

1 **Interactive comment on “Characteristics of ozone and particles in**
2 **the near-surface atmosphere in urban area of the Yangtze River**
3 **Delta, China” by Huimin Chen et al.**

4 **To Editors and Anonymous Referee #2 and #3:**

5 Dear editors and reviewers:

6 Thank you very much for dedicating time to reviewing the manuscript and providing us the important
7 comments and suggestions on our study. We have learned a lot from your advice and made great efforts
8 to improve the manuscript accordingly. A carefully point by point response to your comments has been
9 listed below which we hope meet with approval. The revised details can be referred to the new version
10 of the manuscript.

11 **Relevant changes of the revised manuscript (marked with traces) as well as the change list are**
12 **also enclosed in the last part of this document.**

13
14 **Anonymous Referee #2**

15 Received and published: 5 December 2018

16
17 A major revision of the MS must be made. Reconsideration of the MS is only possible pending the
18 responses from the authors to the points listed below. The MS reports the observational data but
19 barely digs enough into it, let alone a sufficient and reasonable discussion without conceptual
20 mistakes. Moreover, the MS is not comfortably readable and lacks brevity. There are quite a few
21 grammatical errors to be corrected. It would also be better if the language could be polished in the
22 revision.

23
24 **R:** We sincerely thanks for pointing out the problem of manuscript’s analysis and writings. First,
25 according to your suggestions, the authors conduct a more detailed analysis and discussion on the
26 observational data. And we have also checked and corrected the all confusing statements in the
27 manuscript. For example, we describe the similar role CO play in ozone production as volatile organic
28 compounds (VOCs) and the criterion for VOC/NO_x sensitive region in the revised manuscript after a
29 comprehensive study of related work, making the deduction of the VOC-limited region through the CO-
30 NO_x-O₃ correlation in this study more convincing. Also, for a sufficient use of observation data, like the
31 aerosol optical properties, we have further analyzed the optical properties data to some extent for a better
32 understanding of particle characteristics, such as its size and light extinction effects. It would contribute
33 to the analysis of aerosols characteristics. Moreover, the manuscript has been rephrased significantly and
34 shortened in necessarily throughout the whole text. Most parts of the manuscript have been shortened,
35 especially for the Sections 2.2, 3.1, and 3.2. For example, the calculation of the aerosol optical properties
36 and truncation correction of Aurora-3000 (Section 2.2), which have been stated clearly in previous
37 studies (e.g., *Zhuang et al., 2015, 2017; Anderson and Ogren, 1998; Müller et al., 2011, etc.*) have been
38 rephrased to a briefer but more legible version. More details could be found in the revised manuscript,
39 and it’s believed that the revised version of the manuscript is much clearer and more readable.

41 With regard to your comments, questions and suggestions, the manuscript has been rephrased throughout
42 the whole text. The finding(s) of this study have also been refined in better ways of expression, which
43 could be found in most parts of the revised manuscript, including in the sections of Abstract, Introduction,
44 Discussions, as well as Conclusion. Details can be found in the revised manuscript.

45

46 **References:**

47 Zhuang, B. L., Wang, T. J., Liu, J., Ma, Y., Yin, C. Q., Li, S., Xie, M., Han, Y., Zhu, J. L., Yang, X. Q.,
48 Fu, C. B.: Absorption coefficient of urban aerosol in Nanjing, west Yangtze River Delta, China, *Atmos.*
49 *Chem. Phys.*, 15, 13633–13646, doi:10.5194/acp-15-13633-2015, 2015.

50 Zhuang, B. L., Wang, T. J., Liu, J., Li, S., Xie, M., Han, Y., Chen, P. L., Hu, Q. D., Yang X.Q., Fu, C. B.,
51 Zhu, J. L.: The surface aerosol optical properties in the urban area of Nanjing, west GTH River Delta,
52 China. *Atmos. Chem. Phys.*, 17, 1143–1160, doi:10.5194/acp-17-1143-2017, 2017.

53 Anderson, T. L., Ogren, J. A.: Determining aerosol radiative properties using the TSI 3563 integrating
54 nephelometer, *Aerosol Sci. Tech.*, 29, 57–69, 1998.

55 Müller, T., Laborde, M., Kassell, G., Wiedensohler, A.: Design and performance of a three-wavelength
56 LED-based total scatter and backscatter integrating nephelometer, *Atmos. Meas. Tech.*, 4, 1291–1303,
57 doi:10.5194/amt-4-1291-2011, 2011.

58

59 **Main points:**

60 1. The structure of the introduction apparently lacks logic organization. Even more, major
61 scientific issues the MS to be addressed are not clearly stated.

62

63 **R:** According to your suggestions, the structure of the introduction has been reorganized. It is believed
64 to be more readable and easier for readers to grasp the major scientific issues of the study. Please refer
65 to the revised manuscript for more details.

66

67 2. A detailed description of the environment where all instruments are installed should be given
68 in section 2.1. How about the drying system upstream AE-31 and Aurora-3000? The
69 instruments used to measure trace gases should be at least briefly described, instead of having
70 not even a single word on that.

71

72 **R:** Thank you for your suggestions and question. Section 2.1 has been extended to degrees. Description
73 of the environment where all instruments are installed has been included in the revised manuscript. For
74 the drying system, there is no heater for AE-31, which is similar to the settings in other sites (e.g., *Wu et*
75 *al.*, 2012; *Wu et al.*, 2013; *Gong et al.*, 2015, etc.). Both external and internal heaters are equipped for
76 Aurora-3000. However, the internal heater has been turned off during the study period because RH in
77 the tube is mostly lower than 50% in this period. Corresponding statements on settings of AE-31 and
78 Aurora-3000 have also been included in the revised manuscript. For the instruments of the trace gases,
79 more detailed description can be found in the revised manuscript.

80

81 **References:**

82 Wu, Y. F., Zhang, R. J., Pu, Y. F., Zhang, L. M., Ho, K. F., Fu, C.B.: Aerosol optical properties observed
83 at a semi-arid rural site in northeastern China, *Aerosol Air Qual. Res.*, 12, 503–514, 2012.

84 Wu, D., Wu, C., Liao, B., Chen, H., Wu, M., Li, F., Tan, H., Deng, T., Li, H., Jiang, D., Yu, J. Z.: Black

85 carbon over the South China Sea and in various continental locations in South China, Atmos. Chem.
86 Phys., 13, 12257–12270, doi:10.5194/acp-13-12257-2013, 2013.
87 Gong, W., Zhang, M., Han, G., Ma, X., Zhu, Z.: An investigation of aerosol scattering and absorption
88 properties in Wuhan, Central China, Atmosphere, 6, 503–520, 2015

89
90 3. The SC2006 is adopted in this study to correct the systematic biases inherent in the principle
91 of AE-31. What are the parameters used in your procedure? How about the values of your
92 correction factors? The description needs to be more specific.

93
94 **R:** Thanks for your question. Previous investigation indicated that both Weingartner corrected (WC2003
95 for short, hereinafter) and Schmid corrected (SC2006 for short, hereinafter) absorptions show good
96 agreements with the one from the Multi-Angle Absorption Photometer (*Collaud Coen et al., 2010*).
97 Therefore, we have applied several correction algorithms to calculate the aerosol absorption coefficient
98 according to SC2006, WC2003, and indirect calculation (IDC). And the aerosol optical properties and
99 certain parameters used in the correction procedures are based on our observation data and previous work

100 (*Wu et al., 2009; Wu et al., 2013*). Results showed that corrected $\sigma_a \sigma_a$ at 532 nm is consistent with
101 each other among WC2003, SC2006 and IDC. However, the absorption Ångström exponent from
102 SC2006 might be closer to the real ones than WC2003s as suggested in *Zhuang et al. (2015)*. Therefore,
103 the SC2006 is adopted in this study.

104 The parameters in the correction procedure are derived from the local optical properties ($\omega_0 \omega_0$ and α_s
105 α_s were set to 0.922 and 1.51, respectively). The values of correction factors C and R are as follows: $R=1$
106 when $ATN \leq 10$ and $f=1.2$, and C in Nanjing is 2.95, 3.37, 3.56, 3.79, 3.99, 4.51 and 4.64 at 370, 470, 520,
107 590, 660, 880 and 950 nm. Detailed procedures of the calculations could be referred to *Zhuang et al.*
108 (*2015*). Relatively in-depth description has been added in Section 2.2 in the revised manuscript.

109 **References:**

110 Collaud Coen, M., Weingartner, E., Apituley, A., Ceburnis, D., Fierz-Schmidhauser, R., Flentje, H.,
111 Henzing, J. S., Jennings, S. G., Moerman, M., Petzold, A., Schmid, O., Baltensperger, U.:
112 Minimizing light absorption measurement artifacts of the Aethalometer: evaluation of five correction
113 algorithms, Atmos. Meas. Tech. 2010, 3, 457–474.
114 Wu, D., Mao, J. T., Deng, X. J., Tie, X. X., Zhang, Y. H., Zeng, L. M., Li, F., Tan, H. B., Bi, X. Y.,
115 Huang, X. Y., Chen, J., Deng, T.: Black carbon aerosols and their radiative properties in the Pearl
116 River Delta region, Sci. China Ser. D, 52, 1152–1163, doi:10.1007/s11430-009-0115-y, 2009.
117 Wu, D., Wu, C., Liao, B., Chen, H., Wu, M., Li, F., Tan, H., Deng, T., Li, H., Jiang, D., Yu, J. Z.: Black
118 carbon over the South China Sea and in various continental locations in South China, Atmos. Chem.
119 Phys., 13, 12257–12270, doi:10.5194/acp-13-12257-2013, 2013.
120 Zhuang, B. L., Wang, T. J., Liu, J., Ma, Y., Yin, C. Q., Li, S., Xie, M., Han, Y., Zhu, J. L., Yang, X. Q.,
121 Fu, C. B.: Absorption coefficient of urban aerosol in Nanjing, west Yangtze River Delta, China, Atmos.
122 Chem. Phys., 15, 13633–13646, doi:10.5194/acp-15-13633-2015, 2015

123
124
125 4. The truncation correction of Aurora-3000 is based on Mie calculations. If I understand it

126 correctly, Mie calculation is not performed in this study, since obviously there is no
127 measurement of particle number size distribution. Instead, correction parameters are directly
128 taken from the literature in this study. How much uncertainty might be introduced to scattering
129 coefficients due to the choice of the correction factors?
130

131 **R:** Thank you for your question. Mie calculation is not performed due to the lack of measurement of
132 particle number size distribution at the site. However, in Müller *et al.* (2011), it is pointed out that the
133 calculation performed for Aurora-3000 in the study is accurate for a wide range of atmospheric aerosols,
134 and the correction parameters have been used for correction in previous studies (e.g., Virkkula *et al.*,
135 2015; Gong *et al.*, 2015; Perrone *et al.*, 2014; Pandolfi *et al.*, 2014, *etc.*). For the single scattering albedo
136 larger than 0.8, the uncertainty of the correction is not expected to be larger than 3 % (Bond *et al.*, 2009).
137 Here in our study, over 99% of the single scattering albedo is larger than 0.8, thus the uncertainty is about
138 2%~ 3%, which could meet the precision requirements to degrees.
139

140 **References:**

141 Müller, T., Laborde, M., Kassell, G., Wiedensohler, A.: Design and performance of a three-wavelength
142 LED-based total scatter and backscatter integrating nephelometer, *Atmos. Meas. Tech.*, 4, 1291–1303,
143 doi:10.5194/amt-4-1291-2011, 2011.

144 Virkkula, A., Chi, X., Ding, A.J., Shen, Y., Nie, W., Qi, X., Zheng, L., Huang, X., Xie, Y., Wang, J., Petäjä,
145 T., Kulmala, M.: On the interpretation of the loading correction of the aethalometer. *Atmospheric
146 Measurement Techniques*, 8, 10(2015-10-21), 2015, 8(8), 7373-7411.

147 Gong, W., Zhang, M., Han, G., Ma, X., Zhu, Z.: An Investigation of Aerosol Scattering and Absorption
148 Properties in Wuhan, Central China. *Atmosphere*, 2015, 6, 503–520.

149 Perrone, M. R., Romano, S., Orza, J.A.G.: Particle optical properties at a Central Mediterranean site:
150 Impact of advection routes and local meteorology. *Atmospheric Research*, 2014, 145-146:152-167.

151 Pandolfi, M., Ripoll, A., Querol, X., Alastuey, A.: Climatology of aerosol optical properties and black
152 carbon mass absorption cross section at a remote high-altitude site in the western mediterranean basin.
153 *Atmospheric Chemistry and Physics*, 2014, 14(12), 6443-6460.

154 Bond, T. C., Covert, D. S., Müller, T.: Truncation and Angular-Scattering Corrections for Absorbing
155 Aerosol in the TSI 3563 Nephelometer, *Aerosol Sci. Tech.*, 2009, 43, 866–871.
156

157 5. HYSPLIT model is driven by NCEP data with a temporal resolution of 6 hours and a spatial
158 resolution of 2.5 degrees in this study. I doubt that the resolution is adequate for carrying a
159 simulation of near surface transport process.
160

161 **R:** Thanks for your comments. We have checked the data for driving HYSPLIT model according to your
162 comments. Instead of the NCAP data, HYSPLIT model is driven by GDAS (Ground Data Acquisition
163 System, <ftp://arlftp.arlhq.noaa.gov/pub/archives/gdas1>) data with a temporal resolution of 6 hours and a
164 spatial resolution of 1.0 degrees in our study, which is thought to be adequate enough for carrying a
165 simulation of the transport process (e.g., Rolph *et al.*, 2014; Su *et al.*, 2015; Guo *et al.*, 2015, *etc.*).
166

167 **References:**

168 Rolph, G.D., Ngan, F., Draxler, R.R.: Modeling the fallout from stabilized nuclear clouds using the
169 HYSPLIT atmospheric dispersion model. *Journal of Environmental Radioactivity*, 2014, 136:41-55.

170 Su, L., Yuan, Z.B., Fung, J., Lau, A.: A comparison of HYSPLIT backward trajectories generated from
171 two GDAS datasets. *Sci. Total Environ*, 2015, 506-507:527-537.

172 Guo, Z.B., Jiang, W.J., Chen, S.L., Sun, D.L., Shi, L., Zeng, G., Rui, M.L.: Stable isotopic compositions
173 of elemental carbon in PM_{1.1} in north suburb of Nanjing Region, China. *Atmospheric Research*, 2015,
174 168:105-111.

175

176 6. Page 14, Line 283-284, particles especially sub-micron particles could hardly be removed
177 from the atmosphere by rain droplets. It is strong wind before the rain that sweeps them
178 out.

179

180 **R:** Thank you for your comments. We agree with you that strong wind would also play a significant role
181 in removing particles. With regard to your comment, the wind speed is further investigated during the
182 study period. The meteorological data is downloaded from National Climate Data Center
183 (<ftp://ftp.ncdc.noaa.gov/pub/data/noaa/>) and Wunderground Global Weather Precision Forecast
184 (www.wunderground.com), which has also been used in other researches (e.g., *Bolling et al., 2005; Wang*
185 *et al., 2006; Pokharel and Kaplan, 2017; Huang et al., 2018, etc.*) . Results indicate that the monthly
186 averages of daily wind speeds are relatively close to each other in fall and winter, ranging from 1.1
187 (February) to 1.8 m/s (November), whereas the aerosol concentrations are not. For example, the average
188 of PM_{2.5} concentration in October was 35.8 µg/m³ but 42.5 µg/m³ in September, which increased roughly
189 20% in a month. The monthly average wind speed, however, increased only 0.1 m/s from September to
190 October. And the mean precipitation increased from 2.3 mm/h in September to 3.1 mm/h in October
191 correspondingly. Considering the emission rates of these two months are relatively close (emission in
192 October is a little bit stronger according to *Zhang et al., 2006*), it is suggested that a higher precipitation
193 in October thus with a larger scavenging efficiency might have larger contribution to small concentrations
194 of particles.

195

196 **References:**

197 Bolling, B. G., Kennedy, J. H., and Zimmerman, E. G. (2005). Seasonal dynamics of four potential West
198 Nile vector species in north-central Texas., *Journal of Vector Ecology*, 2005, 30(2), 186-194.

199 Wang, Y., Zhuang, G.S., Zhang, X.Y., Huang, K., Xu, C., Tang, A.H., Chen, J.M., An, Z.S.: The ion
200 chemistry, seasonal cycle, and sources of PM_{2.5} and TSP aerosol in Shanghai. *Atmospheric*
201 *Environment*, 2006, 40(16):2935-2952.

202 Ashok, P., Michael, K.: Dust climatology of the NASA Dryden Flight Research Center (DFRC) in
203 Lancaster, California, USA. *Climate*, 2017, 5. 15. 10.3390/cli5010015.

204 Huang, S., Sun, L., Zhou, T., Yuan, D.X., Du, B., Sun, X.W.: Natural stable isotopic compositions of
205 mercury in aerosols and wet precipitations around a coal-fired power plant in Xiamen, southeast China.
206 *Atmospheric Environment*, 2018, 173:72-80.

207 Zhang, Q., Streets, D.G., Carmichael, G.R., He, K.B., Huo, H., Kannari, A., Klimont, Z., Park, I.S.,
208 Reddy, S., Fu, J.S., Chen, D., Duan, L., Lei, Y., Wang, L.T., Yao, Z.L., 2009. Asian emissions in 2006
209 for the NASA INTEX-B mission. *Atmos. Chem. Phys.*2009, 9(14): 5131–5153.

210

211 7. Page 18, Line 385-386, the author states that the diurnal pattern of NO_x is mainly governed
212 by photochemical processes and meteorology. However, emission is a key factor that should
213 not be ignored.

214
215
216
217
218
219
220
221
222
223
224
225
226
227
228
229
230
231
232
233
234
235
236
237
238
239
240
241
242
243
244
245
246
247
248
249
250
251
252
253
254
255
256
257

R: Thanks again. Emission has been stated as a key factor in the current version. The sentence has been rephrased in the revised manuscript.

8. Page 22, Line 454-460, the concept about fog is completely wrong. Fog only occurs above 100% RH, though droplets can exist below 100% due to the hygroscopic growth of particles.

R: Thank you for your advice. We agree with you that fog generally refers to a weather phenomenon created by the condensation of water vapor when the relative humidity approaches 100% (saturated) with the visibility less than 1 km, and we have rephrased the sentence in the revised manuscript.

9. Page 22, Line 467-471, the existence of aerosols might affect solar radiation to some extent and thus ozone photochemical production (not always to a measurable amount). However, the main reason for the observed variation of ozone should not be attributed to aerosols. The author tempts to build a relationship between aerosols and ozone, but I find the analysis of data and deduction not robust and even incorrect, just like here and discussions elsewhere in the MS, e.g., Page 24, Line 503-504.

R: Thanks for the comments.

Firstly, the existence of particulates could affect ozone photochemical production because particulates could inhibit the photolysis reactions near the surface in reducing the photolysis frequencies in the atmosphere, which would result in the decrease of O₃ concentrations near the ground. In our study, the negative correlation between particulates and O₃ coincides with the above assumption, which was also found in various numerical models (e.g., *Li et al., 2005; Bian et al., 2007; Deng et al., 2010; Li et al., 2011; Li et al., 2018, etc.*). Most of the simulated results above showed an obvious change in the amount of ozone concentration and production due to aerosols. For example, *Bian et al. (2007)* reported the ratio of $\Delta[\text{O}_3]/\Delta[\text{AOD}]$ ranged from -4~-16 ppb in Tianjin, and in *Li et al. (2011)*, aerosols decreased the average O₃ → O(¹D) photolysis frequency by 53%, 37% and 21% in the lower, middle and upper troposphere in central east China, and as implied in *Li et al. (2017)*, high concentrations of aerosols result in a 0.1~ 5.0 ppb (12.0%) reduction of near-surface ozone in central Nanjing.

Besides, we agree with you that the main reasons for the observed variation of ozone might be attributed to the effects of radiation, concentrations of precursors, other weather conditions, etc. And we have taken the effects above into consideration when discussing the ozone variation. For example, in Section 3.2, the discussion of ozone temporal variation contains the influence of radiation, precursor concentrations, as well as the meteorology field. And to make a better insight of the correlation and interaction between particles and ozone through observation data, this study further identifies the influence of associated affecting factors, including UV radiation, temperature, and precursors (NO_x, NO_y, and CO) concentrations, on the interaction (Section 3.3). For a more comprehensive overview, we not only analyze the correlation between particulates and ozone but also the one between particulates and the precursor (NO_x and CO). It is found that particles (PM_{2.5} and BC) are well-correlated with precursors (NO_x and CO), which could be another possible reason for the negative correlation between aerosols and ozone. In our study, we have discussed the abovementioned possible reasons for the correlation thoroughly, instead

258 of just laying emphasis on the impact of aerosols on the ozone photochemical production in the revised
259 manuscript. Thus, the main points of our analysis and discussions is to propose the possible reasons for
260 the effects of aerosols on ozone concentration (by influencing the radiation and the precursors
261 concentrations) based on the observation data, rather than regard aerosols as a decisive factor of the
262 observed ozone variation.

263
264 As for the analysis of data and deduction, according to your suggestion, Section 3.3 has been extended
265 to degrees. More in-depth discussions on the aerosol classification and identification have been included
266 in the current version. More details can be found in the revised manuscript.

267

268 **References:**

269 Li, G. H., Zhang, R. Y., Fan, J. W.: Impacts of black carbon aerosol on photolysis and ozone. *Journal of*
270 *Geophysical Research.*, 2005, 110(D23206).

271 Bian, H., Han, S., Tie, X., Sun, M., Liu, A.: Evidence of impact of aerosols on surface ozone
272 concentration in Tianjin, China. *Atmospheric Environment*, 2007, 41, 4672-4681.

273 Deng, J., Wang, T., Liu, L., Jiang, F.: Modeling heterogeneous chemical processes on aerosol surface.
274 *Particuology*, 2010, 8(4):308-318.

275 Li, J., Wang, Z., Wang, X., Yamaji, K., Takigawa, M., Kanaya, Y., Pochanart, P., Liu, Y., Irie, H., Hu, B.,
276 Tanimoto, H., Akimoto, H.: Impacts of aerosols on summertime tropospheric photolysis frequencies
277 and photochemistry over Central Eastern China. *Atmospheric Environment*, 2011, 45(10):1817-1829.

278 Li, M., Wang, T., Xie, M., Li, S., Zhuang, B., Chen, P.: Agricultural fire impacts on ozone photochemistry
279 over the Yangtze River Delta region, East China. *Journal of Geophysical Research: Atmospheres*, 2018.

280 Li, M., Wang, T., Xie, M., Li, S., Zhuang, B., Chen, P.: Impacts of aerosol-radiation feedback on local
281 air quality during a severe haze episode in Nanjing megacity, eastern China, *Tellus B: Chemical and*
282 *Physical Meteorology*, 2017, 69(1):1339548.

283

284 10. Page 23, Line 491-499, the author draws a conclusion that ozone photochemical production
285 is VOC-limited by using CO/particle-O₃-NO_x relationship. I find it very unconvincing.

286 **R:** Thank you for your comments.

287

288 In our study, we have no VOCs measurement, thus CO is chosen as the reference tracer, which is similar
289 to other studies (e.g., *Hsu et al., 2010; Shao et al., 2011; Yao et al., 2012, etc.*). First of all, the measured
290 mixing ratios of CO showed significant correlations with the measured levels of most anthropogenic
291 VOCs, which has been verified in many previous studies (e.g., *Baker et al., 2008; von Schneidmesser*
292 *et al., 2010; Wang et al., 2014, etc.*). In addition, as a significant precursor of ozone, CO also plays a
293 similar role as VOCs. HO₂ produced from oxidation of CO initiates photochemical reactions which result
294 in the net formation of O₃ (*Novelli et al., 1998; Atkinson et al., 2000; Gao et al., 2005*).

295

296 If O₃ formation is under VOC-sensitive regime, the reduction of NO_x will lead to increase in O₃
297 concentrations, which is used for observation data to determine the ozone photochemical production in
298 the region is VOC-limited or NO_x-limited (*Geng et al., 2008; Ding et al., 2013b*). It is found that an
299 increase of CO, as well as PM_{2.5} and BC, always results in higher O₃ concentration for NO_x lower than
300 40 ppb, while NO_x reverses. To be specific, when NO_x reduces for CO lower than 1500 ppb, O₃ has a
301 sharp increase. Also, an increase in the CO level would lead to an increase in the O₃ concentration,

302 especially when NO_x is lower than 40 ppb. Therefore, we suggest that the region is VOC-sensitive.

303

304 **References:**

305 Hsu, Y. K., VanCuren, T., Park, S., Jakober, C., Herner, J., FitzGibbon, M., Blake, D. R., Parrish, D. D.:
306 Methane emissions inventory verification in southern California, *Atmospheric Environment*, 2010,
307 44(1):1-7.

308 Shao, M., Huang, D., Gu, D., Lu, S., Chang, C., Wang, J.: Estimate of anthropogenic halocarbon emission
309 based on measured ratio relative to CO in the Pearl River Delta region, China, *Atmos. Chem. Phys.*,
310 2011, 11((1): 5011–5025.

311 Yao, B., Vollmer, M. K., Zhou, L. X., Henne, S., Reimann, S., Li, P. C., Wenger, A., Hill, M.: In-situ
312 measurements of atmospheric hydrofluorocarbons (HFCs) and perfluorocarbons (PFCs) at the
313 Shangdianzi regional background station, China, *Atmos. Chem. Phys.*, 2012, 12(21): 10181–10193.

314 Baker, A. K., Beyersdorf, A. J., Doezema, L. A., Katzenstein, A., Meinardi, S., Simpson, I. J., Blake, D.
315 R., Rowland, F. S.: Measurements of nonmethane hydrocarbons in 28 United States cities, *Atmos.*
316 *Environ.*, 2008, 42(1): 170–182.

317 von Schneidmesser, E., Monks, P. S., and Plass-Duelmer, C.: Global comparison of VOC and CO
318 observations in urban areas, *Atmos. Environ.*, 2010, 44(39): 5053–5064.

319 Wang, M., Shao, M., Chen, W., Yuan, B., Lu, S., Zhang, Q., Zeng, L., Wang, Q.: A temporally and
320 spatially resolved validation of emission inventories by measurements of ambient volatile organic
321 compounds in Beijing, China. *Atmos. Chem. Phys.*, 2014, 14(12): 5871–5891.

322 Novelli, P.C., Masarile, K. A., Lang, P.M.: Distributions and recent changes of carbon monoxide in the
323 lower troposphere. *Journal of Geophysical Research Atmospheres*, 1998, 103(D15).

324 Atkinson, R.: Atmospheric chemistry of VOCs and NO_x, *Atmos. Environ.*, 2000, 34(12-14), 2063–2101.

325 Gao, J., Wang, T., Ding, A., Liu, C.: Observational study of ozone and carbon monoxide at the summit
326 of mount Tai (1534 m a.s.l.) in central-eastern China. *Atmos. Environ.*, 2005, 39(26), 4779–4791.

327 Geng, F.H., Tie, X.X., Xu, J.M., Zhou, G.Q., Peng, L., Gao, W., Tang, X., Zhao, C.S.: Characterizations
328 of ozone, NO_x, and VOCs measured in Shanghai, China. *Atmos. Environ.*, 2008, 42(29), 6873–6883.

329 Ding, A. J., Fu, C. B., Yang, X. Q., Sun, J. N., Zheng, L. F., Xie, Y. N., Herrmann, E., Nie, W., Petaja, T.,
330 Kerminen, V. -M., and Kulmala, M.: Ozone and fine particle in the western Yangtze River Delta: an
331 overview of 1 yr data at the SORPEs station, *Atmos. Chem. Phys.*, 2013, 13, 5813–5830.

332

333 **Minor points:**

334 1. The full form should be given for the abbreviation of BTH in the abstract.

335

336 **R:** Thanks for your advice. The full form for the abbreviation of BTH has been given in the revised
337 abstract.

338

339 2. The abbreviation of several aerosol optical parameters such as AAC and SC is not common.
340 It would be better to follow the convention in the community.

341

342 **R:** Thanks again for your suggestion. According to your suggestion, in the revised manuscript, aerosol
343 optical parameters, including scattering (SC), back-scattering (Bsp), absorption (AAC), and extinction
344 (EC) coefficient, scattering (SAE) and absorbing (AAE) Ångström exponent, asymmetry parameter
345 (ASP), and single-scattering albedo (SSA), have been adapted to σ_{ts} , σ_{bs} , σ_a , σ_e ,

346 α_{ts} , α_a , g , and ω_0 , respectively (e.g., Hess, 1998; Andreae et al., 2008; Müller et
347 al., 2011, etc.).

348

349 **References:**

350 Hess, M.: Optical properties of aerosols and clouds: The software package OPAC. Bull. Am. Meteor. Soc.
351 1998, 79(5):831-844.

352 Andreae, M.O., Schmid, O., Yang, H., Chanda, D., Yu, J., Zeng, L., Zhang, Y.: Optical properties and
353 chemical composition of the atmospheric aerosol in urban Guangzhou, China. Atmospheric
354 Environment, 2008, 42(25):6335-6350.

355 Müller, T., Laborde, M., Kassell, G., Wiedensohler, A.: Design and performance of a three-wavelength
356 LED-based total scatter and backscatter integrating nephelometer, Atmos. Meas. Tech., 2011, 4,
357 1291–1303.

358

359 3. Page 13, Line 270-274, the sentence beginning with ‘For example’ is supposed to illustrate
360 the point brought forward by the sentence before it. However, I find their connection rather
361 confusing.

362

363 R: Thank you for pointing out the problem. This part has been rephrased to be more intelligible in the
364 revised manuscript.

365

366 **Anonymous Referee #3**

367 Received and published: 21 December 2018

368

369 The paper written by Chen et al., performed the continuous measurements of particles and trace
370 gases in Nanjing during cold seasons. Although the interaction of atmospheric components (e.g.,
371 trace gases, aerosols) and meteorological conditions has been analyzed, the originality should
372 be addressed especially in abstract before publication. Besides, the paper still suffered from
373 many minor flaws throughout the manuscript. Thus, I suggest this paper could be published
374 after revising the minor errors.

375 The detailed suggestions are as follows:

376 1. It was well documented that the air pollutants were closely linked to the weather system
377 and meteorological conditions. (Line 32) The author only revealed the important effects of
378 weather system and human activities on the environment in the YRD region, which has
379 been investigated by many previous studies. The originality was not addressed in the
380 manuscript. In my opinion, the abstract should be rewritten to stress the new contribution
381 of this paper to atmospheric chemistry rather than reporting the pollution level simply.

382

383 R: We sincerely thanks for your comments. In the revised manuscript, the authors stress the originality
384 of the study.

385

386 1. Indeed, some researches on the air pollutants related to weather system and human activities have been
387 carried out in most sites of YRD recently. However, previous studies using observation data in Nanjing
388 often concentrated on characteristics of one of the particles, such as BC and carbonaceous aerosols (e.g.,

389 *Zhuang et al., 2014*), or PMs (e.g., *Deng et al., 2011; Shen et al., 2014*), or ozone and its precursors (e.g.,
390 *Tu et al., 2007; Wang et al., 2008; An et al., 2015*). Thus, it is necessary to achieve a relatively
391 **comprehensive understanding** of the air pollution problem **directly** through analysis of **various species**.
392 In addition, most of them described the temporal and spatial distributions of concentrations, and the
393 influence of meteorological effects. In this study, discussion of aerosols characteristics, especially
394 particles, is **not limited to the concentrations** but taking optical properties into consideration as well.
395 Moreover, most of them lay less emphasis on the **inter-species correlations** and the combined effects of
396 **more than one pollutant**, especially the possible underlying **chemical progress**, during severe pollution
397 episodes except *Ding et al. (2013b)*, who described the characteristics of O₃ and PM_{2.5} with near-surface
398 observation data in **rural** area of Nanjing. As implied in *Zhang et al. (2012)*, aerosols are complicated in
399 compositions and spatial distributions especially in fast developing regions with intense human activities
400 (such as Nanjing). Thus, differences of the aerosol characteristics, for instance, concentrations as well as
401 optical properties, might exist to degrees among the sites located in different parts of Nanjing with
402 different land use. Additionally, a better understanding of spatial and temporal variations of pollutants
403 can contribute to the adoption of effective measures to reduce air pollution on the urban scale. Therefore,
404 it's necessary to investigate the characteristics of air pollutants in **urban** area of west YRD.

405

406 2. To make a better insight of the correlation and interaction between particles and ozone (the two main
407 pollutants) through observation data, this study further identifies the influence of **associated affecting**
408 **factors**, including UV radiation, temperature, and precursor's concentrations on the interaction (Section
409 3.3). Most of previous studies present the findings from various numerical models (e.g., *Li et al., 2005;*
410 *Bian et al., 2007; Deng et al., 2010; Li et al., 2011; Li et al., 2018, etc.*). However, only a few studies
411 discussed the correlation based on observation. In Nanjing, *Ding et al. (2013b)* described a correlation
412 between PM_{2.5} and O₃. But only temperature is regarded as an affecting factor. Thus, it is believed that
413 our study would contribute to a more comprehensive understanding of the underlying mechanisms from
414 observation.

415

416 3. Back to the site, the site is located in the **city center**, one of the highly residential areas of Nanjing,
417 with concentrated human activities with residential areas, schools, institutions and business districts, and
418 the main road of urban transportation around. Therefore, the results could suggest the characteristics and
419 interactions of pollutants in the urban region very well. Also, the results could further imply the effects
420 of the **urban underlying surface** and **human activities** to degrees. Besides, as a typical urban area, the
421 results in this study would probably bring new knowledge of aerosol characteristics, like the pollution
422 level variation in different years and different regions through comparison with previous studies based
423 on observation and numerical simulations.

424

425 Overall, this manuscript presents more comprehensive, systematic and deeper analysis on main pollutants
426 like particles and ozone in urban area of west YRD. Results further indicate the characteristics of the
427 particles and trace gases and reveal the possible chemistry process and interactions among different
428 species and meteorological variables in west YRD. And they are also advantageous to improve the
429 understanding of the detailed variations (seasonal, monthly, and diurnal) and its effects in east regions of
430 China.

431

432 According to your comments, questions and suggestions, not only the abstract, but the introduction,

433 discussion and conclusion have also been rephrased carefully. The originality (listed above) and finding(s)
434 of this study have been refined in better ways of expression. Details can be found in the revised
435 manuscript.

436

437 **References:**

438 Zhuang, B. L., Wang, T. J., Liu, J., Li, S., Xie, M., Han, Y., Chen, P. L., Hu, Q. D., Yang, X. Q., Fu, C.
439 B., Zhu, J. L.: Continuous measurement of black carbon aerosol in urban Nanjing of Yangtze River
440 Delta, China. *Atmospheric Environment*, 2014, 89(Complete):415-424.

441 Deng, J. J., Wang, T. J., Jiang, Z. Q., Xie, M., Zhang, R. J., Huang, X. X., Zhu, J. L.: Characterization of
442 visibility and its affecting factors over Nanjing, China. *Atmospheric Research*, 2011, 101(3), 0-691.

443 Shen, G. F., Yuan, S. Y., Xie, Y. N., Xia, S. J., Li, L., Yao, Y. K., Qiao, Y. Z., Zhang, J., Zhao, Q. Y., Ding,
444 A. J.: Ambient levels and temporal variations of PM_{2.5} and PM₁₀ at a residential site in the mega-
445 city, Nanjing, in the western Yangtze River Delta, China. *J. Environ. Sci. Health Part A*, 2014, 49(2),
446 171–178.

447 Tu, J., Xia, Z. G., Wang, H. S., Li, W. Q.: Temporal variations in surface ozone and its precursors and
448 meteorological effects at an urban site in China, *Atmos. Res.*, 2007, 85(3-4), 310–337.

449 Wang, W., Ren, L., Zhang, Y., Chen, J., Liu, H., Bao, L., Shao, F., Tang, D.: Aircraft measurements of
450 gaseous pollutants and particulate matter over Pearl River Delta in China. *Atmos. Environ.* 2008,
451 42(25), 6187–6202.

452 An, J., Zou, J., Wang, J., Lin, X., Zhu, B.: Differences in ozone photochemical characteristics between
453 the megacity Nanjing and its suburban surroundings, Yangtze River Delta, China. *Environ. Sci. Pollut.*
454 *Res.*, 2015, 22(24), 19607–19617.

455 Ding, A. J., Fu, C. B., Yang, X. Q., Sun, J. N., Zheng, L. F., Xie, Y. N., Herrmann, E., Nie, W., Petaja, T.,
456 Kerminen, V. -M., and Kulmala, M.: Ozone and fine particle in the western Yangtze River Delta: an
457 overview of 1 yr data at the SORPEs station, *Atmos. Chem. Phys.*, 2013, 13, 5813–5830.

458 Zhang, X. Y., Wang, Y. Q., Niu, T., Zhang, X. C., Gong, S. L., Zhang, Y. M., and Sun, J. Y.: Atmospheric
459 aerosol compositions in China: Spatial/temporal variability, chemical signature, regional haze
460 distribution and comparisons with global aerosols, *Atmos. Chem. Phys.*, 12, 779–799,
461 doi:10.5194/acp-12-779-2012, 2012.

462 Li, G. H., Zhang, R. Y., Fan, J. W.: Impacts of black carbon aerosol on photolysis and ozone. *Journal of*
463 *Geophysical Research.*, 2005, 110(D23).

464 Bian, H., Han, S., Tie, X., Sun, M., Liu, A.: Evidence of impact of aerosols on surface ozone
465 concentration in Tianjin, China. *Atmospheric Environment*, 2007, 41(22), 4672-4681.

466 Deng, J., Wang, T., Liu, L., Jiang, F.: Modeling heterogeneous chemical processes on aerosol surface.
467 *Particuology*, 2010, 8(4):308-318.

468 Li, J., Wang, Z., Wang, X., Yamaji, K., Takigawa, M., Kanaya, Y., Pochanart, P., Liu, Y., Irie, H., Hu, B.,
469 Tanimoto, H., Akimoto, H.: Impacts of aerosols on summertime tropospheric photolysis frequencies
470 and photochemistry over Central Eastern China. *Atmospheric Environment*, 2011, 45(10):1817-
471 1829. Li, M., Wang, T., Xie, M., Li, S., Zhuang, B., Chen, P. (2018): Agricultural fire impacts on ozone
472 photochemistry over the Yangtze River Delta region, East China. *Journal of Geophysical Research:*
473 *Atmospheres*, 2018123. <https://doi.org/10.1029/2018JD028582>.

474 Li, M., Wang, T., Xie, M., Li, S., Zhuang, B., Chen, P.: Impacts of aerosol-radiation feedback on local
475 air quality during a severe haze episode in Nanjing megacity, eastern China, *Tellus B: Chemical and*
476 *Physical Meteorology*, 2017, 69(1):1339548.

477

478 2. Line 71, the author said observation-based studies of particles were relatively limited. I
479 think it was very subjective because there were hundreds of observation-based studies
480 about the aerosol particles in the past decades. Meanwhile, in line 75, the author said there
481 were only very limited studies of O₃ in the urban of YRD. Actually, the O₃ concentration
482 has been widely monitored in YRD because it was one of the most important gaseous
483 pollutants in YRD. I think the author should review a large amount of papers before writing
484 this paper.

485

486 **R:** Thanks for your suggestions. We have reviewed more papers and refined the expression in the
487 introduction, making it more integrated. More details could be found in the revised version.

488

489 3. Line 108-112, the author should highlight the objective of the present study. In addition,
490 the sentence between line 110 and line 112 should be replaced by the environmental
491 implication of the research.

492

493 **R:** Thank you for your advice. The sentences have been rewritten to highlight the objective of our study,
494 and readers can find more details in the revised manuscript. Generally speaking, the emphasis of our
495 objective is to improve the insight in the characteristics, interactions of main pollutants, and the influence
496 of integrated meteorology variables based on the observation data at an urban site above ground, and
497 further investigate the possible underlying reasons and mechanisms, which is also helpful to achieve a
498 thorough understanding of particles and trace gases pollution in these polluted areas by just using the
499 conventional observations

500

501 The detailed environmental implication of the research could be concluded as follows.

502

503 1. An in-depth discussion on particles variations is performed, not limited to the concentrations but
504 taking optical properties into consideration as well, to quantify the polluted level in detail to receive
505 an overview of the inter-annual variations in the urban region.

506

507 2. A detailed description of O₃ variations can also be found in our study, including the analysis of the
508 main precursors as trace gases (NO_x, NO_y and CO), to have a general and quantitative insight in O₃
509 pollution situations. Both of the pollutants are analyzed considering the effects of meteorology
510 variables including but not limited to precipitation and temperature.

511

512 3. Analysis of inter-species correlations gives a relatively thorough overview of the interactions among
513 various species, for instance, O₃ and particles (BC and PM_{2.5}), O₃ and precursors (NO_x and CO), and
514 particles (BC and PM_{2.5}) and precursors (NO_x and CO). For a better insight, this study further
515 identifies the influence of associated affecting factors on the interaction, such as UV radiation and
516 temperature. Deduction of the underlying chemical mechanisms and process based on the results
517 and previous studies is also presented in our study.

518

519 4. Backward trajectories analysis is conducted for improving the knowledge of regional/sub-regional
520 transport process in urban Nanjing. Discussion of pollutants in different clusters suggests main

521 transport progress in each season and the effects of air masses coming from various regions.

522

523 5. A case study for high particles and O₃ episode is implemented to emphasize the integrated influence
524 of meteorology fields on regional air pollution.

525

526 4. Line 123, the instruments used to monitor the gaseous pollutants such as O₃ should be added
527 in the methods. Additionally, NO_y generally consisted of a large of N-bearing gaseous
528 pollutants. The detailed NO_y species should be introduced in this part.

529

530 **R:** Thank you for your suggestions. In the revised version, the detailed description of instruments
531 measuring trace gases (CO, NO_x, NO_y and O₃) and the measurement of NO_y species (where NO_y = NO
532 + NO₂ + PAN + HNO₃ + NO₃⁻ + N₂O₅ + HONO + organic nitrates, etc.) has been added in the Section
533 2.1.

534

535 5. Line 263-264, the author did not show the variation trend of BC, PM₁₀, and PM_{2.5}.
536 Furthermore, how do you know the sources of these pollutants shared the similar sources?
537 The relevant references were also missing. Line 265, what does transport emission mean?

538

539 **R:** Thanks for your questions. We agree with you that the statement of the similar pattern without the
540 variation trend is not acceptable enough, thus, the expression has been rephrased to be more precise in
541 the revised manuscript.

542

543 *Chow et al. (2011)* reported a wide range of EC and OC abundances (highly correlated with BC) in PM_{2.5}
544 source profiles, which represented the same source type. *Zhuang et al. (2014)* also reported same
545 emission sources for BC and PM_{2.5} in Nanjing based on the well-correlated relationship, which is also
546 found in this study (R=0.75). *Wang et al. (2008)* suggested that the major constituents of PM_{2.5} were
547 black carbon (BC), cluster elements, nitrates, ammonium salts, and sulfates based on the long-term
548 monitoring data, and PM_{2.5} and PM₁₀ share various common sources, i.e., soil dust, coal combustion,
549 industrial emission, and biomass burning in Beijing. *Schlemicher et al. (2013)* also reported quite similar
550 main sources for both particle size classes. Moreover, it is found in *Gong et al. (2013)* that PM_{2.5} is one
551 of the major contributors to PM₁₀ with a good correlation in Wuhan, especially when the concentration
552 of PM₁₀ is not extremely high. Thus, we assume that these pollutants possibly shared the similar sources.

553

554 Relevant references have been added in the revised manuscript. As for the second question, the sentence
555 has been rewritten to be clearer.

556

557 **References:**

558 Chow, J. C., Watson, J. G., Lowenthal, D. H., Chen, L.-W. A., Motallebi, N.: PM_{2.5} source profiles for
559 black and organic carbon emission inventories. *Atmospheric Environment*, 2011, 45(31): 5407-5414.

560 Zhuang, B. L., Wang, T. J., Liu, J., Li, S., Xie, M., Han, Y., Chen, P. L., Hu, Q. D., Yang, X. Q., Fu, C.
561 B., Zhu, J. L.: Continuous measurement of black carbon aerosol in urban Nanjing of Yangtze River
562 Delta, China. *Atmospheric Environment*, 2014, 89(Complete):415-424.

563 Wang, H.L., Zhuang, Y.H., Wang, Y., Sun, Y.L., Yuan, H., Zhuang, G.S., Hao, Z. P.: Long-term
564 monitoring and source apportionment of PM 2.5/PM 10 in Beijing, China. *Journal of Environmental*

565 Sciences, 2008, 20(11): 1323-1327.

566 Schleicher, N., Cen, K., Norra, S.: Daily variations of black carbon and element concentrations of
567 atmospheric particles in the Beijing megacity – Part 1: General temporal course and source
568 identification. *Chemie der Erde - Geochemistry*, 2013, 73(1):51-60.

569 Gong, W., Zhang, T.H., Zhu, Z.M., Ma, Y.Y, Ma, X., Wang, W.: Characteristics of PM_{1.0}, PM_{2.5} and
570 PM₁₀ and their relation to black carbon in Wuhan, central China. *Atmosphere*, 2015, 6(9): 1377-1387.

571

572 6. Line 272-274, the author said the high loadings of particulate matter in early October was
573 mainly due to the increase in aerosol concentrations with high scatter coefficient (SC). I do
574 not understand the association between PM concentration and the aerosol concentrations
575 with high SC. Please explain the reasons in details.

576

577 **R:** Thanks again for your advice. The high concentrations of PMs in early October are possibly resulted
578 from the increase in scattering aerosols. First of all, scatter coefficient is high during that period. Besides,
579 BC, as one of typical absorbing aerosols, does not show such peak in concentrations during that period.
580 The statement has been rephrased and corresponding reasons have also been discussed in the revised
581 manuscript.

582

583 7. Line 284-286, Nanjing is located in Southeast China. The combustion of fossil fuels for
584 domestic heating is not common in the winter of Nanjing. I do not understand why the
585 increased anthropogenic emission of fossil fuels in the winter of Nanjing contributed to the
586 high aerosol loadings.

587

588 **R:** Thanks for your question. Here in our study, anthropogenic particle emissions from fossil fuel are not
589 limited to those for domestic heating. First, though the combustion of fossil fuels for domestic heating is
590 not common in Nanjing to some degree, the emission rates indeed increase in winter in YRD are higher
591 (*Zhuang et al., 2018; Li et al., 2017*). Besides, burning of crop residues during autumn harvest could also
592 contribute to the high aerosol concentrations to some degrees (*Qian et al., 2014*). Although it has been
593 strictly controlled in China, the influence of crop residues burning still exist and cannot be ignored (e.g.,
594 *Wang and Zhang, 2008; Zhu et al., 2010; Ni et al., 2015; Mehmood et al., 2018, etc.*). Additionally, sub-
595 regional transport also plays an important role, for example, in winter, air masses coming from North
596 China Plain where emission rates from fossil fuels of domestic heating are high, account for 31% and
597 have high particles concentrations (Section 3.4). More details have been added in the revised manuscript.

598

599 **References:**

600 Zhuang, B. L, Li, S., Wang, T. J., Liu, J., Chen, H. M., Chen, P. L., Li, M. M., Xie, M.: Interaction
601 between the Black Carbon Aerosol Warming Effect and East Asian Monsoon Using RegCM4. *Journal*
602 *of Climate*, 2018, 31(22):9367-9388.

603 Li, M., Zhang, Q., Kurokawa, J., Woo, J.-H., He, K. B., Lu, Z. F., Ohara, T., Song, Y., Streets, D. G.,
604 Carmichael, G. R., Cheng, Y. F., Hong, C. P., Huo, H., Jiang, X. J., Kang, S., Liu, F., Su, H., Zheng,
605 B.: MIX: a mosaic Asian anthropogenic emission inventory under the international collaboration
606 framework of the MICS-Asia and HTAP, *Atmos. Chem. Phys.*, 2017, 17, 935–963.

607 Qian, L., Yan, Y., Qian, J.M.: An Observational Study on Physical and Optical Properties of Atmospheric
608 Aerosol in Autumn in Nanjing. *Meteorological and Environmental Research* 2014, 5(2): 24 – 30.

609 Wang, S., Zhang, C.: Spatial and temporal distribution of air pollutant emissions from open burning of
610 crop residues in China. *Science Paper Online*, 2008, 3: 329-333.
611 Zhu, B., Su, J. F., Han, Z. W., Yin, C., Wang, T.: Analysis of a serious air pollution event resulting from
612 crop residue burning over Nanjing and surrounding regions. *China Environmental Science*, 2010,
613 30(5):585-592.
614 Ni, H., Han, Y., Cao, J., Chen, L-W. A., Tian, J., Wang, X. L., Chow, J. C., Watson, J. G., Wang, Q., Wang,
615 P., Li, H., Huang, R.: Emission characteristics of carbonaceous particles and trace gases from open
616 burning of crop residues in China. *Atmospheric Environment.*, 2015, 123: 399-406.
617 Mehmood, K., Chang, S., Yu, S., Wang, L., Li, P., Li, Z., Liu, W., Rosenfield, D., Seinfeld, J.: Spatial and
618 temporal distributions of air pollutant emissions from open crop straw and biomass burnings in China
619 from 2002 to 2016. *Environmental Chemistry Letters*, 2018, 16(1):301-309.

620

621 8. Line 294, the diurnal variation of BC concentration was generally associated with the
622 vehicle volume. I am very curious about the higher BC levels during 8-11 pm. I think
623 Nanjing showed the higher vehicle volume during 5-8 pm. The author should explain the
624 unusual characteristics.

625

626 **R:** Thank you for your question and suggestion. Considering a higher vehicle volume during 5~ 8 pm,
627 the peak occurs during 9~11 pm is probably related to a more stable atmosphere stratification and a lower
628 planetary boundary layer (PBL) after around 4 pm when the temperature decreases (*Qian et al., 2014*,
629 *Chen et al., 2016*), both of which would result the accumulation of BC levels, thus the lag of the peak.

630

631 **References:**

632 Qian, L., Yan, Y., and Qian, J.M.: An Observational Study on Physical and Optical Properties of
633 Atmospheric Aerosol in Autumn in Nanjing. *Meteorological and Environmental Research* 2014, 5(2):
634 24 – 30.

635 Chen, T., He, J., Lu, X., She, J., G, Z.: Spatial and temporal variations of PM2.5 and its relation to
636 meteorological factors in the urban area of Nanjing, China. *International Journal of Environmental*
637 *Research and Public Health*, 2016, 13(9), 921.

638

639 9. Line 336, the author inferred that the BC and CO in the atmosphere were mainly originated
640 from biomass burning. The fire point data should be added to demonstrate the potential
641 source of BC and CO.

642

643 **R:** Thanks for your comments. A remarkable correlation between BC and CO was found in a number of
644 studies (*Jennings et al., 1996; Derwent et al., 2001; Badarinath et al., 2007; Spackman et al., 2008;*
645 *Zhuang et al., 2014*). Additionally, BC is mostly produced by the incomplete combustion of carbonaceous
646 material, and so is CO (*Pan et al., 2011*). Therefore, both BC and CO might come from the same sources.

647

648 BC in Nanjing might mostly come from combustions of domestic bio-fuel, industry-coal, and vehicle-
649 gasoline (*Zhuang et al., 2014; Cheng et al., 2017*), instead of biomass burning only. And during the
650 autumn harvest (September~ November), though not so much as that in summer, the crop burning
651 emissions still make contribution to pollutants (e.g., *Qian et al., 2014; Yang et al., 2008; Yin et al., 2016*,
652 *etc.*). Moreover, in *Yin et al.2016*, spatial distribution of crop residue burning spots number from

653 September to December in 2015 deriving from MODIS data shows that autumn crop residue burning has
654 started in October in YRD, and could cause a rise in pollutants. According to *Huang et al. (2012)* and *Li*
655 *et al. (2016)*, spatiotemporal distribution of agricultural fire occurrences in China during 2003~ 2010 as
656 well as 2012 has been presented associated with the spatial distribution of CO emission from residue
657 open burning. Both of them suggested the crop residue burning in autumn is noteworthy and Jiangsu as
658 well as the surrounding provinces including Henan, Shandong, and Anhui are the regions with highest
659 emissions. The problems of writings might mislead the readers, for example, the explanation is probably
660 not comprehensive enough to degrees. The sentences have been rephrased in the current version.

661

662 **References:**

663 Jennings, S. G., Spain, T. G., Doddridge, B. G., Maring, H., Kelly, B. P., Hansen, A. D. A.: Concurrent
664 measurements of black carbon aerosol and carbon monoxide at Mace Head, *J. Geophys. Res.-Atmos.*,
665 1996, 101(D14), 19447–19454.

666 Derwent, R. G., Ryall, D. B., Jennings, S. G., Spain, T. G., and Simmonds, P. G.: Black carbon aerosol
667 and carbon monoxide in European regionally polluted air masses at Mace Head, Ireland during 1995–
668 1998, *Atmos. Environ.*, 2001, 35(36), 6371–6378.

669 Badarinath, K. V. S., Kharol, S. K., Chand, T. R. K., Parvathi, Y. G., Anasuya, T., Jyothsna, A. N.:
670 Variations in black carbon aerosol, carbon monoxide and ozone over an urban area of Hyderabad,
671 India, during the forest fire season, *Atmos. Res.*, 2007, 85(1), 18–26.

672 Spackman, J. R., Schwarz, J. P., Gao, R. S., Watts, L. A., Thomson, D. S., Fahey, D. W., Holloway, J. S.,
673 de Gouw, J. A., Trainer, M., and Ryerson, T. B.: Empirical correlations between black carbon aerosol
674 and carbon monoxide in the lower and middle troposphere, *Geophys. Res. Lett.*, 2008, 35(19), L19816.

675 Zhuang, B. L., Wang, T. J., Liu, J., Li, S., Xie, M., Han, Y., Chen, P. L., Hu, Q. D., Yang, X. Q., Fu, C.
676 B., Zhu, J. L.: Continuous measurement of black carbon aerosol in urban Nanjing of Yangtze River
677 Delta, China. *Atmospheric Environment*, 2014, 89(Complete):415-424.

678 Pan, X. L., Kanaya, Y., Wang, Z. F., Liu, Y., Pochanart, P., Akimoto, H., Sun, Y. L., Dong, H. B., Li, J.,
679 Irie, H., Takigawa, M.: Correlation of black carbon aerosol and carbon monoxide in the high-altitude
680 environment of Mt. Huang in Eastern China. *Atmospheric Chemistry and Physics*, 2011, 11:9735-
681 9747.

682 Cheng, S., Wang, Y. & An, X. J: Temporal variation and source identification of black carbon at Lin'an
683 and Longfengshan regional background stations in China. *Meteorol Res.*, 2017, 31:1070.

684 Qian, L., Yan, Y., Qian, J.M.: An Observational Study on Physical and Optical Properties of Atmospheric
685 Aerosol in Autumn in Nanjing. *Meteorological and Environmental Research*, 2014, 5(2): 24 – 30.

686 Yang, S. J., He, H. P, Lu, S. L., Chen, D., Zhu, J. X.: Quantification of crop residue burning in the field
687 and its influence on ambient air quality in Suqian, China. *Atmospheric Environment*, 2008,42(9):1961-
688 1969.

689 Yin, S., Wang, X.F, Xiao, Y., Tani, H., Zhong, G.S., Sun, Z.Y.: Study on spatial distribution of crop
690 residue burning and PM2.5 change in China. *Environmental Pollution*, 2016, 220(Pt A):204-221.

691 Huang, X., Li, M., Li, J., Song, Y.: A high-resolution emission inventory of crop burning in fields in
692 China based on MODIS Thermal Anomalies/Fire products. *Atmospheric Environment*, 2012, 50:9-15.

693 Li, J., Bo, Y., Xie, S.: Estimating emissions from crop residue open burning in China based on statistics
694 and MODIS fire products. *Journal of Environmental Sciences*, 2016, 44:158-167.

695

696 10. Line 495-496, what does the sentence mean? The author should point out the relationship

697 between CO and ozone production.

698

699 **R:** Thank you for your question and advice. The sentences have been rephrased. A more detailed and in-
700 depth discussion about the relationship between CO and ozone production has been included in the
701 revised manuscript.

702

703 11. The conclusion should be condensed and stress the new contribution to the atmospheric
704 chemistry.

705

706 **R:** Thanks for your suggestion. Conclusion has been rephrased significantly and shortened necessarily
707 and it's believed that the revised version is much more readable. The readers would more easily grasp
708 the useful information of the results. In the revised version, the authors highlight the contributions to the
709 atmospheric chemistry, especially deduction of the underlying chemical mechanisms based on the results
710 of our study and previous studies through inter-species correlations analysis.

711

712 12. There are many grammar and format errors throughout the paper. I suggest the author
713 should revise all of these minor flaws from words to words carefully.

714

715 **R:** Thanks a lot for figuring out the problems of the manuscript's writings. The manuscript has been
716 rephrased to be clearer. And it's also corrected carefully by Professor J. Liu, who is from University of
717 Toronto and also is a co-author of this study with great contributions.

718

719 **Change List**

720 The manuscript has been rephrased significantly and shortened in necessarily throughout the whole
721 text. Changes in manuscript could be concluded as follows.

722 1. The structures of **Abstract**, **Introduction**, and **Conclusion** have been reorganized to be more
723 readable with major scientific issues clearly addressed. And the originality of this study could
724 also be reflected in the revised version.

725 2. For a sufficient use of the observation data, we have extended certain sections in **Results and**
726 **Discussion**, making our results more convincing and robust.

727 3. Previous work has been referred for a comprehensive understanding of the results in this study,
728 and the related papers have been updated in **References**.

729 4. With respect to the grammar and format errors, the manuscript has been revised from words to
730 words carefully and these minor flaws have been corrected.

731 The revised details could be referred to the new version of the manuscript, with relevant changes
732 marked with traces.

733

734

735

736

737

738

739

740

741

742

743

744

745

746

747

748

749

750

751

752

753

754

755

756

757

758

759

760

761

762

763

764

765

766

767

768

769 **Characteristics of ozone and particles in the near-surface**
770 **atmosphere in urban area of the Yangtze River Delta, China**

771 **Huimin Chen¹, Bingliang Zhuang^{1,*}, Jane Liu^{1,2}, TijianWang^{1,**}, Shu Li¹, Min Xie¹,**
772 **Mengmeng Li¹, Pulong Chen¹, Ming Zhao¹**

773 **¹School of Atmospheric Sciences, CMA-NJU Joint Laboratory for Climate Prediction**

774 **Studies, Jiangsu Collaborative Innovation Center for Climate Change, Nanjing University,**
775 **Nanjing 210023, China**

776 **²Department of Geography and Planning, University of Toronto, Toronto, M5S 3G3, Canada**

777 Correspondence: Bingliang Zhuang (blzhuang@nju.edu.cn) and Tijian Wang (tjwang@nju.edu.cn)

778 **Abstract**

779 Aerosols and ozone have significant influences on air qualities, human health and climate changes.
780 To further understand the characteristics and interactions among different urban air pollutants in the
781 west Yangtze River Delta (YRD) region, continuous measurements of low layer atmospheric
782 particles and trace gases have been performed at an urban site in Nanjing from September 2016 to
783 February 2017 in this study. In urban area of west YRD, the mean PM₁₀ and O₃ concentrations are
784 86.3 μg/m³ and 37.7 ppb, respectively, with significant seasonal and diurnal variations. Particles,
785 which are dominated by fine aerosols, are relatively scattering. And most of their optical properties
786 have the similar variations to the aerosol concentrations. Results also show that west YRD could
787 still suffer severe air pollutions, although the seasonal mean aerosol concentrations have been
788 decreased in recent years. Even in cold seasons, O₃ could have about 40 days excess against to the
789 National Ambient Air Quality Standards during the sampling period. Most of polluted episodes are

790 caused by local and sub-regional emissions. A case study for a typical O₃ and PM_{2.5} episode in
791 December 2016 demonstrates that the episode was generally associated with regional transport and
792 stable weather system. Air pollutants were mostly transported from the western areas with high
793 emissions, as well as with an anticyclone and high-pressure system in this region. Correlation
794 analysis reveals that the interaction between O₃ and PMs are complex with a combination of
795 inhibition and promotion under different conditions. The inhibition effect might result from the
796 reduction of photolysis frequency near surface due to aerosols besides their positive correlations
797 with precursors, while the promotion effect is from the formation of secondary aerosols under high
798 concentrations of oxidants and solar radiation. However, the interaction between O₃ and BC shows
799 an inhibit effect due to its chemical stability. It is also indicated a VOC-sensitive regime for
800 photochemical production of O₃ in this region. This study further improves the insight in the
801 characteristics and interactions of main pollutants, and might have a certain contribution to improve
802 the simulation and prediction of aerosols and gases in urban area of YRD.

803 ~~To improve the understanding of the interactions between particles and trace gases in a typical city~~
804 ~~of the YRD region, continuous measurements of particles and trace gases were made at an urban~~
805 ~~site in Nanjing during cold seasons in 2016 in this study. The average of particles, including black~~
806 ~~carbon (BC), PM_{2.5}, and PM₁₀ are $2.602 \pm 1.720 \mu\text{g}/\text{m}^3$, $58.2 \pm 36.8 \mu\text{g}/\text{m}^3$, and $86.3 \pm 50.8 \mu\text{g}/\text{m}^3$,~~
807 ~~respectively, while the average of trace gases, which contain CO, O₃, NO_x, and NO_y, are $850.9 \pm$~~
808 ~~384.1 , 37.7 ± 33.5 , 23.5 ± 14.7 , and 32.8 ± 22.3 ppb, respectively. Compared to National Ambient~~
809 ~~Air Quality Standards in China (NAAQS-CN), we found 48 days excess of PM_{2.5}, 14 days excess~~
810 ~~of PM₁₀, and 40 days excess of O₃. The particles, CO, and nitrogen oxide concentrations shared a~~
811 ~~similar pattern of seasonality and diurnal cycles, which are different from O₃. The former ones are~~

812 all high in DJF and at rush hours, while the latter one had high loadings in the daytime, especially
813 when the ultra-violet (UV) was high. Correlation analysis reveals the formation of secondary
814 aerosols, especially PM_{2.5}, under high O₃ and temperature conditions, and suggests a VOC-sensitive
815 regime for photochemical production of O₃ in urban Nanjing in cold seasons. Backward trajectory
816 analysis suggests the prevailing winds in Nanjing were northerly and easterly during cold seasons
817 in 2016. Air masses from eastern without passing through the urban agglomeration and those from
818 northern without crossing BTH regions were cleaner, but air masses from local regions were more
819 polluted in winter. A case study for a typical O₃ and PM_{2.5} episode in December 2016 demonstrated
820 that the episode was generally associated with regional transport and stable weather system. Air
821 pollutants were mostly transported from the western areas with high emissions and weather
822 conditions are controlled by anticyclone and high pressure system in this region. This study further
823 reveals the important effects of weather system and human activities on the environment in the YRD
824 region, especially in the urban areas, and it's an urgent need for improving air quality in these areas.

825

826 **1. Introduction**

827 Particles, including black carbon (BC), PM_{2.5}, and PM₁₀, and trace gases, such as carbon monoxide
828 (CO), ozone (O₃), nitric oxide and nitrogen dioxide (NO_x), and total reactive nitrogen (NO_y, which
829 includes NO_x, aerosol nitrates (NO₃⁻), nitric acid (HNO₃), N₂O₅, peroxyacetyl nitrate (PAN), and
830 various nitrogen-containing organic compounds.), are important components in the troposphere
831 because of their impacts on human health, biosphere and climate changes (e.g., Chameides et al.,
832 1999a, b; Jerrett et al., 2009; Allen et al., 2012). Through long-range particle cycles, particles could

833 interact with atmospheric trace gases from complex sources, especially ozone and its precursors,
834 disturbing the earth's radiation budget (Sassen, 2002), or providing reactive surfaces for
835 heterogeneous reactions (Kumar et al., 2014), which leads to a great but hard problem for regional
836 air quality (Zhang et al., 2008; van Donkelaar et al., 2010). ~~BC is mostly from incomplete~~
837 ~~combustion of coal, diesel fuels, biofuels, and outdoor biomass burning (Bond et al., 2004).~~
838 ~~Although BC accounts for a relatively small portion of the total mass concentrations of aerosol~~
839 ~~particles in atmosphere, it plays a significant role in global radiation balance, both directly and~~
840 ~~indirectly. Thus, BC could influence the global and region climate changes and atmospheric~~
841 ~~environment substantially (Jacobson et al., 2002; Bond et al., 2013; Deng et al., 2010). Particulate~~
842 ~~matters (PMs) originate from both natural and anthropogenic emission sources (Kaufman et al.,~~
843 ~~2002). Due to prosperous economic development, rapid industrialization and urbanization in recent~~
844 ~~decades, haze events have frequently occurred in the Beijing Tianjin Hebei (BTH) area, Yangtze~~
845 ~~River Delta (YRD) and Pearl River Delta (PRD) regions, all of which were mainly caused by high~~
846 ~~concentrations of particulate matter. Tropospheric ozone is a typical secondary air pollutant that is~~
847 ~~related to its precursors NO_x and VOCs (Crutzen, 1973) through several complicated reactions. O₃~~
848 ~~could impact tropospheric environment (Monks et al., 2015), and make significant contributions to~~
849 ~~radiative forcing of climate (Intergovernmental Panel on Climate Change (IPCC), 2007).~~
850 ~~Tropospheric O₃ precursors and the interactions between O₃ and its precursors in different~~
851 ~~geographical locations are usually different, and thereby the characterizations of O₃ at different sites~~
852 ~~can vary greatly (Xie et al., 2016). The impact of PMs and BC on surface ozone is a topic that has~~
853 ~~attracted much attention. Jacobson (1998) reported that aerosols containing BC cores reduced~~
854 ~~photolysis rates and resulted in a decrease in ozone concentrations by 5%–8% at ground level in~~

855 ~~Los Angeles. It is also found that a strong reduction in photolysis rate (10%–30%) due to BC-~~
856 ~~containing aerosols (Castro et al., 2001) led to a decrease in surface ozone in Mexico City. Similar~~
857 ~~results have been found in other studies simulating the effects of BC on surface ozone in China (Li~~
858 ~~et al., 2011).—~~

859

860 ~~—Over the decades, China is always one of the major source regions of particles, with BC and dust~~
861 ~~emission accounting for up to 25% of the global anthropogenic sources (Streets et al., 2001; Tegen~~
862 ~~and Schepanski, 2009). Relatively high levels of particle concentrations are mainly distributed in~~
863 ~~Beijin-Tianjin-Hebei area (BTH), Yangtze River Delta (YRD), and Pearl River Delta (PRD) regions~~
864 ~~(e.g., Zhang et al., 2008, 2012; Zhang et al., 2015), along with the rapid economic development.~~
865 ~~These regions consistently have the highest emissions of anthropogenic precursors (e.g., Wang et~~
866 ~~al., 2015; Wang et al., 2009b; Ding et al., 2013b; Zheng et al., 2010), which have led to severe~~
867 ~~region-wide air pollution. Earlier studies on particles mostly focused on concentrations estimation,~~
868 ~~the chemical characteristics, potential sources, as well as climate effects based on numerical~~
869 ~~simulations (e.g., Wu et al., 2012; Song et al., 2014; Xiao et al., 2012; Yu et al., 2015; Kristjánsson,~~
870 ~~2002; Liao and Seinfeld, 2005; Zhuang et al., 2010, 2013, 2013b, 2018). However, a better~~
871 ~~understanding of spatial and temporal variations of particles can contribute to the adoption of~~
872 ~~effective measures to reduce air pollution, and real-time monitoring data is essential to better obtain~~
873 ~~the detailed variations (seasonal, monthly, and diurnal) on the city scale. In China, the research~~
874 ~~based on PMs observations, especially in the polluted regions above, have gradually expanded since~~
875 ~~2012 due to the establishment of China's PM_{2.5} air quality standards and gradual developments of~~
876 ~~nationwide PMs observation. The research is mainly related to the temporal and spatial distribution~~
877 ~~characteristics (e.g., Wang et al., 2015; Chen et al., 2016; Wu et al., 2012), and the effects of~~
878 ~~meteorological variables on aerosols (e.g., Zhang et al., 2015; Yan et al., 2016; Huang et al., 2015).~~
879 ~~In addition, many observations of BC have been made in the recent years, most of which~~
880 ~~concentrated on the analysis of the concentration level and the temporal and spatial variations (e.g.,~~
881 ~~Verma et al., 2010; Wang et al., 2011b; Zhang et al., 2012). Some also revealed the correlations of~~
882 ~~carbonaceous aerosols (Pan et al., 2011; Zhuang et al., 2014b). Besides particles, because of the lack~~

883 of nationwide O₃ monitoring data in earlier years, O₃ and its precursors (NO_x, NO_y, CO and VOCs
884 etc.) pollution situations can only be discerned from limited campaign-type measurements in certain
885 developed regions, for instance, Beijing in BTH area (Shao et al., 2006; Lin et al., 2008; Meng et al.,
886 2009), Guangzhou in PRD region (Zhang et al., 1998; Wang et al., 2003) and Lin'an in YRD region
887 (Luo et al., 2000; Cheung and Wang 2001; Wang et al. 2001a, 2002, 2004; Guo et al. 2004b). Since
888 2005, the number of photochemical studies through observation data has increased in the PRD
889 region in the south (Xue et al., 2014a), the BTH area in the north (Han, 2011), and the YRD region
890 in the east (Shi et al., 2015). However, large gaps and uncertainties remain in the knowledge of
891 characteristics of regional particles and O₃ pollution and its mitigation strategies due to the
892 complexity of main sources, interaction between different aerosols, and changing meteorology filed.
893
894 ~~Most of earlier studies on particles were focused on concentrations estimation, the chemical~~
895 ~~characteristics, potential sources, as well as climate effects of particulate matters based on numerical~~
896 ~~simulations (Wu et al., 2012; Song et al., 2014; Xiao et al., 2012; Yu et al., 2015; Kristjánsson, 2002;~~
897 ~~Liao and Seinfeld, 2005; Zhuang et al., 2010; 2013), while observation-based studies of particles~~
898 ~~were relatively limited. In addition, although a good understanding of the characteristics of O₃ have~~
899 ~~been gained in the BTH area and the PRD region (Wang et al., 2009; Zheng et al., 2010; Lin et al.,~~
900 ~~2008) due to a relatively long history of research limited in the megacities, in the YRD region, there~~
901 ~~were only very limited studies of O₃ made in urban areas in some YRD cities (Tu et al., 2007; Ding~~
902 ~~et al., 2013; Xie et al., 2016), most of which were based on studies of O₃ measurement beginning in~~
903 ~~the 1990s at Lin'an site, a rural region in the southeast YRD (Luo et al., 2000). And most of studies~~
904 ~~in YRD on particles, or particulate matter, were done in the eastern YRD, close to Shanghai, and~~
905 ~~mainly covered short periods of time. In the YRD region, the prevailing winds are from between~~
906 ~~the northeast and southeast. Therefore, western YRD region is under a downwind condition. As~~
907 ~~only few measurement studies have been conducted for western YRD (Tu et al., 2007), large~~

908 ~~knowledge gaps still exist in our understanding of the characteristics and main sources of O₃ and~~
909 ~~particles (Ding et al., 2013) in the region, let alone their interactions.~~

910
911 ~~China is always one of the major source regions of particles. Over recent decades, along with the~~
912 ~~rapid economic development and the growing demand of energy consumption, many areas in China~~
913 ~~are suffering from the elevated O₃ pollution. In the BTH area, the YRD region, and the PRD region,~~
914 ~~all of which are the economically vibrant and densely populated, high levels of ozone precursor~~
915 ~~emissions and O₃ pollution have become one of the major environment problems affecting the public~~
916 ~~(Chan and Yao, 2008; Zhang et al., 2009; Ma et al., 2012; Xie et al., 2016). Because of complex~~
917 ~~sources and chemical reactions, and relatively long atmospheric lifetimes of the pollutants in the~~
918 ~~atmosphere that favors regional and long range transport, all the pollutants are of great concern for~~
919 ~~regional air quality but are very difficult to control (Cooper et al., 2005; Zhang et al., 2008). The~~

920 YRD is located in the eastern part of the Yangtze River Plain, adjacent to the most polluted North
921 China Plain, including large cities of Shanghai, southern Jiangsu and northern Zhejiang. Taking up
922 only 2 percent of the land area in China, this region produces over 20 percent of China's Gross
923 Domestic Product (GDP). Nanjing, as the capital of Jiangsu Province, lies in the middle of YRD. It
924 covers an area over 6000 km², with more than 7.3 million residents (<http://www.njtj.gov.cn/>). Being
925 the second largest commercial center after Shanghai in YRD, even the East China, Nanjing is highly
926 urbanized and industrialized, especially the urban area. In addition, the complex monsoon and
927 synoptic weather may play an important role in air pollution transport and formation in Nanjing.
928 Therefore, the urban atmosphere in Nanjing is also heavily polluted by local emissions and long-
929 distance transport of pollutants, which affects regional climate and air quality (Huang et al., 2013;

930 Yi et al., 2015). Both particles and O₃ concentrations are found to be high in Nanjing, which affects
931 regional climate and air quality (Zhang et al., 2009; Yi et al., 2015). Therefore Thus, the issue of air
932 pollution in Nanjing deserves attentions. Previous studies using observation data in Nanjing often
933 concentrated on characteristics of one of the particles (Deng et al., 2011; Shen et al., 2014; Zhuang
934 et al., 2014b) or ozone and its precursors (Tu et al., 2007; Wang et al., 2008; An et al., 2015),
935 describing the temporal and spatial distributions, and the influence of meteorological effects, but
936 lay less emphasis on the inter-species correlations and the combined effects of pollutants during
937 severe pollution episodes. Ding et al. (2013b) described the characteristics of O₃ and PM_{2.5} with
938 near-surface observation data in rural Nanjing, but the detailed characteristics in urban Nanjing is
939 not clear enough so far.

940

941 To fill the knowledge gap, continuous online measurements of particles, trace gases, and other
942 relevant parameters were carried out at Gulou site in urban Nanjing about 80m above the ground,
943 an integrated measurement platform for the study of atmospheric environment and climate change.
944 In this study, 6-month measurement of particles, trace gases, and other related variables at this site
945 during September 2016~ February 2017 when air pollution occurred frequently is analyzed. Our
946 work gives a synthetic analysis about their characteristics. The emphasis of our objective is to
947 improve the insight in the characteristics, interactions of main pollutants, and the influence of
948 integrated meteorology variables based on the observation data at an urban site above ground, and
949 further investigate the possible underlying reasons and mechanisms. Firstly, an in-depth discussion
950 on particles variations is performed, not limited to the concentrations but taking optical properties
951 into consideration as well, to quantify the polluted level in detail. Secondly, a detailed description
952 of O₃ variations can also be found in our study, including the analysis of the main precursors as trace
953 gases (NO_x, NO_y and CO), to have a general and quantitative insight in O₃ pollution situations. Both
954 of the pollutants are analyzed considering the effects of meteorology variables including but not
955 limited to precipitation and temperature. Thirdly, analysis of inter-species correlations gives a

956 relatively thorough overview of the interactions among various species, and deduction of the
957 underlying chemical mechanisms based on the results of our study and previous studies is also
958 presented in our study. Moreover, backward trajectories analysis is conducted for improving the
959 knowledge of regional/sub-regional transport process in urban Nanjing. Finally, a case study for
960 high particles and O₃ episode is implementing to emphasize the integrated influence of
961 meteorological field on regional air pollution.

962
963 In the following, we describe the methodology in Section 2, which includes the measurement site
964 and instruments. Results and discussions are presented in Section 3, consisting of overall temporal
965 variation, correlation analysis, backward trajectory analysis, and case studies. A summary is given
966 in Section 4.

967 ~~In this study, continuous observations of particles, trace gases and certain aerosol optical properties~~
968 ~~at an urban station in Nanjing (a typical developing city in YRD) have been made in order to~~
969 ~~characterize the air pollution in the city. In the following, we describe the methodology in Section~~
970 ~~2. Results and discussions are presented in Section 3, followed by Conclusions in Section 4.~~

971 **2. Methodology**

972 **2.1 Brief Introduction to the Urban Atmospheric Observational Station**

973 The Urban Atmospheric Observational Station is a regional atmospheric urban station located on
974 the Gulou Campus of Nanjing University in the downtown area of Nanjing (32.05 °N,118.78 °E),
975 and run by School of Atmospheric Sciences, Nanjing University. It is built on the roof of a 79.3m
976 tall building, without any industrial pollution sources within a 30 km radius around but several main
977 roads with evident traffic pollution, especially during rush hours. The sketch map of the site (not
978 shown) and the corresponding climatology have been described in Zhu et al (2012).

979
980 The Particles, O₃, NO_x, NO_y (including most oxides of nitrogen mentioned above with the exception
981 of NH₃ and N₂O), CO, and wavelength-dependent aerosol optical parameters including aerosol
982 aerosol scattering (σ_{ts}), back-scattering (σ_{bs}), and absorption (σ_a) coefficients scattering (SC);
983 ~~back scattering (Bsp), and absorption (AAC) coefficients~~ have been routinely measured at the
984 station during the time period from 1 Sep 2016 to 28 Feb 2017. The σ_a AAC and concentrations
985 of BC were derived from the measurements using a seven-channel Aethalometer (model AE-31,
986 Magee Scientific, USA). The detailed calculation will be discussed below. The AE-31 model
987 measures light attenuation (ATN) at seven wavelengths, including 370, 470, 520, 590, 660, 880 and
988 950 nm. The sample air is taken through a stainless-steel tube into the instruments, with a desired
989 flow rate of 5.0 L min⁻¹ and a sampling interval of 5 min during the whole period. The aerosol σ_{ts}
990 ~~SC~~ and σ_{bs} Bsp were measured with a three-wavelength-integrating Nephelometer (Aurora 3000,
991 Australia). Aurora 3000 measures aerosol light scattering, including σ_{ts} and σ_{bs} at 450, 525 and
992 635 nm, with a sampling interval of 1 min (Zhuang et al. 2017). The sample air was taken through
993 a 2m stainless-steel tube with a sampling interval of 1 min, top of which is 1.5m above the roof. The
994 inlet has a rain cap and an external as well as an internal heater to prevent condensation. In cold
995 seasons when RH in the tube was relatively low, maximum of which was lower than 75% and most
996 of which was lower than 50% during sunny hours, therefore the internal heater was turned off.The
997 ~~AE-31 model measures light attenuation at seven wavelengths, including 370, 470, 520, 590, 660,~~
998 ~~880 and 950 nm, with a desired flow rate of 5.0 L min⁻¹ and a sampling interval of 5 min. Aurora~~
999 ~~3000 measures aerosol light scattering, including SC and Bsp at 450, 525 and 635 nm, with a~~
1000 ~~sampling interval of 1 min (Zhuang et al. 2017); PM_{2.5} and PM₁₀ mass concentrations were measured~~

1001 using a mass analyzer (Thermo Instruments, THOM 1405-DF), which has been used to measure the
1002 mass concentration of PM_{2.5}, PM_{2.5-10}, and PM₁₀ simultaneously. The hourly and daily mean mass
1003 concentrations are updated every 6 minutes, as well as the hourly base and reference mass
1004 concentrations. The sample air is taken through a stainless-steel tube into the instruments. Trace
1005 gases (CO, NO_x, NO_y and O₃) were measured every minute using online analyzers (Thermo
1006 Instruments, TEI 48i, 42i, 42iY, and 49i, respectively). Sample air was drawn from the 1.5m above
1007 the rooftop to the laboratory through a manifold connected to O₃, NO_x and CO analyzers with PFA
1008 Teflon tubes, while a separate sample line with a MoO converter was used for NO_y analyzer (Wang
1009 et al., 2002; Ding et al., 2013b) to convert other reactive nitrogen species including PAN, NO₃⁻ and
1010 HNO₃. Thus, the measured quantity approximates total reactive nitrogen. Precision and instrument
1011 of the measurements in this study are listed in Table 1.

1012
1013 Since aerosols are quite hygroscopic in China (e.g., Eichler et al., 2008; Liu et al., 2011; Ding et al.,
1014 2013b). All the instruments are installed in a laboratory with a constant temperature (24°C) and a
1015 low RH located on the building roof. Routine calibrations and maintenances were carried out for all
1016 these instruments during the sampling periods.

1017
1018 Monthly averaged meteorological parameters during the period from Sep.2016 to Feb.2017 at the
1019 station are shown in Table 2. The air temperature at the site ranged from 6.64°C in Feb.2017 to
1020 24.88°C in Sep.2016. Both higher relative humidity (RH) and more precipitation occurred in fall
1021 than winter, especially in October. The relative humidity (RH) was higher in fall than in winter,
1022 especially in October, while the precipitation was heavier in fall than in winter. Visibility (Vis)

varied in different months. The peak of the ultraviolet radiation (UV) occurred in Sep.2016, after which the radiation became weak till the end of Jan.2017, and rose a little afterwards in Feb.2017.

2.2 Calculation of the aerosol optical properties

The wavelength-dependent σ_a AAC, which is associated with the intensities of the incoming light and remaining light after passing through a medium, can be calculated directly using the measured light attenuations (ATN) through a quartz filter matrix, a percentage to represent the filter attenuation, as well as BC mass concentrations (Petzold et al., 1997; Weingartner et al., 2003; Arnott et al., 2005; Schmid et al., 2006):

$$\sigma_{a, ATN, t}(\lambda) = \frac{(ATN_t(\lambda) - ATN_{t-1}(\lambda))}{\Delta t} \times \frac{A}{V}, \quad (1)$$

where A (in m^2) is the area of the aerosol-laden filter spot, V is the volumetric sampling flow rate (in $L \text{ min}^{-1}$) and Δt is the time interval (=5 min) between t and $t-1$. $\sigma_{a, ATN}$, known as σ_a AAC without any correction, is larger than the actual aerosol absorption coefficient $\sigma_{a, \text{abs}}$ in general. The key factors leading to the bias are as follows: (1). multiple-scattering of light at the filter fibers (multiple-scattering effect), and (2) the instrumental response with increased particle loading on the filter (shadowing effect). The former results in the overestimation of the σ , while the later causes underestimation of the σ_a . Thus, the correction is needed and the calibration factors C and R (shown in Eq. 2) are introduced against the scattering effect and shadowing effect, respectively:

1043
$$\sigma_{\text{abs}, t(\lambda)} = \frac{\sigma_{\text{ATN}, t(\lambda)}}{C \times R}, \sigma_{a, \text{abs}, t(\lambda)} = \frac{\sigma_{a, \text{ATN}, t(\lambda)}}{C \times R} \quad (2)$$

1044
$$R_t(\lambda) = \left(\frac{1}{f} - 1\right) \times \frac{\ln(\text{ATN}_t(\lambda)) - \ln 10}{\ln 50 - \ln 10} + 1, \quad (3) \quad (2)$$

1045 Previous investigation suggested that wavelength-dependent σ_a corrected by Schmid (Schmid et
 1046 al., 2006, SC2006 for short, hereinafter) might be the closest to the real ones in Nanjing (Collaud
 1047 Coen et al., 2010; Zhuang et al., 2015). Therefore, the SC2006 is adopted in this study. In this study,
 1048 the parameters in the correction procedure are derived from local optical properties (ω_0 and α_{ts}
 1049 were set to 0.922 and 1.51, respectively). The values of correction factors C and R are as follows:
 1050 $R=1$ when $\text{ATN} \leq 10$ and $f=1.2$, and C in Nanjing is 2.95, 3.37, 3.56, 3.79, 3.99, 4.51 and 4.64 at 370,
 1051 470, 520, 590, 660, 880 and 950 nm (Zhuang et al., 2015).

1052 ~~Weingartner (Weingartner et al., 2003, WC2003 for short, hereinafter), Arnott (Arnott et al., 2005),~~
 1053 ~~Schmid (Schmid et al., 2006, SC2006 for short, hereinafte), and Virkkula (Virkkula et al., 2007)~~
 1054 ~~corrections, have been developed to eliminate the uncertainties. Zhuang et al. (2015) further~~
 1055 ~~suggested that wavelength dependent AACs corrected by SC2006 might be closer to the real ones~~
 1056 ~~than WC2003s in Nanjing, although 532 nm AACs from these two corrections are close to each~~
 1057 ~~other.~~

1058 ~~Therefore, AACs corrected from SC2006 are used in this study.~~

1059
 1060 Measurement of Aurora 3000, a nephelometer with newly designed light sources based on light
 1061 emitting diodes, needs correction using Mie-theory for measurement artifacts. In this study,
 1062 correction was performed according to Müller et al. (2011). The raw total scattering coefficients
 1063 were corrected first by calculating first the Ångström exponents from the non-corrected scattering

1064 coefficients and then following the formulas presented by Müller et al. (2011) where the tabulated
 1065 factors for no cutoff at the inlet were used, and the raw backward scattering coefficients were
 1066 corrected according to the correction factors for no cutoff. And based on corrected wavelength-
 1067 dependent σ_a and σ_{ts} , α_{ts} and α_a at 550 nm are estimated by the following:

$$1068 \quad \alpha_{a,470/660nm} = -\log(\sigma_{a,470nm} / \sigma_{a,660nm}) / \log(470/660), \quad (4)$$

$$1069 \quad \alpha_{ts,450/635nm} = -\log(\sigma_{ts,450nm} / \sigma_{ts,635nm}) / \log(450/635), \quad (5)$$

1070
 1071 Meanwhile, aerosol asymmetry parameter (g), single-scattering albedo (ω_0) and extinction
 1072 coefficient (σ_e) are further estimated:

$$1073 \quad \omega_0 = \frac{\sigma_{ts}}{\sigma_{ts} + \sigma_a}, \quad (6)$$

$$1074 \quad \sigma_e = \sigma_{ts} + \sigma_a, \quad (7)$$

1075
 1076 Measurement of Aurora 3000, a nephelometer with newly designed light sources based on light
 1077 emitting diodes, needs correction using Mie theory for measurement artefacts. Müller et al. (2011)
 1078 provided parameterizations for the angular sensitivity functions of Aurora 3000, which follows the
 1079 definition of correction factors from Anderson and Ogren (1998), where the ratios of true to
 1080 measured nephelometer values for both total scattering and backscattering are defined by:-

$$1081 \quad C_{ts,\lambda} = \frac{\sigma_{ts,\lambda}^{true} \sigma_{tsR,\lambda}^{neph}}{\sigma_{ts,\lambda}^{neph} \sigma_{tsR,\lambda}^{true}}, \quad (4)$$

1082 **and**

$$1083 \quad C_{bs,\lambda} = \frac{\sigma_{bs,\lambda}^{true} \sigma_{bsR,\lambda}^{neph}}{\sigma_{bs,\lambda}^{neph} \sigma_{bsR,\lambda}^{true}}, \quad (5)$$

1084 where σ_{ts}^{true} and σ_{bs}^{true} are true total scattering coefficient and backscattering coefficient for ideal

1085 angular sensitivity functions, respectively, $\sigma_{tsR,\lambda}$ and $\sigma_{bsR,\lambda}$ are Rayleigh total scattering
1086 coefficient and backscattering coefficient, respectively, and σ_{ts}^{neph} and σ_{bs}^{neph} are nephelometer
1087 total scattering coefficient and backscattering coefficient, respectively. In this study, we assume that
1088 Rayleigh scattering is equivalent to true scattering.

1089
1090 The correction factors can be calculated using measured size distributions or SAE. Anderson and
1091 Ogren (1998), hereinafter denoted as AO98, found a dependency between the SAE and the
1092 correction factor for total scattering. The correction was given by:

$$1093 \quad C_{ts} = a + b \cdot \alpha_{ts}^* \quad (6)$$

1094 where α_{ts}^* is the scattering Ångström exponent derived from uncorrected nephelometer scattering.
1095 According to Müller et al. (2011), for backscattering, there was no correlation between correction
1096 factors and scattering Ångström exponents, which is in agreement with AO98. The parameters a
1097 and b were derived from Mie-calculated true scattering and simulated nephelometer scattering for
1098 ranges of particle sizes and refractive indices.

1099
1100 In this study, we used the correction factors for Aurora 3000 without a sub- μm cut in Müller et al.
1101 (2011), which are shown in the Table 3. According to nephelometer correction factors for angular
1102 nonidealities, which are shown in Table 3(a), original scattering coefficient (SC at 635 nm, 525 nm
1103 and 450 nm) and backscattering coefficient (Bsp at 635 nm, 525 nm and 450 nm) obtained from
1104 the measurements are corrected based on Eqs (4) and Eqs (5). We also calculated correction factors
1105 for total scatter as function of Ångström exponent shown in Table 3.(b), original scattering
1106 coefficient (SC at 635 nm, 525 nm and 450 nm) are corrected based on Eqs (6).

1107

1108 Based on corrected wavelength-dependent AAC and SC, SAE and AAE are estimated by the
1109 following:

1110 ~~$AAE_{470/660nm} = \log(AAC_{470nm} / AAC_{660nm}) / \log(470 / 660),$~~ (7)

1111 ~~$SAE_{450/635nm} = \log(SC_{450nm} / SC_{635nm}) / \log(450 / 635),$~~ (8)

1112 ~~$\sigma_{\lambda} = \sigma_{\lambda_0} \times \left(\frac{\lambda}{\lambda_0}\right)^{-\alpha},$~~ (9)

1113 where σ_{λ} is the coefficient at wavelength λ and α is the corresponding Ångström exponents.

1114

1115 On the basis of Eqs (7)–Eqs (9), SC and Bsp at 550 nm were calculated for comparison. Between
1116 the two ways of corrections, the results of the total scattering coefficients are in agreement with
1117 each other in general, with differences of 10.67%. In this study, we choose the results from the
1118 correction using SAE.

1119 Meanwhile, based on wavelength-dependent SC, Bsp, AAC, aerosol asymmetry parameter (ASP),
1120 single scattering albedo (SSA) and extinction coefficient (EC) are further estimated:

1121 ~~$ASP_{\lambda} = -7.143889\beta_{\lambda}^3 + 7.464443\beta_{\lambda}^2 - 3.9356\beta_{\lambda} + 0.9893,$~~ (10)

1122 ~~$SSA_{\lambda} = \frac{SC_{\lambda}}{SC_{\lambda} + AAC_{\lambda}},$~~ (11)

1123 ~~$EC_{\lambda} = SC_{\lambda} + AAC_{\lambda},$~~ (12)

1124 where is β_{λ} the ratio of Bsp to SC at wavelength λ . Equation (10) is derived from Andrews et al.
1125 (2006).

1126 Table 4 shows the statistical summary of the surface aerosol optical properties in Nanjing after the
1127 correction. The mean value during the cold seasons in 2016 of AAC, SC, Bsp, EC, SSA and ASP
1128 at 550 nm, AAE at 470/660 nm and SAE at 450/635 nm are 23.741, 349.502, 35.469, 373.536 Mm⁻¹

1129 ~~±, 0.929, 0.645, 1.600, and 1.192, with a standard deviation of 15.556, 235.291, 21.488, 247.877~~

1130 ~~Mm⁻¹, 0.028, 0.052, 0.175, and 0.288, respectively.~~

1131

1132 **2.3 HYSPLIT model**

1133 In order to understand the general transport characteristics of air masses recorded at this station, we

1134 conducted a 4 d (96 h) backward trajectory simulations during the cold seasons in 2016 using a

1135 Lagrangian dispersion model Hybrid Single-Particle Lagrangian Integrated Trajectory (HYSPLIT)

1136 (version 4.9) provided by the Air Resource Laboratory (ARL) of the USA National Oceanic and

1137 Atmospheric Administration (NOAA) (Draxler and Hess, 1998). HYSPLIT - 4 Model is capable of

1138 processing multiple gas input fields, multiple physical processes and different types of pollutant

1139 emission sources and has been widely used in the study of transport and diffusion of various

1140 pollutants in various regions (Mcgowan and Clark, 2008; Wang et al., 2011; Wang et al., 2015). It

1141 is one of the most extensively used atmospheric transport and dispersion models for the study of air

1142 parcel trajectories (Draxler and Rolph, 2013; Stein et al., 2016). In this study, backward trajectories

1143 were calculated and clustered using a stand-alone version of the GDAS (Ground Data Acquisition

1144 System) meteorological field (ftp://arlftp.arlhq.noaa.gov/pub/archives/gdas1)~~the NCEP / NCAR~~

1145 ~~reanalyzed meteorological field (http://ready.arl.noaa.gov/archives.php).~~ The NCEP-GDAS data

1146 contains 6-hourly basic meteorological fields on pressure surfaces, with the spatial resolution of

1147 2.51.0°, corresponding to the 00, 06, 12, 18 UTC, respectively. In this study, the data are also

1148 converted to hemispheric 144 by 73 polar stereographic grids, which is the same grid configuration

1149 as the dataset applied in synoptic weather classification. For each synoptic weather pattern, the

backward trajectories were started at Gulou station in Nanjing (32°N, 118.8°E).

3. Results and discussion

3.1 Characteristics of particulate matter in Nanjing

The hourly-mean concentrations of particles at Gulou site during the cold seasons in 2016 are shown in Fig 1. Gaps in the time series are missing values.

Observations show that peaks and valleys of BC, PM_{2.5} and PM₁₀ occur simultaneously in general (Fig 1a), probably because the three particles originate mostly from the same sources, i.e., fossil fuel burning and traffic activities. It has also been addressed in previous work (e.g., Wang et al., 2008; Chow et al., 2011; Schleicher et al., 2013; Zhuang et al., 2014b; Gong et al., 2015).

~~The averaged values of BC, PM_{2.5} and PM₁₀ during the study period are 2.6 ± 1.7 , 58.2 ± 36.8 , and 86.3 ± 50.8 $\mu\text{g}/\text{m}^3$, respectively. The average of particulate matter concentrations during the study period are higher than standard concentrations, which are 35 $\mu\text{g}/\text{m}^3$ for fine and 70 $\mu\text{g}/\text{m}^3$ for PM₁₀. Particles, including BC, PM_{2.5} and PM₁₀ fluctuate similarly, because the three particles originate mostly from the same sources, i.e., transport emissions. BC loadings at Gulou were low in September and October, usually below 6 $\mu\text{g}/\text{m}^3$, while the loadings were high in the other months, such as in mid-November, early and late December, early January, and mid-to-late February, suggesting occurrences of BC pollution events during these periods. PM_{2.5} loadings and PM₁₀ loadings were generally below 120 and 200 $\mu\text{g}/\text{m}^3$, respectively, but higher during early October and in the periods when BC loadings were high. The particle concentrations are affected by various factors and progress. For example, the high loadings of particulate matter in early October was mainly due to the increase in aerosols concentrations with high scatter coefficient (SC), and thus the~~

1171 ~~BC loadings did not show such peak during early October.~~

1172

1173 BC concentration ranged from 0.064 to 15.609 $\mu\text{g}/\text{m}^3$. Seasonal mean of BC concentration was

1174 2.126 $\mu\text{g}/\text{m}^3$ in SON and 3.083 $\mu\text{g}/\text{m}^3$ in DJF, with a standard deviation of 1.457 and 1.827 $\mu\text{g}/\text{m}^3$,

1175 respectively. It was low in September and October, usually below 6 $\mu\text{g}/\text{m}^3$, but higher in other

1176 months. Although BC concentration was relatively low, it was extremely high in particular periods,,

1177 such as in mid-November, early and late December, early January, and mid-to-late February,

1178 suggesting occurrences of substantial BC pollution events. $\text{PM}_{2.5}$ and PM_{10} concentration ranged

1179 from 0.8 to 256.4 $\mu\text{g}/\text{m}^3$ and from 1.1 to 343.4 $\mu\text{g}/\text{m}^3$, respectively. Seasonal mean of $\text{PM}_{2.5}$

1180 concentration was 43.1 $\mu\text{g}/\text{m}^3$ in SON and 73.2 $\mu\text{g}/\text{m}^3$ in DJF, with a standard deviation of 25.4 and

1181 40.0 $\mu\text{g}/\text{m}^3$, respectively. PM_{10} averaged 67.6 $\mu\text{g}/\text{m}^3$ in SON and 105.0 $\mu\text{g}/\text{m}^3$ in DJF, with a standard

1182 deviation of 39.1 and 54.0 $\mu\text{g}/\text{m}^3$, respectively. $\text{PM}_{2.5}$ and PM_{10} concentration were generally below

1183 120 and 200 $\mu\text{g}/\text{m}^3$, respectively. Remarkable increases existed especially when BC concentration

1184 was high. Additionally, the high concentrations of PMs in early October possibly resulted from the

1185 increase in scattering aerosols, since absorption coefficient and BC, one of typical absorbing

1186 aerosols, did not show such peak, while scatter coefficient experienced a sharp increase during that

1187 period. It is found that both BC and PMs levels in Nanjing became lower compared to those in

1188 earlier years, which is possibly due to the strengthening energy conservation and reduction of

1189 pollution emissions from 2014. For instance, seasonal average in SON and DJF were reported 4339

1190 and 4189 ng/m^3 in urban Nanjing during 2012 in Zhuang et al. (2014b), and Ding et al. (2013b)

1191 stated a 1-year average about 75 $\mu\text{g}/\text{m}^3$ of $\text{PM}_{2.5}$ in rural area of Nanjing from August 2011 to July

1192 2012, while Wang et al. (2014) suggested that annual average of $\text{PM}_{2.5}$ and PM_{10} were 75 and 135

1193 µg/m³ in Nanjing during 2013, respectively.

1194

1195 Monthly variations of particles in the cold seasons in 2016 were obvious (Fig.2). The concentrations

1196 increased from October to December and decreased a little afterwards but remained relatively high

1197 in January and February. High particle concentrations were observed from November to February

1198 while the low ones were in September and October. The lowestsmallest monthly concentrations of

1199 BC, PM_{2.5}, and PM₁₀ occurred in October, being 1.8, 39.2, and 59.8 µg/m³, respectively, while the

1200 largest monthly concentrations occurred in December, being 3.7, 85.0, and 123.1 µg/m³,

1201 respectively, which were about twice of those in October. Monthly variations of BC were different

1202 from those in previous studies in YRD. For instance, Pan et al. (2011) pointed out an extremely high

1203 concentration in October in Mt. Huang, which was attributed to combustion of biomasses as well as

1204 the dynamic transport and stable planetary boundary layer (PBL) stratification in the transitional

1205 periods of the winter monsoon (October). For PMs, monthly behavior was basically similar to what

1206 has been reported in previous studies in YRD, increasing from September to December in general

1207 (Chen et al., 2016), except the decrease in October. In generalGenerally, there are two key factors

1208 that could impact particle concentrations: meteorology and emissions. Heavy precipitation with a

1209 strong scavenging effect in October when average rainfall was 3.1 mm, and the frequency of daily

1210 rainfall exceeding 50mm was over 30% might directly lead to small loadings of particles (Table.2),

1211 had a strong scavenging effect, which might directly lead to low levels of particles despite the

1212 influence of biomass burning addressed in Pan et al. (2011). Anthropogenic particle emissions from

1213 fossil fuel over China increased after summer and showed a sharp increase from November to

1214 January (Zhang et al., 2009), and emission rates in southwest (Sichuan basin), central to north, and

1215 northeast China, as well as YRD and PRD were higher in winter (Zhuang et al., 2018), especially
1216 in residential, industry and power emissions (Li et al., 2017)which may explain the high partiele
1217 concentrations during those periods. And during the autumn harvest (September~ November),
1218 though not so much as that in summer, the crop burning emissions in still make contribution to
1219 pollutants (Yang et al., 2008). Yin et al. (2016) discussed the spatial distribution of crop residue
1220 burning from September to December in 2015, suggesting autumn crop residue burning in
1221 surrounding regions like Shandong, Anhui and Henan Provinces, thus, particles in Nanjing might
1222 also be subject to these large-scale burning of crop residues (Qian et al., 2014). According to Huang
1223 et al. (2012) and Li et al. (2016), spatiotemporal distribution of agricultural fire occurrences in China
1224 during 2003~ 2010 as well as 2012 has been presented associated with the spatial distribution of
1225 CO emission from residue open burning. Both of them suggested the crop residue burning in autumn
1226 is noteworthy and Jiangsu as well as the surrounding provinces are the regions with highest
1227 emissions. Besides, sub-regional transport also plays an important role, for example, in winter, air
1228 masses coming from North China Plain, which accounts for 31%, have high particles concentrations
1229 (Sect 3.4).

1230 ~~Qian et.al (2014) believed that high particle loadings in Nanjing from late October to early~~
1231 ~~November resulted from the large-scale burning of crop residues. However, PM_{2.5} and PM₁₀~~
1232 ~~concentrations reached a relative maximal in early October, while the emission in October is relative~~
1233 ~~low compared to the following months (Zhang et al., 2009).~~

1234

1235 Substantial diurnal cycles of the particles are also observed (Fig.3). Particles levels were high during
1236 7:00~9:00 and 22:00~0:00 LT but low in afternoon (13:00~15:00 LT).BC levels were high at rush

1237 hours (7~9 am and 8~11 pm) but low in afternoon (1~3 pm). High concentrations during 7:00~9:00
1238 LT Zhuang et al. (2014) mentioned that high BC concentrations in these times of the day might be
1239 caused by the vehicle emissions (as mentioned in Section 2, several main roads with apparent traffic
1240 pollution surround the station). A higher vehicle volume showed during 17:00~ 20:00 LT in Nanjing,
1241 while the high concentrations occurred during 22:00~ 0:00 LT. A lower temperature and a more
1242 stable atmosphere stratification after sunset (17:00~18:00 LT) often lead to frequent temperature
1243 inversion and low height of planetary boundary layer (Jiang et al., 2014), which is not conducive
1244 to the diffusion of pollutants, and the concentrations of particles accumulate and remain high from
1245 the evening to early morning. In addition, temperature was low after midnight, and the atmosphere
1246 stratification was stable. Therefore, it was easy for temperature inversion to appear, which was not
1247 conductive to the diffusion of pollutants, and the concentrations of particles accumulated and
1248 reached a peak at around 8 am. Atmosphere stratification became stable again as the temperature
1249 decreased after around 4 pm, which may also explain the peak during 9~11 pm (Qian et al., 2014).
1250 For low levels in afternoon, it is mainly induced by well-developed boundary layer. Because the
1251 atmosphere become less stable with the increasing temperature, and strong turbulent exchange as
1252 well as vertical diffusion are favorable to the diffusion of pollutants, particles concentrations
1253 decrease to a minimum in the afternoon. As to the low BC in afternoon, which occurred at around
1254 3 pm, it was mainly induced by well-developed boundary layer. Because the atmosphere became
1255 less stable with increasing temperature, and strong turbulent exchange and vertical diffusion were
1256 favorable to the diffusion of pollutants, BC concentrations decreased to a minimum in the afternoon.
1257 Similar phenomenon of PMs has been observed in previous studies in Nanjing (Chen et al., 2016;
1258 Ding et al., 2013b), while a different pattern is discussed in Pan et al. (2011) in Mt. Huang, a rural

1259 site in YRD, due to different emission sources (less vehicle emission) and meteorology effects
1260 (effect of valley breezing). Fig. 3 also shows that the peak values of fine particle concentrations
1261 often occurred ~~one or two hours~~ 1~ 2 h later than those of BC concentrations, with high values at
1262 around 10 ~~am:00~~ and low values at around 5 ~~pm~~ 17:00 LT. According to Roberts and Friedlander
1263 (1976) and Khoder (2002), atmospheric photochemical reactions are extremely active under
1264 conditions of strong radiation and high temperature, especially during daytime, thus, during which
1265 ~~more secondary aerosol particles (like sulfate particles) generated, so more secondary aerosol~~
1266 particles (like sulfate particles) are likely to generate, and the concentrations of fine particles in the
1267 atmosphere will increase. ~~When solar radiation was strong, ultra-fine particles generated during~~
1268 ~~photochemical reactions contributed greatly to the concentrations of aerosol particles.~~

1269 ~~Generally, the diurnal cycles of BC had a bimodal distribution with two peaks, while PM_{2.5} and~~
1270 ~~PM₁₀ had only one peak. However, both magnitude and temporal variations of particles were~~
1271 ~~changed in winter, and there is another peak at around 2 am (see S1), which was possibly due to~~
1272 ~~the affection of BC pollution episodes at night.~~

1274 **3.2 Characteristics of gaseous pollutants in Nanjing**

1275 Fig.4 shows hourly-mean concentrations of gaseous pollutants at Gulou during the cold seasons in
1276 2016, ~~in which, there were few gaps for invalid values.~~ In general, as main precursors of O₃, NO_x,
1277 NO_y, and CO generally show different pattern with O₃, such as when the precursors levels remained
1278 high from November to January, O₃ levels were relatively low (Xie et al., 2016; Wang et al., 2017).
1279 Also, the precursors concentrations varied greatly, especially in DJF (with several peaks), possibly

1280 because of the frequent shifting of air masses from the clean interior continent and heavily polluted
1281 urban plumes in the heating period (normally from November to March in Northern China) (Pan et
1282 al., 2011).

1283 Concentrations of trace gases, including CO (176~ 2852 ppb), NO_x (2.7~ 80.0 ppb), NO_y (3.6~
1284 158.4 ppb), and O₃ (0.2~ 235.7 ppb), varied a lot in the study period. Seasonal mean of O₃ was 42.3
1285 ppb in SON and 33.1 ppb in DJF, with a standard deviation of 40.1 and 24.4 ppb, respectively. The
1286 averaged concentrations during the fall and winter of CO, O₃, NO_x and NO_y at the site are 851 ±
1287 384, 37.7 ± 33.5, 23.5 ± 14.7, and 32.8 ± 22.3 ppb, respectively. As shown in Fig.4, O₃
1288 concentrations in the site were was extremely high during the entire-whole September in 2016, with
1289 a maximum over 200 ppb, and decreased sharply after mid-October, basically keeping a low level
1290 below 100 ppb, until early February when it began to increase, which was mainly due to the strong
1291 solar radiation and the high temperature lasting in September. O₃ concentrations began to increase
1292 in February because of enhanced solar radiation, after a low concentration period since late October,
1293 during which O₃ concentrations were below 100 ppb. Seasonal averages of NO_x and NO_y were 21.4
1294 and 28.6ppb in SON, with a deviation of 20.5, and 40.1 ppb, respectively. In DJF, mean
1295 concentrations of NO_x and NO_y were 27.6 and 37.0 ppb, with a deviation of 15.5 and 23.1 ppb. And
1296 seasonal averages of CO were 753 ppb in SON, and 950 ppb in DJF, with a deviation of 353 and
1297 388 ppb, respectively. The precursors concentrations were high from November to mid-January,
1298 and low in September. NO_x and NO_y have a similar pattern: the concentrations were high in
1299 November, December and February (Fig.5). Moreover, it is suggested that O₃ concentration is
1300 higher compared to the results in previous studies in Nanjing (Xie et al., 2016; An et al., 2015; Ding
1301 et al., 2013b), implying a more pressing environmental issue of near-surface O₃ problem in urban

1302
1303
1304
1305
1306
1307
1308
1309
1310
1311
1312
1313
1314
1315
1316
1317
1318
1319
1320
1321
1322
1323

area.

It is noticeable that the daily variation of CO concentrations was similar to that of BC. A remarkable correlation between BC and CO is found in a number of studies (Jennings et al., 1996; Derwent et al., 2001; Badarinath et al., 2007; Spackman et al., 2008), suggesting that both of the pollutants are greatly affected by anthropogenic sources and biomass burning in eastern China.

Monthly variations of trace gases are shown in Fig.5. Fig.5 illustrates monthly variations of O₃, nitrogen oxides (NO_y and NO_x), and CO in the cold seasons in 2016. It is noticeable that the different patterns occur in O₃ and its precursors. Observations show that O₃ concentration decreased after the lasting extremely high level in September until November and increased a little afterwards. Highest concentration of O₃ was found in September and lowest in November, being 74.8 and 23.4 ppb, respectively. This pattern might be attributed to the solar radiation and emissions. For instance, in September when solar radiation was strong (maximum UV over 55 W/m²), it would contribute greatly to O₃ formation, and precursors were at relatively high levels (CO, NO_x, and NO_y were about 600, 15 and 20 ppb, respectively), though not as high as those in cold days. CO, NO_x and NO_y peaked in December correspondingly at 1064, 31.8 and 41.7 ppb. The precursors reached the lowest level in September, being 620, 14.5, and 20.8 ppb, respectively. In addition, the pattern of precursors is analogous to those in previous studies (Xie et al., 2016; Ding et al., 2013b), but with a relatively lower concentration, especially NO_x and NO_y, which might also result from the large-scale reduction of pollution emissions.

O₃ peaked in September at 74.8 ppb while NO_y and NO_x peaked in December at 31.8 and 41.7 ppb, respectively. O₃ reached minimum at 23.4 ppb in November and NO_y and NO_x were lowest in

1324 September, being 14.5, and 20.8 ppb, respectively. O₃ is a secondary pollutant and complicatedly
1325 related to its precursors, including NO_x and VOCs. O₃ precursors and their effects on O₃ formation
1326 are different at different geographical locations, and thus the characterizations of O₃ at different
1327 sites can vary greatly. O₃-NO_x-VOCs relationships can be described by the following reactions:



1335 where (R4), (R5), and (R2) reactions establish an “NO_x-cycle” that could produce O₃ without
1336 consumption of NO_x, the other important chemistry cycle is the so-called “RO_x (RO_x=OH+HO₂+
1337 RO₂) radical cycle” that could continuously supply HO₂ and RO₂ to oxidize NO to NO₂, and (R7)
1338 is usually referred as NO_x titration, which is an important O₃ removal process related to freshly
1339 emitted NO. In general, when NO_x concentrations were high, O₃ concentrations may experience a
1340 depression process since excessive NO are not favorable for the O₃ production (Xie et al., 2016;
1341 Wang et al., 2018). The CO concentrations varied greatly in winter because of the frequent shifting
1342 of air masses from the clean interior continent and heavily polluted urban plumes in the heating
1343 period (normally from November to March in Northern China, (Pan et al., 2011). In September and
1344 October, the CO concentrations at Gulou apparently decreased owing to frequent intrusions of clean
1345 air mass from the Pacific Ocean, and this seasonal trend was confirmed by HYSPLIT-4 model (see

1346 ~~detailed discussion in Section.4).~~

1347

1348 Fig. 6 (a) shows the ~~mean~~ diurnal variations of the gaseous pollutants (O₃, NO_x, NO_y, and CO) ~~at~~

1349 ~~Gulou during the cold seasons in 2016.~~ The concentrations of O₃ ~~were~~ is the lowest around 7:00

1350 LT ~~am~~ and rises rapidly until reaching the peak in the middle of the day at 15:00 LT. ~~went up~~

1351 ~~rapidly corresponding with the increase of solar radiation. After reaching the peak in the middle of~~

1352 ~~the day at 3 pm, It keeps decreasing sharply after the afternoon peak till sunset. During the nighttime,~~

1353 the concentration of O₃ decreases slowly and remains low. ~~the O₃ concentrations kept decreasing~~

1354 ~~rapidly until sunset. During the nighttime, the concentrations of O₃ decreased slowly and maintained~~

1355 ~~low values, attributed to the process of NO_x titration and the lack of solar radiation.~~ With respect to

1356 NO_x and NO_y, peak appears at around 9:00 LT, with another high value occurring at night (21:00~

1357 0:00 LT), both of which coincide with the rush hours in the city, when two peaks appeared in the

1358 ~~diurnal cycles, one around 9 am and the other at 8 pm. Both peaks coincided with the rush hours in~~

1359 ~~the city, during which~~ large amounts of vehicle emissions ~~were~~ are released. The morning peak

1360 is slightly higher than the ~~evening-night~~ one in general. ~~Besides emissions, According to Xie~~

1361 ~~et al. (2016),~~ these diurnal variation patterns of O₃ and NO_x ~~are~~ mainly resulted from the

1362 photochemical processes and the meteorological conditions. Simultaneous measurement of O₃ and

1363 UV shows that the O₃ concentration is highly correlated to UV (R=0.71, Fig. 9(a)). The ultraviolet

1364 irradiance (UV) at Gulou ~~start~~ sed to increase at about 7-am:00 LT (Fig.6 (b)), which could induce a

1365 series of photochemical reactions including the formation of peroxy radicals (HO₂ and RO₂ etc.)

1366 and the photolysis of NO₂. From 8-am:00 to 3-pm15:00 LT, the increase in UV ~~enhanced~~ enhances

1367 the O₃ formation by promoting the production processes of NO₂ and OH from NO and peroxy

1368 radicals(R4)–(R5). Simultaneous measurement of O₃ and UV shows that the O₃ concentrations are
1369 highly correlated to UV, with a correlation coefficient of 0.47. The diurnal range of O₃ concentration
1370 (the difference between the maximum at 15:00 LT and the minimum at 7:00 LT) is relatively high
1371 (45.1 ppb), suggesting the active chemical reactions as well. It is also noticeable that ~~the~~ O₃ peaks
1372 ~~maximum was~~ 2 h after the UV maximum, suggesting the time to take for the chemical reactions.
1373 The slightly reduction of O₃ and NO_x after the midnight in the early morning (3:00~7:00 LT) is likely
1374 due to ~~of~~ NO_x titration. The development of the planetary boundary layer (PBL) can also modulate
1375 pollutant concentrations. The concentrations of a pollutant ~~are~~ is diluted when PBL rises during the
1376 daytime and enhanced in the low nocturnal PBL that favors pollutant accumulation, after comparing
1377 Fig.6 (a) with the reported diurnal variation of PBL height in Nanjing (Jiang et al., 2014; Xie et al.,
1378 2016). And that is also the reason for the difference of peak time between the emission rate and NO_x
1379 (NO_y) concentration, which is similar to particles to some degree. The abovementioned diurnal
1380 cycles in O₃ and NO_x (NO_y) concentrations follow the typical patterns at other sites in Nanjing (Tu
1381 et al., 2007; Ding et al., 2013b; Xie et al, 2016). The daily variation of CO concentration is found
1382 to be similar to that of BC, such as morning peak during rush hours, afternoon dip at around 15:00
1383 LT, and accumulation at night. A remarkable correlation has been found in a number of previous
1384 studies (e.g., Jennings et al., 1996; Derwent et al., 2001; Badarinath et al., 2007; Spackman et al.,
1385 2008; Pan et al., 2011; Zhuang et al., 2014b). Besides, BC is mostly produced by the incomplete
1386 combustion of carbonaceous material, and so is carbon monoxide (CO) (Pan et al., 2011), thus, both
1387 BC and CO might come from the same sources, mostly from combustions of domestic bio-fuel,
1388 industry-coal, and vehicle-gasoline (Zhuang et al., 2014b). The effect of meteorology, i.e., the
1389 development of PBL, influences the diurnal pattern as mentioned in Section 3.1, especially the

1390 afternoon dip and night accumulation. Moreover, as one of main precursors of O₃, increase in O₃
1391 levels in the afternoon might also contribute to the lowest concentration at 15:00 LT.

1392
1393 Table 7-5 further provides the statistics of O₃, PM_{2.5} and PM₁₀ mass concentrations with a
1394 comparison to the National Ambient Air Quality Standards in China (NAAQS-CN), which were
1395 released in 2012 by the China State Council and will be implemented nationwide in 2016 (MEP,
1396 2012). According to NAAQS-CN for PM_{2.5} and PM₁₀ (75 µg/m³ of PM_{2.5} concentrations and 150
1397 µg/m³ of PM₁₀ concentrations for 24h average), there were 48 days of PM_{2.5} exceedances,
1398 accounting for about 30% of the 6 months period, and 14 days of PM₁₀ exceedances, lower than the
1399 PM_{2.5} exceedances. Days of ~~particulate-matter~~PMs exceedances mainly occurred during DJF. The
1400 days of exceedances decreased. ~~Donkelaar et al. (2010) reported that a multi-year average of PM_{2.5}~~
1401 ~~mass concentrations was over 80 µg/m³ in eastern China by using satellite data during 2001–2006,~~
1402 ~~and Ding et al. (2013b) reported stated 99 days of PM_{2.5} exceedances in total from September 2011~~
1403 ~~to February 2012, and Wang et al. (2014) suggested that non-attainment rates in Nanjing from~~
1404 ~~September 2013 to February 2014 were over 40% and 70% in SON and DJF, respectively. an 1-~~
1405 ~~year average about 75 µg/m³ in rural area of Nanjing from August 2011 to July 2012. Therefore, the~~
1406 ~~means in Table 7 show lower particle concentrations than what were reported. The days of~~
1407 ~~exceedances also were fewer than in 2011 (Ding et al., 2013), during which 99 days of PM_{2.5}~~
1408 ~~exceedances happened during the cold seasons.~~ These results suggest that particles control policies
1409 are well-implemented in Nanjing although particles remain a severe pollution problem in the YRD
1410 region. According to NAAQS-CN for O₃ (160 µg/m³ for 8 h average and 200 µg/m³ for 1 h average),
1411 37 days of exceedances occurred (Table 7 Table 5), covering 20% of the period and mostly appearing

1412 in September and February when the air temperature was relatively high. In contrast to particulate
1413 matter, ~~days of O₃ exceedances increases greatly. O₃ concentrations increased from 2011 to 2016,~~
1414 ~~and the exceedance days were 10 times of those in 2011. Wang et al. (2014) reported a 11.4%~~
1415 ~~contribution of O₃ as the major pollutant on non-attainment days in cold seasons in 2013 in south-~~
1416 ~~east China, and Tu et al. (2007) reported frequency of days with O₃ exceedance for cold seasons in~~
1417 ~~2000~2002 in urban Nanjing was 6.3%. It was found in previous studies that~~ O₃ levels in the rural
1418 areas ~~were~~ are generally higher than those in the city centers (Zhang et al., 2008; Geng et al., 2008;
1419 Xie et al., 2016). Thus, high O₃ concentrations and severe air pollution in Gulou, an urban site,
1420 ~~probably suggest imply~~ a severer O₃ pollution problem in the entire YRD region. ~~Moreover, N~~note
1421 that this study only discussed the O₃ concentrations in the cold seasons when ~~the concentrations of~~
1422 ~~O₃ are lower than in the warm season it is relatively low, and it might suggest the problem can be a~~
1423 severer problem in the warm seasons. ~~The emissions of O₃ precursors (VOCs and NO_x) in Nanjing~~
1424 ~~have significantly increased with the increases of residents (over 200,000 increase since 2011), the~~
1425 ~~number of automobiles (over 65% increase since 2011), and GDP (gross domestic production)~~
1426 ~~(nearly 70% increase since 2011). Consequently, O₃ concentrations at ground level has gradually~~
1427 ~~risen (<http://www.njtj.gov.cn/>).~~

1428

1429 **3.3 Inter-species correlations**

1430 Correlations between different species ~~were~~ have been analyzed to help interpret the data and gain
1431 insights into the underlying mechanisms/processes. Because precipitation could impact wet
1432 scavenging processes for particles and other aerosols (~~see S2Table 6~~), the data in rainy condition

1433 ~~has been eliminated. we eliminated the data in rainy condition.~~

1434

1435 The scatter plot of O₃ measured at the site and NO_x color-coded with air temperature is given in

1436 Fig.7 (a). ~~As discussed in previous studies (Xie et al., 2016; Ding et al., 2013b), measured O₃~~

1437 ~~presents an overall negative correlation with NO_x.The negative correlation suggests a titration effect~~

1438 ~~of freshly emitted NO with O₃ in the cold seasons. The negative correlation mainly exists for data~~

1439 ~~of relatively low air temperature, suggesting a titration effect of freshly emitted NO_x with O₃,~~

1440 ~~especially at nighttime. However, the slope gets less rigid when air temperature rises, and tend to~~

1441 ~~be positive with a high temperature (over 25°C) and low level of NO_x (below 30 ppb).In addition,~~

1442 ~~the slope decreased when air temperature rose.~~ These results possibly suggest a strong

1443 photochemical production of O₃ in this region under high temperature with strong radiation like in

1444 September during high air temperature, leading to resulting in the seasonal cycle pattern of O₃ shown

1445 in Fig. 5 (a) ~~(Ding et.al, 2013).~~

1446

1447 Fig.7 (b) provides a scatter plot of PM_{2.5} and visibility (Vis) color-coded with relative humidity

1448 (RH). Previous research has shown that visibility has a good correlation with the concentrations of

1449 particles and relative humidity. For a better understanding of the relationship between the variables,

1450 we have performed a linear fit of the visibility with the PM_{2.5} concentration when RH ≤ 70%, 70%

1451 <RH ≤ 80%, and 80% < RH ≤ 90%, to find out the relationship among these factors, and the fitting

1452 curves are [PM_{2.5}] = 366.72[Vis]^{-0.745} (R² = 0.7196), [PM_{2.5}] = 337.16[Vis]^{-0.855} (R² = 0.8692), and

1453 [PM_{2.5}] = 248.6[Vis]^{-0.852} (R² = 0.8279), respectively. It is found that visibility decreases with the

1454 concentration of PM_{2.5} in a power function with a negative exponent, and the inverse relationship

1455 between visibility and aerosols concentrations as well as relative humidity has also been discussed
 1456 in previous studies based on the observations in YRD (e.g., Deng et al., 2011; Xiao et al., 2011;
 1457 Jiang et al., 2018). The correlation is stronger than that in Lin'an, a rural site not far from Nanjing
 1458 (Jiang et al., 2018). With an increase in the PM_{2.5} concentrations, visibility decreases exponentially
 1459 ~~(Fig.7 (b)), because t~~The concentrations of particles would increase scattered and absorption
 1460 extinction coefficients, while the visibility (Vis) is related to the coefficients through:

$$1461 \quad Vis = \frac{3.91}{\sigma} \quad (138)$$

1462 where Vis is the visibility and σ is the extinction coefficient (EC) (Larson et.al, 1989). As for the
 1463 effect of relative humidity (RH) on the visibility, according to Mie theory, with the increase of the
 1464 relative humidity, the radius of the wet particle also increases, and so does the extinction coefficient,
 1465 which leads to the decrease in visibility increases. Therefore, the visibility decrease. Moreover,
 1466 when $RH \leq 80\%$, the effect of partiele concentrations on visibility could become smog, and when
 1467 $80\% < RH \leq 90\%$, the effect could form smog and fog at the same time. Thus, we performed a
 1468 linear fit of the visibility with differing concentrations of PM_{2.5} when $RH \leq 70\%$, $70\% < RH \leq$
 1469 80% , and $80\% < RH \leq 90\%$, to find out the relationship among these factors. Although there is
 1470 no precipitation, there are still water droplets in the air when $RH > 90\%$, which become fog.
 1471 Therefore, we eliminated those data. It is found that the fitting curves are as follows: $[PM_{2.5}] =$
 1472 $366.72[Vis]^{-0.745}$ ($R^2 = 0.7196$), $[PM_{2.5}] = 337.16[Vis]^{-0.855}$ ($R^2 = 0.8692$), and $[PM_{2.5}] = 248.6[Vis]^{-$
 1473 0.852 ($R^2 = 0.8279$).

1474
 1475 According to the scatter plots of PM_{2.5}-O₃ and BC-O₃ color-coded with air temperature (Fig.8),
 1476 PM_{2.5} and BC are negatively correlated with O₃ in general. To figure out the interaction between

1477 particles and O_3 , we give scatter plots of $PM_{2.5}$ - O_3 and BC - O_3 (Fig.8), in which data points are
1478 color-coded with air temperature. Overall, particulate matters and black carbon are negatively
1479 correlated with O_3 . It is also noticeable that a negative correlation between $PM_{2.5}$ and O_3 could be
1480 found for low air temperature samples while a positive correlation exists for those under a high
1481 temperature. Similar results were also found at a rural site in Nanjing (Ding et al., 2013b). Besides,
1482 BC is in a negative correlation with O_3 under low air temperature, but tend less-correlated with O_3
1483 when the temperature rises. $PM_{2.5}$ is well-correlated with O_3 precursors, such as NO_x (Fig.10 (b))
1484 and CO . Therefore, the anti-correlation in Fig.8 (a) for cold air is likely due to the titration effect of
1485 high NO concentrations associated with high primary $PM_{2.5}$ levels. ~~And~~ Additionally, the increasing
1486 slope under ~~the positive correlation for high air temperature is~~ might be related to the formation of
1487 secondary fine particles associated with high concentrations of O_3 , which may be related
1488 to especially the high conversion rate of SO_2 to sulfate under the effect of high concentrations of
1489 oxidants (Khoder, 2002 O_3) and solar radiation (Roberts and Friedlander, 1976; Khoder, 2002).
1490 Previous studies of $PM_{2.5}$ chemical compositions in Shanghai and Nanjing (Wang et al., 2002, 2006)
1491 and Nanjing (Ding et al., 2013b) suggested that sulfate was the most dominate ion in $PM_{2.5}$. Ding et
1492 al. (2013b) also suggested formation of secondary organic aerosols with high O_3 concentration could
1493 lead to the positive correlation because biogenic emission of VOCs is high under a condition of high
1494 air temperature and solar radiation in summer. However, the study is performed during cold seasons
1495 when air temperature is relatively lower and the biogenic emission of VOCs are likely lower, so the
1496 positive correlation is less pronounced. As for BC , it also shows a good correlation with NO_x (Fig.10
1497 (c)) and CO , which contributes to the inverse correlation for cold air. ~~Since black carbon~~ BC is
1498 insoluble in polar and non-polar solvents and remains stable when air or oxygen is heated to 350 ~

1499 ~~400°C, it's hard it cannot to be generated nor cleared through chemical reactions. And that is~~
1500 ~~probably the reason why~~ Thus, when air temperature rises, the correlation between BC and O₃
1501 ~~becomes~~ is obscurer compared to the one between PM_{2.5} and O₃ ~~when air temperature rises.~~
1502 Moreover, as shown in Fig.9, O₃ is well correlated with UV (daily averages are used due to the
1503 remarkable diurnal variation), suggesting the significant role UV plays in O₃ production, while
1504 PM_{2.5} is generally negatively correlated with UV. Previous findings based on various numerical
1505 models also suggest that particles can affect actinic flux of UV radiation, and inhibit the photolysis
1506 reactions near surface in reducing the photolysis frequencies in the atmosphere, like the frequency
1507 of O₃ → O(¹D) (e.g., Li et al., 2005; Deng et al., 2010; Li et al., 2011; Li et al., 2018). In central
1508 Nanjing, as implied in Li et al. (2017), high concentrations of aerosols could result in a 0.1–5.0 ppb
1509 (12.0%) reduction of near-surface O₃. Thus, they might result in the decrease of O₃ concentration
1510 near the ground to some degree. because particulates inhibit the photolysis reactions near the surface,
1511 reducing the photolysis frequencies in the atmosphere, and resulting in the decrease of O₃
1512 concentrations near the ground, which is also addressed using the chemical transport model (HANK)
1513 (Li et al., 2005). It is noticeable that a negative correlation could be found for low air temperature
1514 samples while a pronounced positive correlation existed for high temperature data points. The
1515 negative correlation for cold air is mainly due to the titration effect of high NO concentrations,
1516 which was associated with high primary PM_{2.5} in the cold seasons as well. And the positive
1517 correlation for high air temperature is related to the formation of secondary fine particles associated
1518 with high concentrations of O₃, which may be related to high conversion rate of SO₂ to sulfate under
1519 high concentrations of oxidants (Khoder, 2002). Previous studies of PM_{2.5} chemical compositions
1520 in Shanghai and Nanjing (Wang et al., 2002, 2006) suggested that sulfate was the most dominate

1521 ~~ion in PM_{2.5}.~~ However, ~~T~~the detailed mechanisms still need to be further ~~investigated~~addressed by
1522 long-term measurement of aerosol chemical composition combined with numerical models. ~~Since~~
1523 ~~black carbon is insoluble in polar and non-polar solvents and remains stable when air or oxygen is~~
1524 ~~heated to 350–400°C, it cannot be generated nor cleared through chemical reactions. Thus, when~~
1525 ~~air temperature rises, the correlation between BC and O₃ becomes obscurer compared to the one~~
1526 ~~between PM_{2.5} and O₃.~~
1527
1528 Scatter plots of CO–NO_x, PM_{2.5}–NO_x, and BC–NO_x, are given in Figs. ~~9~~10 (a)–~~9~~10(c), with data
1529 points color-coded with concentrations of O₃. Fig. ~~9~~10 (b) and ~~9~~10(c) show a good positive correlation
1530 between PM_{2.5} and NO_x, as well as BC and NO_x as mentioned above, suggesting that the particles
1531 at the site ~~in Nanjing University Gulou Campus were~~are mainly associated with combustion sources
1532 ~~(Wang et al., 2006; Ding et al., 2013b; Zhuang et al., 2014b).~~, ~~which is also the reason for the~~
1533 ~~negative correlation between particles and O₃.~~ It is found that high O₃ levels are generally associated
1534 related with to air masses of high CO/NO_x or particles/NO_x ratio. An increase in CO, as well as
1535 PM_{2.5} and BC, always results in higher O₃ concentration for NO_x lower than 40 ppb, while NO_x
1536 reverses. and when NO_x concentrations was lower than 40 ppb, an increase in CO or particular
1537 matter concentrations would cause a sharp increase in O₃ concentrations while NO_x reverses. To be
1538 specific, when NO_x reduces for CO lower than 1500 ppb, O₃ has a sharp increase, and an increase
1539 in the CO level would lead to an increase in the O₃ concentration, especially when NO_x is lower
1540 than 40 ppb. The concentration of O₃ is sensitive to the level of its precursors, and the O₃ formation
1541 regime often includes NO_x-sensitive O₃ formation regime and VOCs-sensitive O₃ formation regime.
1542 If O₃ formation is under VOC-sensitive regime, a reduction in the NO_x concentration will lead to an

1543 increase in the O₃ concentration, which is used to determine the O₃ photochemical production in the
1544 region is VOC-limited or NO_x-limited based on observation data (Geng et al., 2008; Ding et al.,
1545 2013b). In our study, we have no VOCs measurement, thus CO is chosen as the reference tracer,
1546 because mixing ratios of CO showed significant correlations with the measured levels of most
1547 anthropogenic VOCs, which has been verified in many previous studies (e.g., Baker et al., 2008;
1548 von Schneidmesser et al., 2010; Wang et al., 2014). In addition, as a significant precursor of O₃,
1549 CO also plays a similar role as VOCs. HO₂ produced from the oxidation reaction of CO with OH
1550 radicals could initiate photochemical reactions which result in the net formation of O₃ (Novelli et
1551 al., 1998; Atkinson et al., 2000; Gao et al., 2005). Thus, the CO–O₃–NO_x relationship may reflect
1552 the correlation of VOCs, NO_x and O₃ in this region to some degree. And we suggest that the region
1553 is VOC-sensitive. As discussed in Atkinson et.al (2000), volatile organic compounds (VOCs)
1554 generally have good correlation with CO and play a role similar to CO in the photochemical ozone
1555 production. Particles also have good correlation with CO, so the particles–O₃–NO_x relationship may
1556 indicate a VOC-sensitive regime of O₃ formation in this region, as the CO–O₃–NO_x relationship.
1557 Geng et al. (2008) reported a VOC-sensitive regime in Shanghai combining the measured and
1558 modeling results by using measured and modeling results, and Ding et al. (2013b) also reported a
1559 VOC-sensitive regime in rural ~~area in~~ Nanjing using the observation data. And the PM_{2.5}-O₃-NO_x
1560 and BC-O₃-NO_x relationship show the similar pattern, possibly because they are well-correlated
1561 with CO.

1562
1563 Correlations of PM_{2.5}–O₃ in daytime when UV radiation is relatively strong and nighttime when UV
1564 radiation is approximately 0 are shown in Fig.10. It is found that the correlation is better with a

1565 clearer tendency and O_3 are higher during daytime, suggesting strong photochemistry progresses
1566 during daytime. Some data in the nighttime plots show relatively high O_3 . Most occurred in
1567 September and February when O_3 concentrations were extremely high. It is also found that some
1568 show relatively high NO_x associated with relatively low $PM_{2.5}$. After a further backward trajectories
1569 analysis (Section 3.4), we found that these data are most likely corresponded to air masses coming
1570 from the nearby and northwest in November and December, which may contain high NO_x plumes
1571 and transport to Nanjing during nighttime.

1572 3.4 Backward Trajectories Analysis

1573 The cluster means of the backward ~~trajectories~~ trajectory at 100 m from Gulou, Nanjing, in 2016
1574 fall (Fig. 11) and winter (Fig. 13) suggest different air flows that were transported to Nanjing from
1575 long distances. In general, the aerosol kinds and optical properties are characterized differently with
1576 different air masses in the two seasons, which are further analyzed by their origins in SON and DJF
1577 (Figs. 12 and 14). Figs. 12 and 14 show the main concentrations of particles and trace gases, the ratio
1578 of $PM_{2.5}$ to PM_{10} , as well as the values of the aerosol optical properties of different clusters during
1579 SON and DJF, respectively. Because PM_{10} varies similarly to $PM_{2.5}$, while NO_x varies similarly
1580 to NO_y , we only show the variations of $PM_{2.5}$ and NO_y with cluster with cluster here. Also, because
1581 σ_a , σ_{ts} and σ_{bs} AAC, SC and Bsp have good correlations with particle concentrations (Zhuang
1582 et al., 2014a) and g Asp is greatly affected by relative humidity (RH), we discuss the variation of
1583 α_{ts} and ω_0 SAE and SSA with cluster here.
1584 ~~Most of air masses came from the oceans in fall (40 %, cluster 4 in Fig. 11) and from the north and~~
1585 ~~north-west of China in winter (49 %, clusters 1 and 4 in Fig. 13). Although air masses came from~~

1586 north in both fall (cluster 4) and winter (cluster 4), the trajectory cluster in fall came from the oceans
1587 more than the one in winter. In winter, considerable air masses arriving at the site were also from
1588 places near Nanjing (35%, cluster 2 in Fig. 13). Therefore, the aerosol kinds and optical properties
1589 at the study site are characterized differently with different air masses in the two seasons, which are
1590 further analyzed by their origins in SON and DJF (Figs.12 and 14).

1591
1592 Figs. 12 and 14 show the main concentrations of particles and trace gases, the ratio of $PM_{2.5}$ to PM_{10} ,
1593 as well as the values of the aerosol optical properties of different clusters during SON and DJF,
1594 respectively. Because PM_{10} vary similarly to $PM_{2.5}$, while NO_x varies similarly to NO_y , we only
1595 show the variations of $PM_{2.5}$ and NO_y with cluster here. Also, because AAC, SC and Bsp have good
1596 correlations with particle concentrations (Zhuang et al., 2014) and Asp is greatly affected by relative
1597 humidity (RH), we discuss the variation of SAE and SSA with cluster here.

1598
1599 In SON, the dominant air masses are from the East China Sea (passing through urban agglomeration
1600 regions (cluster 3), and less-developed regions (cluster 2) of the YRD, and from northern continent
1601 away from Nanjing (cluster 4) (passing through oceans and urban agglomeration regions (cluster
1602 4)). It is found that although air masses in cluster 3, cluster 4 and cluster 2 all pass through the
1603 oceans and have the same level of relative humidity (RH), differences still exist among the clusters.
1604 The air masses have to cross the urban agglomeration (from Shanghai to Nanjing) of YRD when
1605 they arrive in Nanjing in cluster 3 but past less-developed regions (north
1606 Jiangsu Province) in cluster 4 and cluster 2. In YRD, emissions of the aerosols and trace gases are
1607 much stronger in urban agglomeration regions than those in other areas (Zhang et al., 2009; Zhuang

1608 et al., 2013). It is also noticeable that concentrations of aerosols in cluster 4 are mostly lower, which
1609 may result from its avoidance from BTH regions, also a megacities and urban agglomeration. In
1610 addition, air masses from the west of cluster 1 contain the highest ~~concentrations levels~~ of ~~particulate~~
1611 ~~matter~~ ~~PMs and precursors, CO and NO_y, which Air masses may result from crossing pass~~ central
1612 China with high emissions of ~~CO particles and precursors according to MERRA data~~
1613 ~~(<https://gmao.gsfc.nasa.gov/reanalysis/MERRA>)~~. ~~Particulate matter and NO_y mainly have the same~~
1614 ~~sources as CO, according to MERRA data (<https://gmao.gsfc.nasa.gov/reanalysis/MERRA>) and~~
1615 ~~Zhuang et al. (2018); and h~~ Also, high concentrations of these aerosols are also reflected in a high
1616 AOD according to the MISR data (<https://giovanni.gsfc.nasa.gov/giovanni>). ~~Zhuang et al. (2015)~~
1617 ~~also suggested that high emission occurred in central China. As for the ratio of PM_{2.5} to PM₁₀, the~~
1618 ~~ratio represents the amount number of particles deriving from secondary pollution progress~~
1619 ~~compared to those from primary pollution progress to some extent. In SON, ratios of clusters 1~3~~
1620 ~~are relatively close (all over 60%) with a maximum of cluster 3. Clusters 1-3 had relatively similar~~
1621 ~~ratios in SON, all over 60% except cluster 4, with the maximum of cluster 3, which means particles~~
1622 ~~deriving~~ ~~generating~~ from secondary pollution progress in the three clusters have a similar rate. O₃
1623 concentrations among the ~~four~~ 4 cluster were different. Despite negative correlations of O₃ with its
1624 precursors and particles, the concentrations of O₃ in cluster 3 was higher than in cluster 4, ~~possibly~~
1625 ~~because radiation in cluster 3 is stronger~~ as UV in cluster 3 was higher than in cluster 4. The size of
1626 the aerosols in cluster 1 were finest (α_{ts} SAE is the largest in Fig. 12g), because the other three
1627 ~~clusters all passed through oceans before arriving Nanjing, are more humid going through~~
1628 ~~oceans~~ with higher relative humidity (RH), making it easier for particles' hygroscopic growth. ω_0
1629 SSA is also the largest in cluster 1, which means aerosols in cluster 1 are more scattering.

1630 (<https://giovanni.gsfc.nasa.gov/giovanni>). Zhuang et al. (2015) also suggested that high emission
1631 occurred in central China. As for the ratio of PM_{2.5} to PM₁₀, the ratio represents the amount of
1632 particles deriving from secondary pollution progress compared to those from primary pollution
1633 progress. Clusters 1-3 had relatively similar ratios in SON, all over 60% except cluster 4, with the
1634 maximum of cluster 3, which means particles deriving from secondary pollution progress in the
1635 three clusters have a similar rate. O₃ concentrations among the four clusters were different. Despite
1636 negative correlations of O₃ with its precursors and particles, the concentrations of O₃ in cluster 3
1637 was higher than in cluster 4, as UV in cluster 3 was higher than in cluster 4. The size of the aerosols
1638 in cluster 1 were finest (SAE is the largest in Fig. 12g), because the other three clusters all passed
1639 through oceans before arriving Nanjing, with higher relative humidity (RH), making it easier for
1640 particles' hygroscopic growth. SSA is also the largest in cluster 1, which means aerosols in cluster
1641 1 are more scattering.

1642

1643 In DJF, the air masses come from the local region were from the places near Nanjing (cluster 2),
1644 north-west areas northern continent away from Nanjing (cluster 1), and northern regions northern
1645 continent away far from Nanjing passing through oceans and urban agglomeration regions (cluster
1646 4). Air masses from cluster 1 and cluster 2 both account for over 30% of the total aerosol
1647 characteristics and are more polluted with relatively high levels of particles, CO, and NO_x. Air
1648 masses in cluster 1 come from Shandong Province while those in cluster 2 come from local areas.
1649 Particles and trace gases concentrations of cluster 2 are higher than those of cluster 1 to some extent,
1650 implying the severer air pollution problem in YRD region. This is different from that in SON.
1651 Therefore, besides what has been discussed of cluster 3 and cluster 4 in SON, it is found that air

1652 masses from cluster 1 and cluster 2 both account for over 30% of the total characteristics of the
1653 aerosol optical properties and are main sources of pollutants in DJF (particles, CO, and NO_x are
1654 higher in Fig.14). Air masses in cluster 1 came from Shandong Province while those in cluster 2
1655 came from areas nearby. Particles and trace gases concentrations of cluster 2 are higher than those
1656 of cluster 1 to some extent, which may result from the severer pollution in southern YRD than in
1657 Shandong Province. The concentrations of O₃, similar to that in SON, is affected by radiation
1658 besides precursors levels. Thus, O₃ concentration in cluster 2 is a little higher than that in cluster 1.
1659 was affected by the UV (O₃ concentrations in cluster 2 is a little higher than that in cluster 1 in
1660 Fig.14). The ratios of PM_{2.5} to PM₁₀ of cluster 1 and cluster 2 are approximately equal in DJF, over
1661 70%. The size of aerosols in cluster 1 and 2 are coarser, however, probably due to the higher RH
1662 (over 65%). finer without passing through oceans, so SAE are larger (Fig.12g). Aerosols in cluster
1663 1 are scatter to some extent compared to those in cluster 2. The trajectories of cluster 3 and cluster
1664 4 are analogous to those in SON, respectively, but more polluted, probably due to more emissions
1665 in DJF especially in north China and weaker flow from ocean in DJF.

1668 3.5 Case Study

1669 For further understanding of the causes for high pollutants episodes, especially high particulate and
1670 O₃ episodes, detailed analysis of a typical episode from 2016 December 3-6 is presented in this
1671 section. we choose a typical episode from 2016 December 3-6 for a detailed analysis.

1673 Fig.15 (a) and (b) show that high O₃ concentrations (over 80 ppb) occurred on December 4 with
1674 broad O₃ peaks (over 60 ppb) in the following days, while the average O₃ during the cold seasons
1675 was 37.7 ppb. Though there is a lack of particulate matter concentrations because of the instrument
1676 breakdown, ~~we could see the~~ high concentrations of ~~particulate matter~~PMs might possibly occur
1677 referring to ~~from~~ the relatively high σ_e ~~EC~~ value (over 500 Mm⁻¹) and BC concentrations (over 6
1678 $\mu\text{g}/\text{m}^3$) on December 4th, ~~and~~ ~~both~~ PMs reach a maximum on December 5th (PM_{2.5} over 200
1679 $\mu\text{g}/\text{m}^3$ and PM₁₀ over 300 $\mu\text{g}/\text{m}^3$), over 3 times of the average concentrations. Besides, NO_x, NO_y,
1680 have reached high levels since December 4th (NO_x over 70 ppb and NO_y over 100 ppb). It is also
1681 noticeable that ω_0 SSA has a relatively sharp decrease from December 4th, especially on December
1682 5th when particle concentrations were extremely high, ~~representing probably suggesting~~ that the
1683 ratio of PM₁₀ became higher. Meanwhile, a relatively sharp increase occurred in α_{ts} ~~SAE~~, without
1684 any obvious variation in α_a ~~AAE~~, though, ~~which shows~~ implying that scattering aerosols could take
1685 the leading role during this episode. ~~are the main components~~. It is also found that this case occurred
1686 under calm conditions before the passage of a cold front, which was ~~at~~ in the front of a continental
1687 high pressure system originating from Mongolia and sweeping over Nanjing (Fig.15 (c)), ~~and~~
1688 And the decrease in temperature with high pressure system dominating eastern China ~~were~~ were also
1689 detected on December 6th. Backward ~~trajectories~~ trajectory analysis for the past 96 hours (Fig.15
1690 (d)) ~~were~~ was conducted ~~for~~ from December 5th at 8 ~~pm~~ 20:00 LT, ~~for~~ including the maximum
1691 concentrations of O₃ on December 4th and ~~particulate matter~~PMs on December 5th, ~~which~~ It is
1692 suggested that predominant wind was just in time from the NW directions. Therefore, air masses
1693 with high particles and O₃ concentrations would be transported to Nanjing, ~~which were~~ It was also
1694 clearly detected in Nanjing during these days, such as the relatively high O₃ during nighttime on

1695 December 5th and 6th. The highest O₃ concentration on December 4th together with high particles
1696 and primary pollutants NO_x and NO_y suggests a strong in situ photochemical production in mixed
1697 regional plumes under the influence of ~~high-the high~~-pressure system. Previous studies (Luo et al.,
1698 2000; Wang et al., 2006; Ding et al., 2013b) Guo et al. (2009) reported that the anticyclonic
1699 conditions, e.g., sunny weather and low wind velocities, are favorable for pollution accumulation
1700 and O₃ production. Results in this case clearly demonstrate sub-regional transport of primary and
1701 secondary air pollutants within the YRD region under such weather system.

1702 **4. Conclusion**

1703
1704 In this study, particles (BC and PMs) and trace gases (O₃ and related precursors) in polluted seasons,
1705 are investigated based on continuous measurements of concentrations and optical properties in the
1706 urban area of Nanjing. The characteristics and underlying reasons are comprehensively discussed
1707 from perspectives of temporal variations, inter-species correlations, trajectories analysis, and case
1708 studies associated with weather data and Lagrangian dispersion modeling.

1709 ~~In this paper, an overview of particles and O₃ concentrations, together with trace gases, during 2016~~
1710 ~~the cold seasons in urban Nanjing, China, has been presented based on continuous measurements~~
1711 ~~of aerosols concentrations and optical properties at the Gulou site. The particles, O₃ and trace gases~~
1712 ~~concentrations are comprehensively characterized from perspectives of temporal variations, inter-~~
1713 ~~species correlations, trajectories analysis, and case studies based on weather data and Lagrangian~~
1714 ~~dispersion modeling.~~

1715

1716 Measurements show that average concentrations of PM₁₀ was 86.3 μg/m³, with BC and PM_{2.5}
1717 accounting for 3% and 67%, respectively. 48 and 14 days of PM_{2.5} and PM₁₀ exceeded NAAQS-CN,
1718 respectively. The results suggested that both BC and PMs levels in Nanjing have decreased because
1719 of energy conservation since 2014. The average concentration of O₃ was 37.7 ppb with 40 days of
1720 exceedance. Precursor concentrations, including CO, NO_x and NO_y, averaged 753, 28.4, and 28.6
1721 ppb, respectively. Contrast to particles, O₃ concentration has increased in urban Nanjing, implying
1722 a severer pollution in rural area and entire YRD region. All the aerosols have substantially monthly
1723 and diurnal variations. Both particles and precursors reached maximum values in December and
1724 minimum values in October due to higher emission and less precipitation. O₃ showed a peak in
1725 September because of stronger radiation. Diurnal variations of BC and PMs were similar with peaks
1726 around 7:00~9:00 and 22:00~0:00 LT. Both of the peaks were influenced by traffic emissions in
1727 rush hours and accumulation of air pollution especially at night-time. The peaks of PMs often
1728 occurred 1~ 2 h later than those of BC, possibly due to the production of secondary particles.
1729 Precursors and particles varied similarly in time, and the diurnal variation of O₃ was analogous to
1730 that of radiation with peak around 15:00 LT.

1731 Measurements show that hourly mean particle concentrations, including BC, PM_{2.5}, and PM₁₀ at
1732 Gulou site, Nanjing, China, are 2.602 ± 1.720 μg/m³, 58.2 ± 36.8 μg/m³, and 86.3 ± 50.8 μg/m³,
1733 respectively, with ranges of 0.064-15.608 μg/m³, 0.8-256.2 μg/m³, and 1.1-343.4 μg/m³,
1734 respectively. During the six months, 48 and 14 days when PM_{2.5} and PM₁₀, respectively, exceeded
1735 Class II NAAQS. Measurements also showed that hourly mean O₃ concentrations in urban Nanjing
1736 ranged from 0.2 to 235.7 ppb, with average concentrations of 37.7 ± 33.5 ppb. There were 40 days
1737 excess of O₃ during the period, suggesting a severe air pollution problem in the region.

1738

1739 PM_{2.5} has a quasi-power-law distribution with Vis under RH of different ranges. The correlation is
1740 stronger than that in a rural region in YRD, implying greater effects of air pollution on visibility in
1741 urban Nanjing. O₃ shows an anti-correlation with NO_x generally, but it tends to be positive with a
1742 relatively high temperature and low level of NO_x. PM_{2.5} and BC are overall negatively correlated
1743 with O₃. A positive correlation between PM_{2.5} and O₃ exists under high temperatures, while it is not
1744 found in BC-O₃ correlation. The negative correlation is related to the titration effect of high NO
1745 concentration, which is highly correlated with particles due to similar emission sources. And the
1746 negative correlation between PM_{2.5} and UV suggests particles could decrease actinic flux of
1747 radiation, and thus inhibit the photolysis reactions near surface to degrees. The positive correlation
1748 implies the formation of secondary aerosols under the effects of the high concentrations of oxidants
1749 and solar radiation. BC is hard to be generated through chemical reactions, which might explain
1750 why the correlation between BC and O₃ is obscurer when temperature rises. An increase in CO, as
1751 well as PM_{2.5} and BC, always results in higher O₃ concentration, while NO_x reverses, which
1752 indicates a VOC-sensitive regime for photochemical production of O₃ in urban Nanjing.

1753

1754 ~~The correlation analysis shows a negative PM_{2.5}-Vis correlation as well as RH, both of which would~~
1755 ~~promote the extinction coefficient. Negative O₃-NO_y correlation occurs when temperature is~~
1756 ~~relatively low but the correlation becomes weaker when temperature becomes higher. PM_{2.5}-O₃-T~~
1757 ~~correlations reveal the formation of secondary aerosols, especially fine particulate matter under high~~
1758 ~~O₃ concentration and temperature conditions, while BC-O₃-T correlations not. CO-NO_y-O₃ and~~
1759 ~~PM_{2.5}-NO_y-O₃ correlations suggest that a VOC-sensitive regime for photochemical production of~~

1760 ~~O₃ in urban Nanjing.~~

1761
1762 Backward trajectories indicate that Nanjing could be affected by local air flow (35% in DJF) and
1763 long-distance air flows mostly from western (11% in SON), northwestern (31% in DJF), northern
1764 (up to 50 % in SON and DJF), eastern (40% in SON and 17% in DJF). Considerable air pollution
1765 in the urban area of Nanjing is due to local and sub-regional emissions. Basically, air masses from
1766 the oceans and remote or less-developed areas are relatively clean with low aerosols concentrations.

1767 α_{ts} at the site is usually low when the relative humidity of air masses is high, possibly suggesting
1768 the increased hygroscopicity and more secondary aerosols production under higher RH.

1769 ~~The backward trajectory analysis suggests that the prevailing winds in Nanjing were from the north~~
1770 ~~and east during the cold seasons in 2016. Air masses that are either from the east without passing~~
1771 ~~through the urban agglomeration and from northern without crossing BTH regions were clean with~~
1772 ~~low pollution concentrations. In contrast, air masses from local regions were polluted in winter,~~
1773 ~~suggesting a severe air quality problem in YRD region. SAE and SSA were further studied,~~
1774 ~~indicating that particles from oceans were coarser and less scattering because the airmasses were~~
1775 ~~under high RH condition and less secondary pollutants were produced.~~

1776
1777 A case study for a typical high O₃ and PM_{2.5} episode in December 2016 illustrates the important
1778 influences of sub-regional transport of pollutants from strong source regions and local synoptic
1779 weather on the episode. Stable conditions such as an anticyclonic system make it easy for pollutants
1780 to accumulate in this region. Results from this case reveal the mechanisms of sub-regional transport
1781 of primary and secondary air pollutants within the YRD region.

1782

1783 Overall, this work highlights the interactions and mechanisms of various aerosols and metrological
1784 fields besides the important environmental impact from human activities and meteorological
1785 conditions in the urban area in YRD region. Considering both results in this study and previous
1786 work, it is suggested that collaborative control measures among different administrative regions are
1787 urgently needed including but not limited to energy conservation and reduction of pollution
1788 emissions to improve air quality in the western part of YRD region.

1789

1790 *Data availability.* The ~~automobile numbers and GDP~~ are data is from <http://www.njtc.gov.cn/>.
1791 Satellite CO data are available at: <https://gmao.gsfc.nasa.gov/reanalysis/MERRA>. The aerosols
1792 AOD data are available at: <https://giovanni.gsfc.nasa.gov/giovanni>. The Lagrangian dispersion
1793 model Hybrid Single-Particle Lagrangian Integrated Trajectory (HYSPLIT) was supplied by NOAA:
1794 http://ready.arl.noaa.gov/HYSPLIT_traj.php. The meteorological data for HYSPLIT are accessible
1795 from <ftp://arlftp.arlhq.noaa.gov/pub/archives/gdas1>.

1796

1797 *Competing interests.* The authors declare that they have no conflict of interest.

1798

1799 *Author Contributions.* Huimin Chen, Bingliang Zhuang and Tijian Wang designed research; Huimin
1800 Chen, Bingliang Zhuang, Jane Liu, and Shu Li performed research; Huimin Chen, Bingliang Zhuang,
1801 Min Xie, Mengmeng Li, Pulong Chen and Ming Zhao analyzed data; and Huimin Chen, Bingliang
1802 Zhuang, and Jane Liu wrote the paper.

1803

1804 *Acknowledgements.* This work was supported by the National Key R&D Program of China
1805 (2017YFC0209803, 2014CB441203, 2016YFC0203303), the National Natural Science
1806 Foundation of China (41675143, 91544230, 41621005). The authors would like to thank all
1807 members in the AERC of Nanjing University for maintaining instruments.

1808

1809 **References:**

1810 Allen, R. J., Sherwood, S. C., Norris, J. R., and Zender, C.S.: Recent Northern Hemisphere tropical
1811 expansion primarily driven by black carbon and tropospheric ozone, *Nature*, 485,
1812 doi:10.1038/nature11097, 350–353, 2012.

1813 Anderson, T. L. and Ogren, J. A.: Determining aerosol radiative properties using the TSI 3563
1814 integrating nephelometer, *Aerosol Sci. Tech.*, 29, 57–69, 1998.

1815 An, J., Zou, J., Wang, J., Lin, X., Zhu, B., 2015. Differences in ozone photochemical characteristics
1816 between the megacity Nanjing and its suburban surroundings, Yangtze River Delta, China.
1817 *Environ. Sci. Pollut. Res.* 22, 19607–19617.

1818 ~~Andrews, E., Sheridan, P. J., Fiebig, M., McComiskey, M., Ogren, J. A., Arnott, P., Covert, D.,~~
1819 ~~Elleman, R., Gasparini, R., Collins, D., Jonsson, H., Schmid, B., and Wang, J.: Comparison of~~
1820 ~~methods for deriving aerosol asymmetry parameter, *J. Geophys. Res.*, 111, D05S04,~~
1821 ~~doi:10.1029/2004JD005734, 2006.~~

1822 Arnott, W. P., Hamasha, K., Moosmuller, H., Sheridan, P. J., and Ogren, J. A.: Towards aerosol
1823 light-absorption measurements with a 7-wavelength aethalometer: evaluation with a
1824 photoacoustic instrument and 3-wavelength nephelometer, *Aerosol Sci. Technol.*, 39, 17–29,
1825 doi:10.1080/027868290901972, 2005.

1826 Atkinson, R.: Atmospheric chemistry of VOCs and NO_x, *Atmos. Environ.*, 34, 2063–2101,

1827 doi:10.1016/S1352-2310(99)00460-4, 2000.

1828 Badarinath, K. V. S., Kharol, S. K., Chand, T. R. K., Parvathi, Y. G., Anasuya, T., and Jyothsna, A.
1829 N.: Variations in black carbon aerosol, carbon monoxide and ozone over an urban area of
1830 Hyderabad, India, during the forest fire season, *Atmos. Res.*, 85(1), 18–26, 2007.

1831 Baker, A. K., Beyersdorf, A. J., Doezema, L. A., Katzenstein, A., Meinardi, S., Simpson, I. J., Blake,
1832 D. R., Rowland, F. S.: Measurements of nonmethane hydrocarbons in 28 United States cities,
1833 *Atmos. Environ.*, 2008, 42(1): 170–182.

1834 ~~Bond, T. C., Doherty, S. J., Fahey, D. W., Forster, P. M., Berntsen, T., DeAngelo, B. J., Flanner, M.~~
1835 ~~G., Ghan, S., Karcher, B., Koch, D., Kinne, S., Kondo, Y., Quinn, P. K., Sarofim, M. C.,~~
1836 ~~Schultz, M. G., Schulz, M., Venkataraman, C., Zhang, H., Zhang, S., Bellouin, N., Guttikunda,~~
1837 ~~S. K., Hopke, P. K., Jacobson, M. Z., Kaiser, J. W., Klimont, Z., Lohmann, U., Schwarz, J. P.,~~
1838 ~~Shindell, D., Storerlmo, T., Warren, S. G., and Zender, C. S.: Bounding the role of black carbon~~
1839 ~~in the climate system: A scientific assessment, *J. Geophys. Res.: Atmos.*, 118, 5380–5552,~~
1840 ~~doi:10.1002/jgrd.50171, 2013.~~

1841 ~~Bond, T. C., Streets, D. G., Yarber, K. F., Nelson, S. M., Woo, J. H., and Klimont, Z.: A technology-~~
1842 ~~based global inventory of black and organic carbon emissions from combustion, *J. Geophys.*~~
1843 ~~*Res.*, 109(D14), D14203, doi:10.1029/2003jd003697, 2004.~~

1844 ~~Castro, T., Madronich, S., Rivale, S., Muhlia, A., and Mar, B.: The influence of aerosols on~~
1845 ~~photochemical smog in Mexico City, *Atmos. Environ.*, 35, 1765–1772, 2001.~~

1846 ~~Chameides, W.L., Bergin, M., 2002. Soot takes center stage. *Science* 297 (5590), 2214–2215.~~

1847 Chameides, W. L., Li, X., Tang, X., Zhou, X., Luo, C., Kiang, C. S., John, J. St., Saylor, R. D., Liu,
1848 S. C., Lam, K. S., Wang, T., and Giorgi, F.: Is ozone pollution affecting crop yields in China,

1849 [Geophys. Res. Lett., 26, 867–870, 1999b.](#)

1850 [Chameides, W. L., Yu, H., Liu, S. C., Bergin, M., Zhou, X., Mearns, L., Wang., G., Kiang, C. S.,](#)

1851 [Saylor, R. D., Luo, C., Huang, Y., Steiner, A., and Giorgi, F.: Case study of the effects of](#)

1852 [atmospheric aerosols and regional haze on agriculture: An opportunity to enhance crop yields in](#)

1853 [China through emission controls?, PNAS, 96, 13626–13633, 1999a.](#)

1854 [Chen, T.; He, J.; Lu, X.W.; She, J.F.; Guan, Z.Q. Spatial and Temporal Variations of PM2.5 and Its](#)

1855 [Relation to Meteorological Factors in the Urban Area of Nanjing, China. Int. J. Environ. Res.](#)

1856 [Public Health 2016, 13, 921.](#)

1857 [Cheung, V.T.F., Wang, T., 2001. Observational study of ozone pollution at a rural site in the Yangtze](#)

1858 [Delta of China. Atmos. Environ. 35, 4947–4958.](#)

1859 [Chow, J. C., Watson, J. G., Lowenthal, D. H., Chen, L.-W. A., Motallebi, N.: PM2.5 source profiles](#)

1860 [for black and organic carbon emission inventories. Atmospheric Environment, 2011, 45\(31\):](#)

1861 [5407-5414.](#)

1862 [Collaud Coen, M., Weingartner, E., Apituley, A., Ceburnis, D., Fierz-Schmidhauser, R., Flentje, H.,](#)

1863 [Henzing, J. S., Jennings, S. G., Moerman, M., Petzold, A., Schmid, O., and Baltensperger, U.:](#)

1864 [Minimizing light absorption measurement artifacts of the Aethalometer: evaluation of five](#)

1865 [correction algorithms, Atmos. Meas. Tech., 3, 457–474, doi:10.5194/amt-3-457-2010, 2010.](#)

1866 [Deng, J.J., Wang, T.J., Liu, L., Jiang, F.: Modeling heterogeneous chemical processes on aerosol](#)

1867 [surface. Particuology 8 \(4\), 308-318, 2010.](#)

1868 [Deng, J., Wang, T., Jiang, Z., Xie, M., Zhang, R., Huang, X., Zhu, J., 2011. Characterization of](#)

1869 [visibility and its affecting factors over Nanjing, China. Atmospheric Research 101, 681-691.](#)

1870 [Chan, C.K., Yao, X., 2008. Air pollution in mega-cities in China. Atmos. Environ. 42, 1–42.](#)

1871 [Collaud Coen, M., Weingartner, E., Apituley, A., Ceburnis, D., Fierz-Schmidhauser, R., Flentje, H.,](#)

1872 [Henzing, J. S., Jennings, S. G., Moerman, M., Petzold, A., Schmid, O., and Baltensperger, U.:](#)

1873 ~~Minimizing light absorption measurement artifacts of the Aethalometer: evaluation of five~~
1874 ~~correction algorithms, Atmos. Meas. Tech., 3, 457–474, doi:10.5194/amt-3-457-2010, 2010.~~

1875 ~~Crutzen P. 1973. A discussion of the chemistry of some minor constituents in the stratosphere and~~
1876 ~~troposphere[J]. Pure Appl. Geophys., 106–108 (1): 1385–1399, doi: 10.1007/BF00881092.~~

1877 ~~Deng, J.J., Wang, T.J., Liu, L., Jiang, F.: Modeling heterogeneous chemical processes on aerosol~~
1878 ~~surface. Particuology 8 (4), 308–318, 2010.~~

1879 Derwent, R. G., Ryall, D. B., Jennings, S. G., Spain, T. G., and Simmonds, P. G.: Black carbon
1880 aerosol and carbon monoxide in European regionally polluted air masses at Mace Head,
1881 Ireland during 1995–1998, Atmos. Environ., 35(36), 6371–6378, 2001.

1882 Ding, A. J., Fu, C. B., Yang, X. Q., Sun, J. N., Zheng, L. F., Xie, Y. N., Herrmann, E., Nie, W.,
1883 Petaja, T., Kerminen, V. -M., and Kulmala, M.: Ozone and fine particle in the western Yangtze
1884 River Delta: an overview of 1 yr data at the SORPEs station, Atmos. Chem. Phys., 13, 5813–
1885 5830, 2013b.

1886 Draxler, R. R. and Hess, G. D.: An overview of the HYSPLIT 4 modeling system for trajectories
1887 dispersion and deposition, Aust. Meteor. Mag., 47, 295–308, 1998.

1888 Draxler, R.R. and Rolph, G.D. (2013) HYSPLIT (HYbrid Single-Particle Lagrangian Integrated
1889 Trajectory) Model Access Via NOAA ARL READY Website, NOAA Air Resources
1890 Laboratory, Silver Spring, MD [online].

1891 Eichler, H., Cheng, Y. F., Birmili, W., Nowak, A., Wiedensohler, A., Brüggemann, E., Gnauk, T.,
1892 Herrmann, H., Althausen, D., Ansmann, A., Engelmann, R., Tesche, M., Wendisch, M., Zhang, Y.
1893 H., Hu, M., Liu, S., and Zeng, L. M.: Hygroscopic properties and extinction of aerosol particles at
1894 ambient relative humidity in South-Eastern China, Atmos. Environ., 42, 25, 6321–6334.

1895 [doi:10.1016/j.atmosenv.2008.05.007](https://doi.org/10.1016/j.atmosenv.2008.05.007), 2008.

1896 Gao, J., Wang, T., Ding, A., and Liu, C.: Observational study of ozone and carbon monoxide at the
1897 summit of mount Tai (1534 m a.s.l.) in central-eastern China. *Atmos. Environ.* 39, 4779–4791,
1898 2005.

1899 Geng, F.H., Tie, X.X., Xu, J.M., Zhou, G.Q., Peng, L., Gao, W., Tang, X., Zhao, C.S.:
1900 Characterizations of ozone, NO_x, and VOCs measured in Shanghai, China. *Atmos. Environ.*
1901 42, 6873–6883, 2008.

1902 [Gong, W., Zhang, T.H., Zhu, Z.M., Ma, Y.Y, Ma, X., Wang, W.: Characteristics of PM1.0, PM2.5
1903 and PM10 and their relation to black carbon in Wuhan, central China. *Atmosphere*, 2015, 6\(9\):
1904 1377-1387.](#)

1905 [Guo, H., Wang, T., Simpson, I., Blake, D., Yu, X., Kwok, Y., et al., 2004b. Source contributions to
1906 ambient VOCs and CO at a rural site in eastern China. *Atmos. Environ.* 38, 4551–4560.](#)

1907 [Han, S., 2011. Analysis of the relationship between O₃, NO and NO₂ in Tianjin, China. *Aerosol Air
1908 Qual. Res.*](#)

1909 [Huang, F., Li, X., Wang, C., Xu, Q., Wang, W., Luo, Y., Tao, L., Gao, Q., Guo, J., Chen, S.: PM2.5
1910 spatiotemporal variations and the relationship with meteorological factors during 2013–2014 in
1911 Beijing, China. *PLoS ONE* 2015, 10, e0141642.](#)

1912 [Huang, X., Li, M., Li, J., Song, Y.: A high-resolution emission inventory of crop burning in fields
1913 in China based on MODIS Thermal Anomalies/Fire products. *Atmospheric Environment*, 2012,
1914 50:9-15.](#)

1915 [Huang, X. X., Wang, T. J., Jiang, F., Liao, J. B., Cai, Y. F., Yin, C. Q., Zhu, J. L., Han, Y., 2013.
1916 Studies on a severe dust storm in East Asia and its impact on the air quality of Nanjing, China.
1917 *Aerosol Air Qual. Res.* 13, 179e193.](#)

1918 ~~Jacobson, M.Z., 2002. Control of fossil-fuel particulate black carbon and organic matter, possibly
1919 the most effective method of slowing global warming. *Journal of Geophysical Research* 107
1920 (D19), 4410.~~

1921 ~~Jacobson, M. Z.: Studying the effects of aerosols on vertical photolysis rate coefficient and~~
1922 ~~temperature profiles over an urban airshed, J. Geophys. Res., 103, 10593–10604,~~
1923 ~~doi:10.1029/95JD00287, 1998.~~

1924 Jennings, S. G., Spain, T. G., Doddridge, B. G., Maring, H., Kelly, B. P., and Hansen, A. D. A.:
1925 Concurrent measurements of black carbon aerosol and carbon monoxide at Mace Head, J.
1926 Geophys. Res.-Atmos., 101(D14), 19447–19454, 1996.

1927 Jennings, S. G., Spain, T. G., Doddridge, B. G., Maring, H., Kelly, B. P., and Hansen, A. D. A.:
1928 Concurrent measurements of black carbon aerosol and carbon monoxide at Mace Head, J.
1929 Geophys. Res. Atmos., 101(D14), 19447–19454, 1996.

1930 Jerrett, M., Finkelstein, M. M., Brook, J. R., Arain, M. A., Kanaroglou, P., Stieb, D. M., Gilbert, N.
1931 L., Verma, D., Finkelstein, N., Chapman, K. R., and Sears, M. R.: A Cohort Study of Traffic-
1932 Related Air Pollution and Mortality in Toronto, Ontario, Canada. Environmental Health
1933 Perspectives, 2009, 117(5):772-777.

1934 Jiang, J., Zheng, Y.F., Liu, J.J., and Fan, J.J.: Observational research on planetary boundary layer
1935 by lidar over Nanjing city. Environ. Sci. Technol. 37, 22–27 (in Chinese), 2014.

1936 Jiang, L., Zhang, Z. F., Zhu, B., Shen, Y., Wang, H. L., Shi, S. S., Sha, D. D.: Comparison of
1937 parameterizations for the atmospheric extinction coefficient in Lin'an, China. The Science of the
1938 total environment., 2018, 621. 507-515. 10.1016/j.scitotenv.2017.11.182.

1939 Kaufman, Y.J.; Tanré, D.; Boucher, O. A satellite view of aerosols in the climate system. Nature
1940 2002, 419, 215–223.

1941 ~~Kristjánsson, J.E., 2002. Studies of the aerosol indirect effect from sulfate and black carbon aerosols.~~
1942 ~~Journal of Geophysical Research 107 (D15), 4246.~~

1943 Khoder, M. I.: Atmospheric conversion of sulfur dioxide to particulate sulfate and nitrogen dioxide

1944 to particulate nitrate and gaseous nitric acid in an urban area, *Chemosphere*, 49, 675–684, 2002.

1945 [Kristjánsson, J.E., 2002. Studies of the aerosol indirect effect from sulfate and black carbon aerosols.](#)

1946 [Journal of Geophysical Research 107 \(D15\), 4246.](#)

1947 [Kumar, R., Barth, M.C., Madronich, S., Naja, M., Carmichael, G.R., Pfister, G.G., Knute, C.,](#)

1948 [Brasseur, G.P., Ojha, N., Sarangi, T., 2014. Effects of dust aerosols on tropospheric chemistry](#)

1949 [during a typical pre-monsoon season dust storm in northern India. *Atmos. Chem. Phys.* 14,](#)

1950 [6813-6834.](#)

1951 ~~Lal, S., Naja, M., and Subbaraya, B.H.: Seasonal variations in surface ozone and its precursors over~~

1952 ~~an urban site in India. *Atmos. Environ.* 34, 2713–2724, 2000.~~

1953 ~~Lam, K.S., Wang, T.J., Chan, L.Y., Wang, T., and Harris, J.: Flow patterns influencing the seasonal~~

1954 ~~behavior of surface ozone and carbon monoxide at a coastal site near Hong Kong. *Atmos.*~~

1955 ~~*Environ.* 35, 3121–3135, 2001.~~

1956 Larson, S.M., and Cass, G.R.: Characteristics of summer midday low-visibility events in the Los

1957 Angeles area. *Environmental Science & Technology*. 23-281, 1989.

1958 Liao, H., Seinfeld, J.H., 2005. Global impacts of gas-phase chemistry aerosol interactions on direct

1959 radiative forcing by anthropogenic aerosols and ozone. *Journal of Geophysical Research* 110,

1960 D18208.

1961 Li, G.H., Zhang, R.Y., and Fan, J.W.: Impacts of black carbon aerosol on photolysis and ozone. [J].

1962 *Journal of Geophysical Research*. Vol. 110, D23206, doi:10.1029/2005JD005898, 2005.

1963 [Li, J., Bo, Y., Xie, S.: Estimating emissions from crop residue open burning in China based on](#)

1964 [statistics and MODIS fire products. *Journal of Environmental Sciences*, 2016, 44:158-167.](#)

1965 Li, J., Wang, Z., Wang, X., Yamaji, K., Takigawa, M., Kanaya, Y., Pochanart, P., Liu, Y., Irie, H.,

1966 Hu, B., Tanimoto, H., and Akimoto, H.: Impacts of aerosols on summertime tropospheric

1967 photolysis frequencies and photochemistry over Central Eastern China, *Atmos. Environ.*, 45,
1968 1817–1829, doi:10.1016/j.atmosenv.2011.01.016, 2011.

1969 Li, M., Wang, T., Xie, M., Li, S., Zhuang, B., Chen, P.: Agricultural fire impacts on ozone
1970 photochemistry over the Yangtze River Delta region, East China. *Journal of Geophysical*
1971 *Research: Atmospheres*, 2018.

1972 Li, M., Wang, T., Xie, M., Li, S., Zhuang, B., Chen, P.: Impacts of aerosol-radiation feedback on
1973 local air quality during a severe haze episode in Nanjing megacity, eastern China. *Tellus B:*
1974 *Chemical and Physical Meteorology*, 2017, 69(1):1339548.

1975 Li, M., Zhang, Q., Kurokawa, J., Woo, J.-H., He, K. B., Lu, Z. F., Ohara, T., Song, Y., Streets, D.
1976 G., Carmichael, G. R., Cheng, Y. F., Hong, C. P., Huo, H., Jiang, X. J., Kang, S., Liu, F., Su, H.,
1977 Zheng, B.: MIX: a mosaic Asian anthropogenic emission inventory under the international
1978 collaboration framework of the MICS-Asia and HTAP. *Atmos. Chem. Phys.*, 2017, 17, 935–963.

1979 Lin, W., Xu, X., Ge, B., Zhang, X., 2009. Characteristics of gaseous pollutants at Gucheng, a rural
1980 site southwest of Beijing. *J. Geophys. Res. Atmos.* 114, D00G14.

1981 Lin, W., Xu, X., Zhang, X., Tang, J., 2008. Contributions of pollutants from North China Plain to
1982 surface ozone at the Shangdianzi GAW Station. *Atmos. Chem. Phys.* 8, 5889–5898.

1983 Liu, P. F., Zhao, C. S., Gobel, T., Hallbauer, E., Nowak, A., Ran, L., Xu, W. Y., et al.: Hygroscopic
1984 properties of aerosol particles at high relative humidity and their diurnal variations in the North
1985 China Plain. *Atmos. Chem. Phys.*, 3479–3494, doi:10.5194/acp-11-3479-2011, 2011.

1986 Luo, C., St. John, J. C., Zhou, X. J., Lam, K. S., Wang, T., and Chameides, W. L.: A nonurban
1987 ozone air pollution episode over eastern China: Observation and model simulation, *J. Geophys.*
1988 *Res.*, 105, 1889–1908, 2000.

1989 Ma, J.Z., Xu, X.B., Zhao, C.S., Yan, P., 2012. A review of atmospheric chemistry research in China:
1990 photochemical smog, haze pollution, and gas-aerosol interactions. *Adv. Atmos. Sci.* 29, 1006–
1991 1026.

1992 McGowan, H. and Clark, A.: Identification of dust transport pathways from Lake Eyre, Australia

1993 using Hysplit, Atmos. Environ., 42, 6915–6925, 2008.

1994 [Meng, Z.Y., Xu, X.B., Yan, P., Ding, G.A., Tang, J., Lin, W.L., et al., 2009. Characteristics of trace](#)

1995 [gaseous pollutants at a regional background station in Northern China. Atmos.Chem. Phys. 9,](#)

1996 [927–936.](#)

1997 [Ministry of Environmental Protection of China \(MEP\), Ambient air quality standards \(GB 3095–](#)

1998 [2012\), 12 pp., China Environmental Science Press, Beijing, 2012.](#)

1999 Müller, T., Laborde, M., Kassell, G., and Wiedensohler, A.: Design and performance of a three-

2000 wavelength LED-based total scatter and backscatter integrating nephelometer, Atmos. Meas.

2001 Tech., 4, 1291–1303, doi:10.5194/amt-4-1291-2011, 2011.

2002 ~~[Monks, P.S., Archibald, A.T., Colette, A., Cooper, O., Coyle, M., Derwent, R., Fowler, D., Granier,](#)~~

2003 ~~[C., Law, K.S., Mills, G.E., Stevenson, D. S., Tarasova, O., Thouret, V., von Schneidmesser,](#)~~

2004 ~~[E., Sommariva, R., Wild, O., and Williams, M. L.: Tropospheric ozone and its precursors](#)~~

2005 ~~[from the urban to the global scale from air quality to short lived climate forcer, Atmos. Chem.](#)~~

2006 ~~[Phys., 15, 8889–8973, doi:10.5194/acp-15-8889-2015, 2015.](#)~~

2007 ~~Tropospheric ozone and its precursors... (PDF Download Available). Available from:~~

2008 ~~[https://www.researchgate.net/publication/278623484_Tropospheric_ozone_and_its_precursors_fr](https://www.researchgate.net/publication/278623484_Tropospheric_ozone_and_its_precursors_from_the_urban_to_the_global_scale_from_air_quality_to_short_lived_climate_forcer#pdf)~~

2009 ~~[om_the_urban_to_the_global_scale_from_air_quality_to_short_lived_climate_forcer#pdf](#)~~

2010 ~~[accessed Jun 24 2018].~~

2011 [Novelli, P.C., Masarile, K. A., Lang, P.M.: Distributions and recent changes of carbon monoxide](#)

2012 [in the lower troposphere. Journal of Geophysical Research Atmospheres, 1998, 103\(D15\).](#)

2013 Pan, X.L., Kanaya, Y., Wang, Z.F., Liu, Y., Pochanart, P., Akimoto, H., Sun, Y.L., Dong, H.B., Li,

2014 J., Irie, H., Takigawa, M., 2011. Correlation of black carbon aerosol and carbon monoxide in

2015 the high-altitude environment of Mt. Huang in Eastern China. Atmospheric Chemistry and

2016 Physics 11, 9735-9747.

2017 Petzold, A., Kopp, C., and Niessner, R.: The dependence of the specific attenuation cross-section
2018 on black carbon mass fraction and particle size, *Atmos. Environ.*, 31, 661–672, 1997.

2019 Qian, L., Yan, Y., and Qian, J.M.: An Observational Study on Physical and Optical Properties of
2020 Atmospheric Aerosol in Autumn in Nanjing [J]. *Meteorological and Environmental Research*
2021 2014, 5(2): 24 – 30.

2022 Roberts, P. T., Friedlander, S. K.: Analysis of sulfur in deposited aerosol particles by vaporization
2023 and flame photometric detection. *Atmospheric Environment*, 1976, 10(5), 403-408.

2024 Sassen, K., 2002. Indirect climate forcing over the western US from Asian dust storms. *Geophys.*
2025 *Res. Lett.* 29.

2026 Schleicher, N., Cen, K., Norra, S.: Daily variations of black carbon and element concentrations of
2027 atmospheric particles in the Beijing megacity – Part 1: General temporal course and source
2028 identification. *Chemie der Erde - Geochemistry*, 2013, 73(1):51-60.

2029 Schmid, O., Artaxo, P., Arnott, W. P., Chand, D., Gatti, L. V., Frank, G. P., Hoffer, A., Schnaiter,
2030 M., and Andreae, M. O.: Spectral light absorption by ambient aerosols influenced by biomass
2031 burning in the Amazon Basin. I: Comparison and field calibration of absorption measurement
2032 techniques, *Atmos. Chem. Phys.*, 6, 3443–3462, doi:10.5194/acp-6-3443-2006, 2006.

2033 Shao, M., Tang, X., Zhang, Y., Li, W., 2006. City clusters in China: air and surface water pollution.
2034 *Front. Ecol. Environ.* 4, 353–361.

2035 Shen, G. F., Yuan, S. Y., Xie, Y. N., Xia, S. J., Li, L., Yao, Y. K., Qiao, Y. Z., Zhang, J., Zhao, Q.Y.,
2036 Ding, A. J.: Ambient levels and temporal variations of PM_{2.5} and PM₁₀ at a residential site in
2037 the mega-city, Nanjing, in the western Yangtze River Delta, China. *J. Environ. Sci. Health Part A*
2038 2014, 49, 171–178.

2039 Shi, C., Wang, S., Liu, R., Zhou, R., Li, D., Wang, W., et al., 2015. A study of aerosol optical
2040 properties during ozone pollution episodes in 2013 over Shanghai, China. *Atmos. Res.* 153, 235–
2041 249.

2042 Schneidmesser, E., Sommariva, R., Wild, O., and Williams, M. L.: Tropospheric ozone and its

2043 ~~precursors from the urban to the global scale from air quality to short lived climate forcer,~~
2044 ~~Atmos. Chem. Phys., 15, 8889–8973, doi:10.5194/acp-15-8889-2015, 2015.~~

2045 Song, W.; Jia, H.; Huang, J.; Zhang, Y. A satellite-based geographically weighted regression model
2046 for regional PM_{2.5} estimation over the Pearl River Delta region in China. Remote Sens.
2047 Environ. 2014, 154, 1–7.

2048 Spackman, J. R., Schwarz, J. P., Gao, R. S., Watts, L. A., Thomson, D. S., Fahey, D. W., Holloway,
2049 J. S., de Gouw, J. A., Trainer, M., and Ryerson, T. B.: Empirical correlations between black
2050 carbon aerosol and carbon monoxide in the lower and middle troposphere, Geophys. Res. Lett.,
2051 35(19), L19816, doi:10.1029/2008GL035237, 2008.

2052 Stein, A. F., Draxler, R. R., Rolph, G. D., Stunder, B. J. B., Cohen, M. D., and Ngan, F.: NOAA'S
2053 Hysplit Atmospheric Transport and Dispersion Modeling System, Bull. Amer. Meteor. Soc.,
2054 96, 2059–2077. doi: <http://dx.doi.org/10.1175/BAMS-D-14-00110.1>, 2016.

2055 Streets, D.G., Gupta, S., Waldhoff, S.T., Wang, M.Q., Bond, T.C., Bo, Y.Y., 2001. Black carbon
2056 emissions in China. Atmospheric Environment 35, 4281-4296.

2057 Tegen, I., Schepanski, K.:The global distribution of mineral dust. IOP Conference Series: Earth and
2058 Environmental Science, 2009, 7:012001.

2059 Tu, J., Xia, Z. G., Wang, H. S., and Li, W. Q.: Temporal variations in surface ozone and its
2060 precursors and meteorological effects at an urban site in China, Atmos. Res., 85, 310–337, 2007.

2061 van Donkelaar, A., Martin, R. V., Brauer, M., Kahn, R., Levy, R., Verduzco, C., and Villeneuve, P.
2062 J.: Global estimates of ambient fine particulate matter concentrations from satellite-based
2063 aerosol optical depth: development and application, Environ. Health Perspectives, 118, 847–
2064 855, 2010.

2065 [Verma, R.L., Sahu, L.K., Kondo, Y., Takegawa, N., Han, S., Jung, J.S., Kin, Y.J., Fan, S., Sugimoto,](#)
2066 [N., Shammaa, M.H., Zhang, Y.H., Zhao, Y., 2010. Temporal variations of black carbon in](#)
2067 [Guangzhou, China, in summer 2006. Atmospheric Chemistry and Physics 10, 6471-6485.](#)

2068 [Virkkula, A., Makela, T., Hillamo, R., Yli-Tuomi, T., Hirsikko, A., Hameri, K., and Koponen, I. K.:](#)
2069 [A simple procedure for correcting loading effects of aethalometer data, J. Air Waste Manage.,](#)
2070 [57, 1214–1222, doi:10.3155/1047-3289.57.10.1214, 2007.](#)

2071 [von Schneidmesser, E., Monks, P. S., and Plass-Duelmer, C.: Global comparison of VOC and CO](#)
2072 [observations in urban areas, Atmos. Environ., 2010, 44\(39\): 5053–5064.](#)

2073 Wang, G. H., Huang, L. M., Gao, S. X., Gao, S. T., and Wang, L.S.: Characterization of watersoluble
2074 species of PM₁₀ and PM_{2.5} aerosols in urban area in Nanjing, China, Atmos. Environ.,
2075 36,1299–1307, 2002.

2076 [Wang, H. L., Zhuang, Y. H., Wang, Y., Sun, Y. L., Yuan, H., Zhuang, G. S., Hao, Z. P.: Long-term](#)
2077 [monitoring and source apportionment of PM_{2.5}/PM₁₀ in Beijing, China. Journal of](#)
2078 [Environmental Sciences, 2008, 20\(11\): 1323-1327.](#)

2079 [Wang, M., Shao, M., Chen, W., Yuan, B., Lu, S., Zhang, Q., Zeng, L., Wang, Q.: A temporally and](#)
2080 [spatially resolved validation of emission inventories by measurements of ambient volatile organic](#)
2081 [compounds in Beijing, China. Atmos. Chem. Phys., 2014, 14\(12\): 5871–5891.](#)

2082 Wang, M.Y., Cao, C.X., Li, G.S., and Singh, R.P.: Analysis of a severe prolonged regional haze
2083 episode in the Yangtze River Delta, China, Atmos. Environ., 102, 112-121, 2015.

2084 [Wang, P., Zhao, W.: Assessment of ambient volatile organic compounds \(VOCs\) near major roads](#)
2085 [in urban Nanjing, China\[J\]. Atmospheric Research, 2008, 89\(3\):0-297.](#)

2086 [Wang, T., Cheung, V.T.F., Anson, M., Li, Y.S., 2001a. Ozone and related gaseous pollutants in the](#)
2087 [boundary layer of eastern China: overview of the recent measurements at a rural site. Geophys.](#)
2088 [Res. Lett. 28, 2373–2376.](#)

2089 [Wang, T., Cheung, T., Li, Y., Yu, X., Blake, D., 2002. Emission characteristics of CO, NO_x, SO₂](#)
2090 [and indications of biomass burning observed at a rural site in eastern China. J. Geophys. Res.-](#)

2091 [Atmos. 107.](#)

2092 [Wang, T., Poon, C.N., Kwok, Y.H., Li, Y.S., 2003. Characterizing the temporal variability and](#)

2093 [emission patterns of pollution plumes in the Pearl River Delta of China. Atmos. Environ.37,](#)

2094 [3539–3550.](#)

2095 [Wang, T., Wong, C., Cheung, T., Blake, D., Arimoto, R., Baumann, K., et al., 2004. Relationships](#)

2096 [of trace gases and aerosols and the emission characteristics at Lin'an, a rural site in eastern China,](#)

2097 [during spring 2001. J. Geophys. Res.-Atmos. 109.](#)

2098 Wang, T., Xue, L. K., Brimblecombe, P., Lam, Y.F., Li, L., and Zhang, L.: Ozone pollution in China:

2099 A review of concentrations, meteorological influences, chemical precursors, and effects.

2100 Science of the Total Environment., 575, 1582–1596, 2017.

2101 ~~Wang, T.J., Lam, K.S., Xie, M., Wang, X.M., Carmichael, G., and Li, Y.S.: Integrated studies of a~~

2102 ~~photochemical smog episode in Hong Kong and regional transport in the Pearl River Delta of~~

2103 ~~China. Tellus Ser. B Chem. Phys. Meteorol. 58, 31–40, 2006.~~

2104 Wang, T. J., Zhuang, B. L., Li, S., Liu, J., Xie, M., Yin, C. Q., Zhang, Y., Yuan, C., Zhu, J. L., Ji,

2105 L. Q., and Han, Y.: The interactions between anthropogenic aerosols and the East Asian

2106 summer monsoon using RegCCMS. J. Geophys. Res. Atmos., 120,

2107 doi:10.1002/2014JD022877, 2015.

2108 Wang, X., Li, J., Zhang, Y., Xie, S., Tang, X., 2009b. Ozone source attribution during a severe

2109 photochemical smog episode in Beijing, China. Sci. China, Ser. B: Chem. 52, 1270–1280.

2110 Wang, Y.Q., Stein, A.F., Draxler, R.R., de la Rosa, J.D., and Zhang, X.Y.: Global sand and dust

2111 storms in 2008: Observation and HYSPLIT model verification, Atmos. Environ., 45, 6368-

2112 6381, 2011.

2113 [Wang, Y., Ying, Q., Hu, J., Zhang, H.: Spatial and temporal variations of six criteria air pollutants](#)

2114 [in 31 provincial capital cities in China during 2013–2014. Environment International, 2014,](#)
2115 [73:413–422.](#)

2116 [Wang, Y., Wang, X., Kondo, Y., Kajino, M., Munger, J.W., Hao, J., 2011b. Black carbon and its](#)
2117 [correlation with trace gases at a rural site in Beijing: top-down constraints from ambient](#)
2118 [measurements on bottom-up emissions. Journal of Geophysical Research 116, D24304.](#)

2119 Wang, Y., Zhuang, G. S., Zhang, X. Y., Huang, K., Xu, Chang, Tang, A. H., Chen, J. M., and An,
2120 Z. S.: The ion chemistry, seasonal cycle, and sources of PM_{2.5} and TSP aerosol in Shanghai,
2121 Atmos. Environ., 40, 2935–2952, 2006.

2122 [Wang, Z., Li, J., Wang, X., Pochanart, P., Akimoto, H.: Modeling of Regional High Ozone Episode](#)
2123 [Observed at Two Mountain Sites \(Mt. Tai and Huang\) in East China. Journal of Atmospheric](#)
2124 [Chemistry, 2006, 55\(3\):253-272.](#)

2125 [Wang, Z., Li, Y., Chen, T., Zhang, D., Sun, F., Pan, L.: Spatial-temporal characteristics of PM_{2.5} in](#)
2126 [Beijing in 2013. Acta Geogr. Sin. 2015, 70, 110–120.](#)

2127 Weingartner, E., Saathoff, H., Schnaiter, M., Streit, N., Bitnar, B., and Baltensperger, U.:
2128 Absorption of light by soot particles: determination of the absorption coefficient by means of
2129 aethalometers, J. Aerosol Sci., 34, 1445–1463, doi:10.1016/S0021-8502(03)00359-8, 2003.

2130 [Wu, D., Liu, Q., Lian, Y., Bi, X., Li, F., Tan, H., Liao, B., Chen, H., Hazy weather formation and](#)
2131 [visibility deterioration resulted from fine particulate \(PM_{2.5}\) pollutions in Guangdong and](#)
2132 [Hong Kong. J. Environ. Sci. Circumst. 2012, 32, 2660–2669.](#)

2133 ~~Wu, D., Wu, C., Liao, B., Chen, H., Wu, M., Li, F., Tan, H., Deng, T., Li, H., Jiang, D., and Yu, J.~~
2134 ~~[Z.: Black carbon over the South China Sea and in various continental locations in South China,](#)~~
2135 ~~[Atmos. Chem. Phys., 13, 12257–12270, doi:10.5194/acp-13-12257-2013, 2013.](#)~~

2136 Wu, Y.; Guo, J.; Zhang, X.; Tian, X.; Zhang, J.; Wang, Y.; Duan, J.; Li, X. Synergy of satellite and
2137 ground based observations in estimation of particulate matter in eastern China. Sci. Total

2138 Environ. 2012, 433, 20–30.

2139 Xiao, Z., Bi, X., Feng, Y., Wang, Y., Zhou, J., Fu, X., Weng, Y., 2012. Source apportionment of
2140 ambient PM10 and PM2.5 in urban area of Ningbo City. Res. Environ. Sci. (China) 5, 549–
2141 555.

2142 Xiao, Z. M., Zhang, Y. F., Hong, S. M., Bi, X. H., Jiao, L., Feng, Y. C., Wang, Y. Q.: Estimation of
2143 the Main Factors Influencing Haze, Based on a Long-term Monitoring Campaign in Hangzhou,
2144 China. Aerosol & Air Quality Research., 2011, 11, 873-882.

2145 Xie, M., Zhu, K.G., Wang, T.J., Chen, P.L., Han, Y., Li, S., Zhuang, B.L., and Shu, L., Temporal
2146 characterization and regional contribution to O3 and NOx at an urban and a suburban site in
2147 Nanjing, China. Science of the Total Environment., 551–552, 533–545, 2016.

2148 Xue, L., Wang, T., Louie, P.K.K., Luk, C.W.Y., Blake, D.R., Xu, Z., 2014a. Increasing external
2149 effects negate local efforts to control ozone air pollution: a case study of Hong Kong and
2150 implications for other Chinese cities. Environ. Sci. Technol. 48, 10769–10775.

2151 Yang, S. J., He, H. P., Lu, S. L., Chen, D., Zhu, J. X.: Quantification of crop residue burning in the
2152 field and its influence on ambient air quality in Suqian, China. Atmospheric Environment,
2153 2008,42(9):1961-1969.

2154 Yan, S.; Cao, H.; Chen, Y.; Wu, C.; Hong, T.; Fan, H. Spatial and temporal characteristics of air
2155 quality and air pollutants in 2013 in Beijing. Environ. Sci. Pollut. Res. 2016, 23, 1–12.

2156 Yin, S., Wang, X.F, Xiao, Y., Tani, H., Zhong, G.S., Sun, Z.Y.: Study on spatial distribution of crop
2157 residue burning and PM2.5 change in China. Environmental Pollution, 2016, 220(Pt A):204-221.

2158 Yang, Y., Liu, X., Qu, Y., Wang, J., An, J., Zhang, Y., Zhang, F.: Formation mechanism of
2159 continuous extreme haze episodes in the megacity Beijing, China, in January 2013. Atmos.
2160 Res. 155, 192–203, 2015.

2161 Yan, P., Tang, J., Huang, J., Mao, J. T., Zhou, X. J., Liu, Q., Wang, Z. F., and Zhou, H. G.: The
2162 measurement of aerosol optical properties at a rural site in Northern China, Atmos. Chem.

2163 ~~Phys., 8, 2229–2242, doi:10.5194/acp-8-2229-2008, 2008.~~

2164 Yi, R., Wang, Y.L., Zhang, Y.J., Shi, Y., Li, M.S., 2015. Pollution characteristics and influence
2165 factors of ozone in Yangtze River Delta. *Acta Sci. Circumst.* 35, 2370–2377 (in Chinese).

2166 Yu, J., Wang, W., Zhou, J., Xu, D., Zhao, Q., He, L., 2015. Analysis of pollution characteristics and
2167 sources of PM_{2.5} in winter of Ningbo City. *Environ. Sci. Technol. (China)* 8, 150–155.

2168 Zhang, Q., Streets, D.G., Carmichael, G.R., He, K.B., Huo, H., Kannari, A., Klimont, Z., Park, I.S.,
2169 Reddy, S., Fu, J.S., Chen, D., Duan, L., Lei, Y., Wang, L.T., Yao, Z.L., 2009. Asian emissions
2170 in 2006 for the NASA INTEX-B mission. *Atmos. Chem. Phys.* 9, 5131–5153.

2171 Zhang, Y. H., Hu, M., Zhong, L. J., Wiedensohler, A., Liu, S. C., Andreae, M. O., Wang, W., Fan, S.
2172 J.: Regional integrated experiments on air quality over Pearl River Delta 2004 (PRIDE-
2173 PRD2004): overview. *Atmos. Environ.* 42, 6157–6173, 2008.

2174 Zhang, X. Y., Wang, Y. Q., Niu, T., Zhang, X. C., Gong, S.L., Zhang, Y.M., Sun, T.Y., 2012.
2175 Atmospheric aerosol compositions in China: spatial/temporal variability, chemical signature,
2176 regional haze distribution and comparisons with global aerosols. *Atmospheric Chemistry and*
2177 Physics 12, 779-799.

2178 Zhang, X.Y., Wang, Y.Q., Zhang, X.C., Guo, W., Gong, S.L., 2008. Carbonaceous aerosol
2179 composition over various regions of China during 2006. *Journal of Geophysical Research* 113,
2180 D14111.

2181 Zhang, Y. L., Cao, F. Fine particulate matter (PM_{2.5}) in China at a city level. *Sci. Rep.* 2015, 5,
2182 14884.

2183 Zhang, Y., Shao, K., Tang, X., 1998. The study of urban photochemical smog pollution in China.
2184 *Acta Scientiarum Naturalium-Universitatis Pekinensis* 34, 392–400.

2185 Zheng, J., Zhong, L., Wang, T., Louie, P.K.K., Li, Z., 2010. Ground-level ozone in the Pearl River

2186 Delta region: analysis of data from a recently established regional air quality monitoring
2187 network. *Atmos. Environ.* 44, 814–823.

2188 ~~Zhang, Y.H., Hu, M., Zhong, L.J., Wiedensohler, A., Liu, S.C., Andreae, M.O., Wang, W., Fan,~~
2189 ~~S.J.: Regional integrated experiments on air quality over Pearl River Delta 2004 (PRIDE-~~
2190 ~~PRD2004): overview. *Atmos. Environ.* 42, 6157–6173, 2008.~~

2191 Zhu, J. L., Wang, T. J., Talbot, R. H., Mao, H. T., Hall, C. B., Yang, X. Q., Fu, C. B., Zhuang, B.
2192 L., Li, S., Han, Y., Huang, X., 2012. Characteristics of atmospheric Total Gaseous Mercury
2193 (TGM) observed in urban Nanjing, China. *Atmospheric Chemistry and Physics* 12, 12103-
2194 12118.

2195 Zhuang, B.L., Liu, L., Shen, F.H., Wang, T.J., Han, Y., 2010. Semidirect radiative forcing of
2196 internal mixed black carbon cloud droplet and its regional climatic effect over China. *Journal*
2197 *of Geophysical Research* 115, D00K19.

2198 Zhuang, B.L., Liu, Q., Wang, T.J., Yin, C.Q., Li, S., Xie, M., Jiang, F., Mao, H.T., 2013.
2199 Investigation on semi-direct and indirect climate effects of fossil fuel black carbon aerosol
2200 over China. *Theoretical and Applied Climatology* 114, 651-672.

2201 Zhuang, B. L., Li, S., Wang, T. J., Deng, J. J., Xie, M., Yin, C. Q., and Zhu, J. L.: Direct radiative
2202 forcing and climate effects of anthropogenic aerosols with different mixing states over China,
2203 *Atmos. Environ.*, 79, 349–361, doi:10.1016/j.atmosenv.2013.07.004, 2013b.

2204 Zhuang, B. L., Li, S., Wang, T. J., Liu, J., Chen, H. M., Chen, P. L., Li, M. M., Xie, M.: Interaction
2205 between the Black Carbon Aerosol Warming Effect and East Asian Monsoon Using RegCM4.
2206 *Journal of Climate*, 2018, 31(22):9367-9388.

2207 Zhuang, B. L., Wang, T. J., Liu, J., Li, S., Xie, M., Han, Y., Chen, P. L., Hu, Q. D., Yang X.Q., Fu,
2208 C. B., and Zhu, J. L.: The surface aerosol optical properties in the urban area of Nanjing, west

2209 GTH River Delta, China. Atmos. Chem. Phys., 17, 1143–1160, doi:10.5194/acp-17-1143-
2210 2017, 2017.

2211 Zhuang, B. L., Wang, T. J., Liu, J., Li, S., Xie, M., Yang, X. Q., Fu, C. B., Sun, J. N., Yin, C. Q.,
2212 Liao, J. B., Zhu, J. L., and Zhang, Y.: Continuous measurement of black carbon aerosol in urban
2213 Nanjing of Yangtze River Delta, China, Atmos. Environ., 89, 415–424, 2014b.

2214 Zhuang, B. L., Wang, T. J., Liu, J., Ma, Y., Yin, C. Q., Li, S., Xie, M., Han, Y., Zhu, J. L., Yang,
2215 X. Q., and Fu, C. B.: Absorption coefficient of urban aerosol in Nanjing, west Yangtze River
2216 Delta, China, Atmos. Chem. Phys., 15, 13633–13646, doi:10.5194/acp-15-13633-2015, 2015.

2217 Zhuang, B. L., Wang, T. J., Li, S., Liu, J., Talbot, R., Mao, H. T., Yang, X. Q., Fu, C. B., Yin, C. Q.,
2218 Zhu, J. L., Che, H. Z., and Zhang, X. Y.: Optical properties and radiative forcing of urban aerosols
2219 in Nanjing, China, Atmos. Environ., 83, 43–52, 2014a.

2220

2221

2222

2223

2224

2225 **Figure Caption**

2226 Fig 1. Time series of the concentrations of PM₁₀, PM_{2.5}, and BC from September 2016 to February
2227 2017 at Gulou site, Nanjing, China.

2228 Fig 2. Seasonal variations of (a) BC, (b) PM_{2.5}, and (c) PM₁₀. Red markers represent the monthly
2229 averages at Gulou site, Nanjing, China.

2230 Fig 3. 6-month mean diurnal variations of BC, PM_{2.5}, and PM₁₀ at Gulou site, Nanjing, China from
2231 September 2016 to February 2017.

2232 Fig.4 Time series of particles from September 2016 to February 2017 at Gulou site.

2233 Fig 5. Seasonal variations of (a) O₃, (b) NO_x, (c) CO, and (d) NO_y. The 10, 25, 50, 75, and 90%
2234 percentile values of each are shown in black, and red markers represent the monthly averages.

2235 Fig 6. 6-month mean diurnal variations of (a) trace gases and (b) UV (ultra-violet radiation) at
2236 Gulou site from September 2016 to February 2017.

2237 Fig 7. Scatter plots of (a) O₃-NO_x color-coded with air temperature (T) and (b) PM_{2.5}-Vis color-
2238 coded with relative humidity (RH).

2239 Fig 8. Scatter plots of (a) PM_{2.5}-O₃ and (b) BC-O₃ color-coded with air temperature (T).

2240 Fig 9. Scatter plots of (a) O₃-UV and (b) PM_{2.5}-UV color coded with O₃. Fig 10. Scatter plots of (a)
2241 CO-NO_x, (b) PM_{2.5}-NO_x, and (c) BC-NO_x color-coded with O₃.

2242 Fig 11. Clusters of 96 h back trajectories arriving at the study site at 100 m in 2016 fall.

2243 Fig 12. The 10, 25, 50, 75, and 90% percentile values in each cluster of back trajectories in 2016
2244 fall of (a) BC, (b) PM_{2.5}, (c) PM_{2.5}/PM₁₀, (d) CO, (e) O₃, (f) NO_y, (g) α_{ts} , and (h) ω_0 . Black
2245 markers represent the averages.

2246 Fig 13. Clusters of 96 h back trajectories arriving at the study site at 100m in 2016 winter.

2247 Fig 14. The 10, 25, 50, 75, and 90% percentile values in each cluster of back trajectories in 2016
2248 winter of (a) BC, (b) PM_{2.5}, (c) PM_{2.5}/PM₁₀, (d) CO, (e) O₃, (f) NO_y, (g) α_{ts} , and (h) ω_0 . Black
2249 markers represent the averages.

2250 Fig 15. Time series during December 3-6, 2016, for (a) PM_{2.5}, BC and O₃ with associated
2251 meteorological parameters, trace gases and (b) optical parameters. Red markers represent O₃ over
2252 daily maximum average during winter. Weather charts on (c) 4th and (d) 5th December. (f) 96h
2253 backward trajectories analysis ending at 1200 UTC on 5th December

2254
2255

2256

Table

2257

Table 1 Measurements at Gulou site.

Measurement		Instrument	Resolution
Meteorological parameters	T (°C)	Thermo Instruments, THOM 1405-DF	
	P (atm)	Thermo Instruments, THOM 1405-DF	
	RH (%)	Thermo Instruments, THOM 1405-DF	
	Rainfall (mm)		
	Vis (m)	Visibility Meter, GSN-1	
	UV (W/m ²)		
Particles	BC (ng/m ³)	Aethalometer, Model AE-31	1 ng/m ³
	PM _{2.5} (µg/m ³)	Thermo Instruments, THOM 1405-DF	0.1 µg/m ³
	PM ₁₀ (µg/m ³)	Thermo Instruments, THOM 1405-DF	0.1 µg/m ³
Gaseous pollutant	CO (ppb)	Thermo Instruments, TEI 48i	1 ppb
	NO _x (ppb)	Thermo Instruments, TEI 42i	0.4 ppb
	NO _y (ppb)	Thermo Instruments, TEI 42iY	0.4 ppb
	O ₃ (ppb)	Thermo Instruments, TEI 49i	0.01 ppb
Optical parameters	SC (Mm ⁻¹)	Nephelometer, Aurora 3000	10 ⁻³ Mm ⁻¹
	BSP (Mm ⁻¹)	Nephelometer, Aurora 3000	10 ⁻³ Mm ⁻¹
	AAC (Mm ⁻¹)	Aethalometer, Model AE-31	10 ⁻³ Mm ⁻¹

2258

2259

2260

Table 2 Statistics of general meteorological parameters at Gulou site for the 6-month period

2261

September 2016~ February 2017.

Month	Temp (°C)	Pres (hPa)	RH (%)	Rainfall (mm)	Vis (km)	UV (W/m ²)
Sep	24.88	996.97	69.41	2.34	11.84	10.36
Oct	18.37	1003.01	85.01	3.12	9.07	5.28
Nov	12.36	1007.87	77.15	1.19	8.99	5.67
Dec	8.74	1010.53	70.33	0.81	7.61	5.03
Jan	6.49	1010.89	70.65	0.59	9.23	4.94
Feb	7.72	1009.65	59.99	0.45	10.24	7.04

2262

2263

2264

2265

2266 Table 3 Statistics of the three particles during the study period at Gulou site, Nanjing, China

	SON	DJF	Cold seasons		
	Mean \pm STD	Mean \pm STD	Mean \pm STD	Maximum	Minimum
BC ($\mu\text{g}/\text{m}^3$)	2.126 \pm 1.457	3.083 \pm 1.827	2.602 \pm 1.720	15.609	0.064
PM _{2.5} ($\mu\text{g}/\text{m}^3$)	43.1 \pm 25.4	73.2 \pm 40.0	58.2 \pm 36.8	256.2	0.8
PM ₁₀ ($\mu\text{g}/\text{m}^3$)	67.6 \pm 39.1	105.0 \pm 54.0	86.3 \pm 50.8	343.4	1.1

2267

2268

2269 Table 4 Statistics of trace gases during the study period

	SON	DJF	Cold seasons		
	Mean \pm STD	Mean \pm STD	Mean \pm STD	Maximum	Minimum
CO (ppb)	753 \pm 353	950 \pm 388	851 \pm 384	2852	176
NO _x (ppb)	21.4 \pm 13.4	25.6 \pm 15.5	23.5 \pm 14.7	80.0	2.7
NO _y (ppb)	28.6 \pm 20.5	37.0 \pm 23.1	32.8 \pm 22.3	158.4	3.6
O ₃ (ppb)	42.3 \pm 40.1	33.1 \pm 24.4	37.7 \pm 35.5	235.7	0.2

2270

2271

2272 Table 5 Statistics of maximum and number of exceedances of O₃ and PM_{2.5} compared with the

2273 National Ambient Air Quality Standards in China.

Aerosol	Mean \pm STD ($\mu\text{g}/\text{m}^3$)	Max ($\mu\text{g}/\text{m}^3$)	N.o.E.
PM _{2.5}	58.2 \pm 36.8	256.2	48
PM ₁₀	86.3 \pm 50.8	343.4	14
O ₃	80.8 \pm 71.8	235.7	37

2274 N.o.E. of PM_{2.5} accounts for days with 24 h average over 75 $\mu\text{g}/\text{m}^3$. N.o.E. of PM₁₀ accounts for days2275 with 24 h average over 150 $\mu\text{g}/\text{m}^3$. N.o.E. of O₃ accounts for days with maximum 8 h average exceed2276 160 $\mu\text{g}/\text{m}^3$.

2277

2278

2279

2280

2281

2282

2283

2284

2285

2286

2287 Table 6 Statistics of aerosols at Gulou site with and without rainfall for the 6-month period

2288

September 2016~ February 2017

Aerosols	With Rainfall			Without Rainfall		
	Mean \pm STD	Maximum	Minimum	Mean \pm STD	Maximum	Minimum
BC ($\mu\text{g}/\text{m}^3$)	1.676 ± 1.261	8.256	0.064	2.723 ± 1.735	15.608	0.211
PM _{2.5} ($\mu\text{g}/\text{m}^3$)	31.2 ± 27.6	218.4	1.2	61.9 ± 36.3	256.2	0.8
PM ₁₀ ($\mu\text{g}/\text{m}^3$)	54.3 ± 44.8	307.3	3.9	89.1 ± 47.3	319.6	4.5
CO (ppb)	659 ± 240	2194	176	876 ± 392	2852	228
NO _x (ppb)	20.4 ± 12.7	75.5	2.9	23.9 ± 14.9	80	2.7
NO _y (ppb)	25.2 ± 16.8	110.3	3.6	33.8 ± 22.8	158.4	5.2
O ₃ (ppb)	22.3 ± 17.1	81.7	0.3	39.7 ± 34.6	235.7	0.2

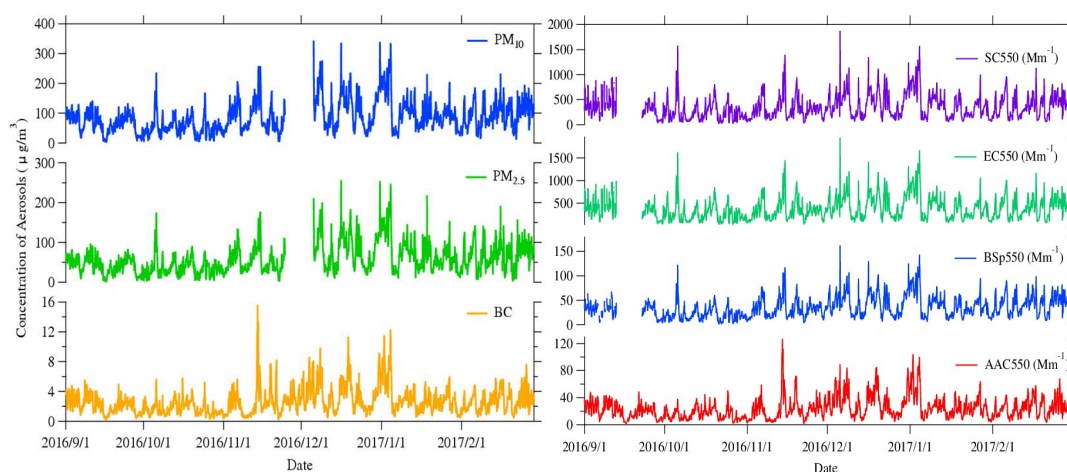
2289

2290

2291

2292

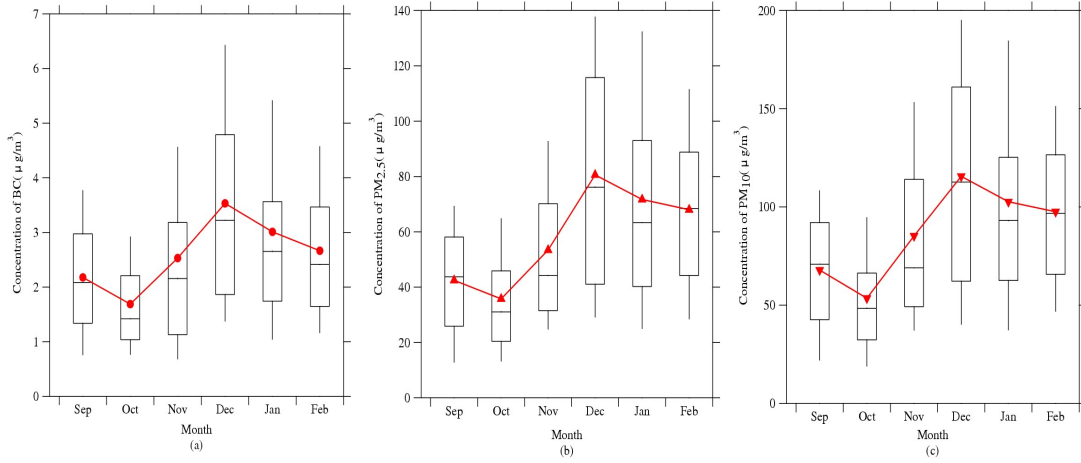
2293

Figures

2294

2295 Fig 1. Time series of (a) concentrations and (b) optical properties of PM₁₀, PM_{2.5}, and BC from
 2296 September 2016 to February 2017 at Gulou site, Nanjing, China.

2297

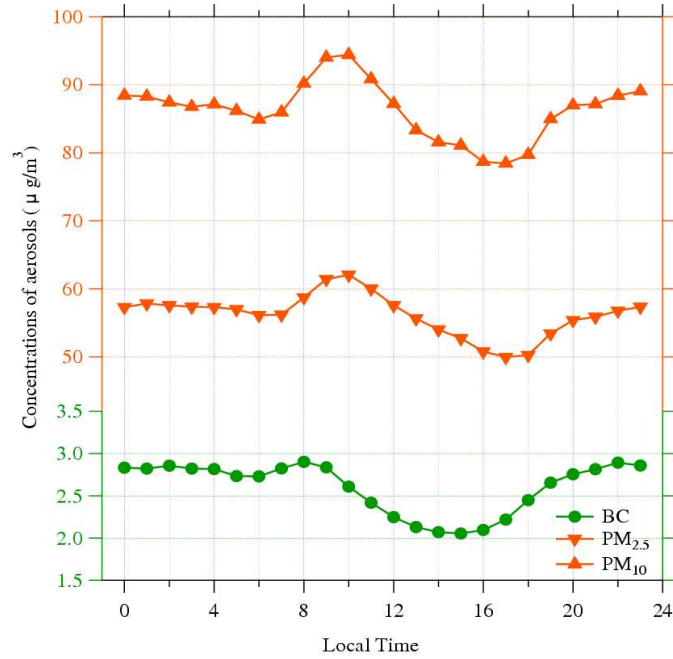


2298

2299 Fig 2. Seasonal variations of (a) BC, (b) PM_{2.5}, and (c) PM₁₀. Red markers represent the monthly

2300

averages at Gulou site, Nanjing, China.

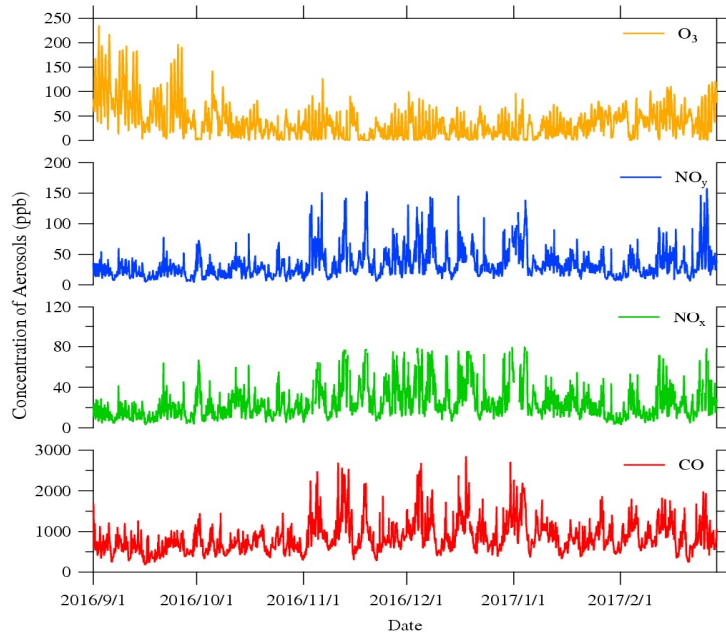


2301

2302 Fig 3. 6-month mean diurnal variations of BC, PM_{2.5}, and PM₁₀ at Gulou site, Nanjing, China

2303

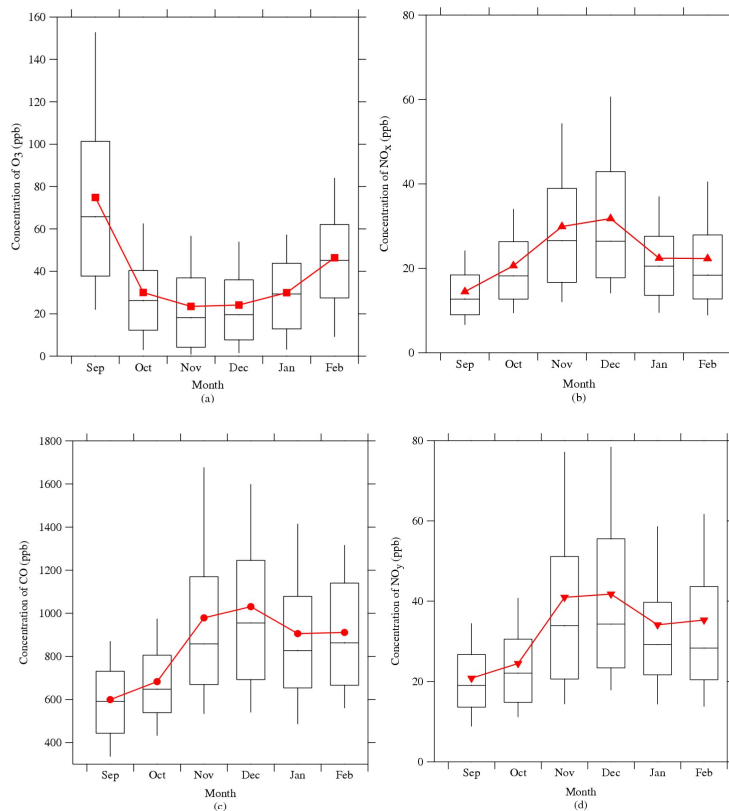
from September 2016 to February 2017



2304

2305

Fig.4 Time series of particles from September 2016 to February 2017 at Gulou site.



2306

2307

2308

Fig 5. Seasonal variations of (a) O₃, (b) NO_x, (c) CO, and (d) NO_y. The 10, 25, 50, 75, and

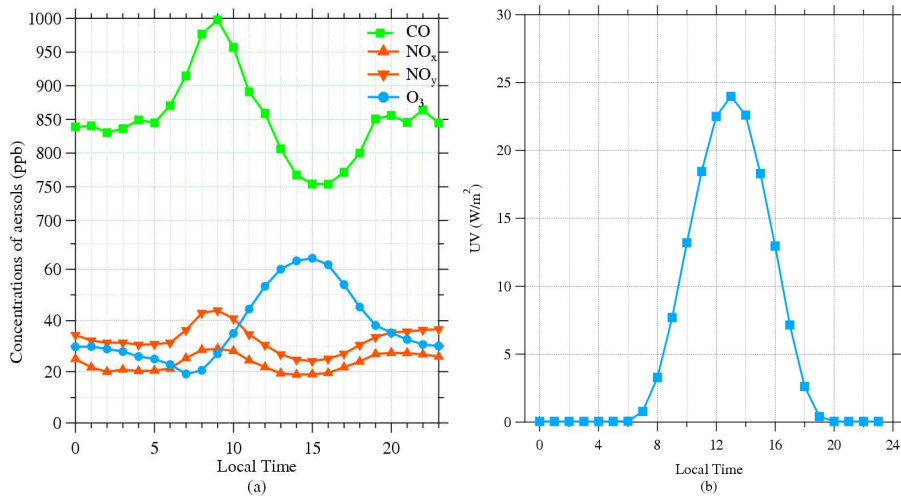
2309

90% percentile values of each are shown in black, and red markers represent the monthly

2310

averages.

2311



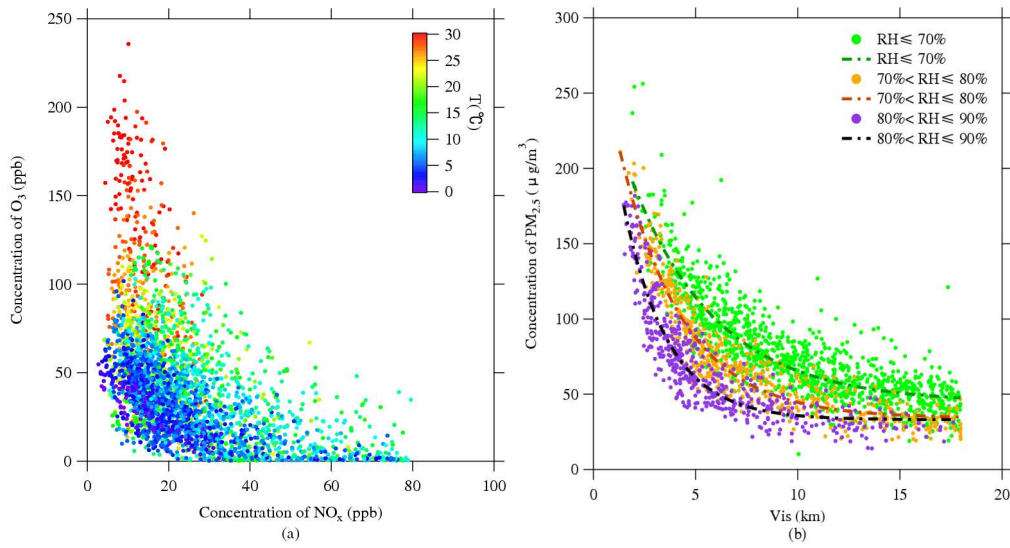
2312

2313 Fig 6. 6-month mean diurnal variations of (a) trace gases and (b) UV (ultra-violet radiation) at

2314

Gulou site from September 2016 to February 2017.

2315



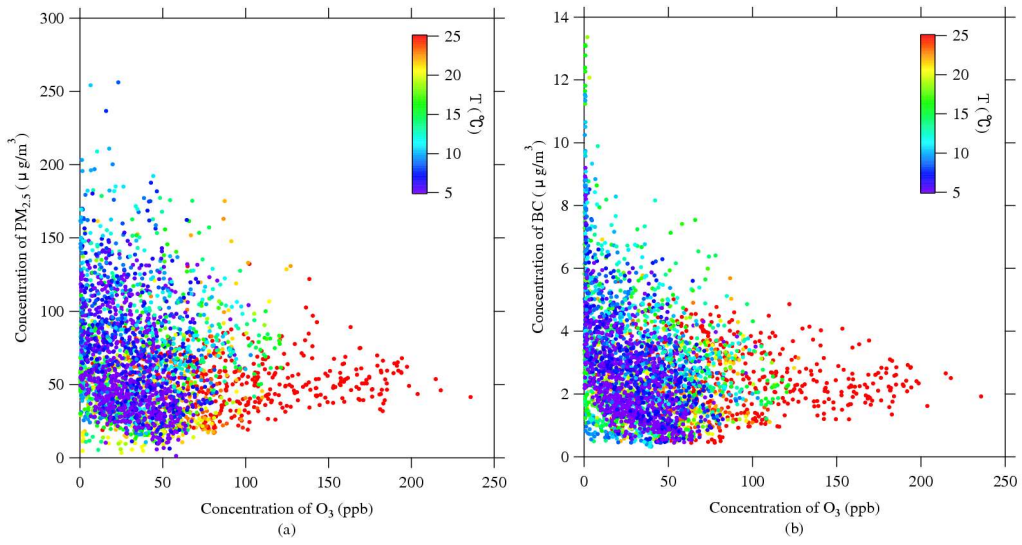
2316

2317 Fig 7. Scatter plots of (a) O₃-NO_x color-coded with air temperature (T) and (b) PM_{2.5}-Vis color-

2318

coded with relative humidity (RH).

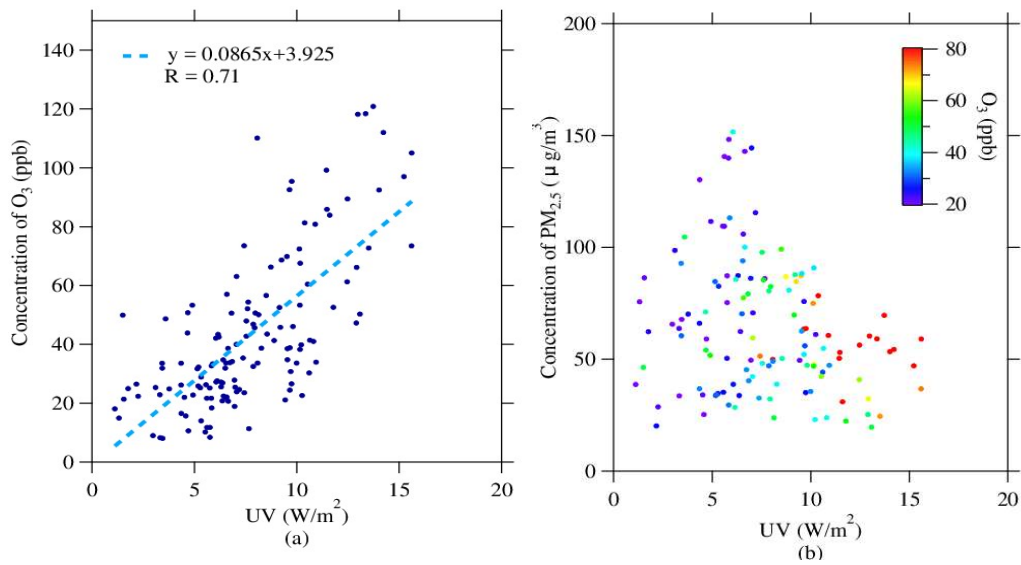
2319



2320

2321 Fig 8. Scatter plots of (a) PM_{2.5}-O₃ and (b) BC-O₃ color-coded with air temperature (T).

2322

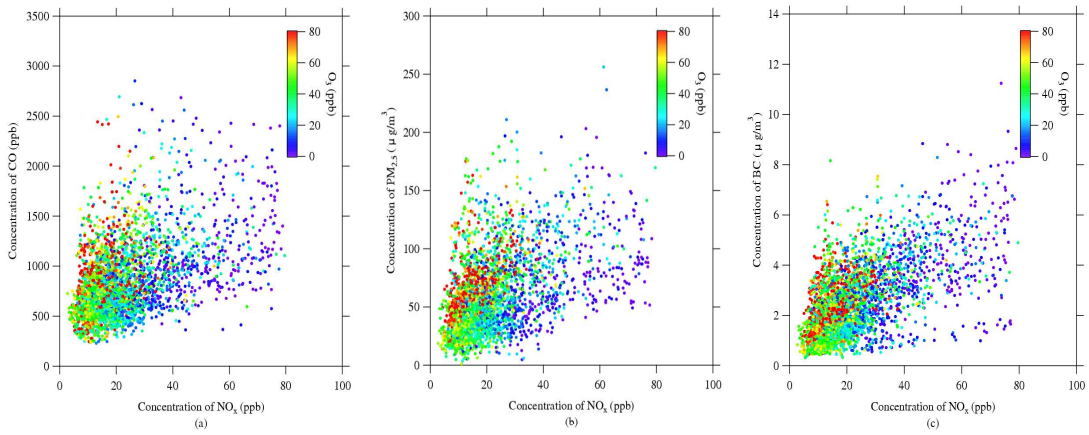


2323

2324

Fig 9. Scatter plots of (a) O₃-UV and (b) PM_{2.5}-UV color coded with O₃.

2325

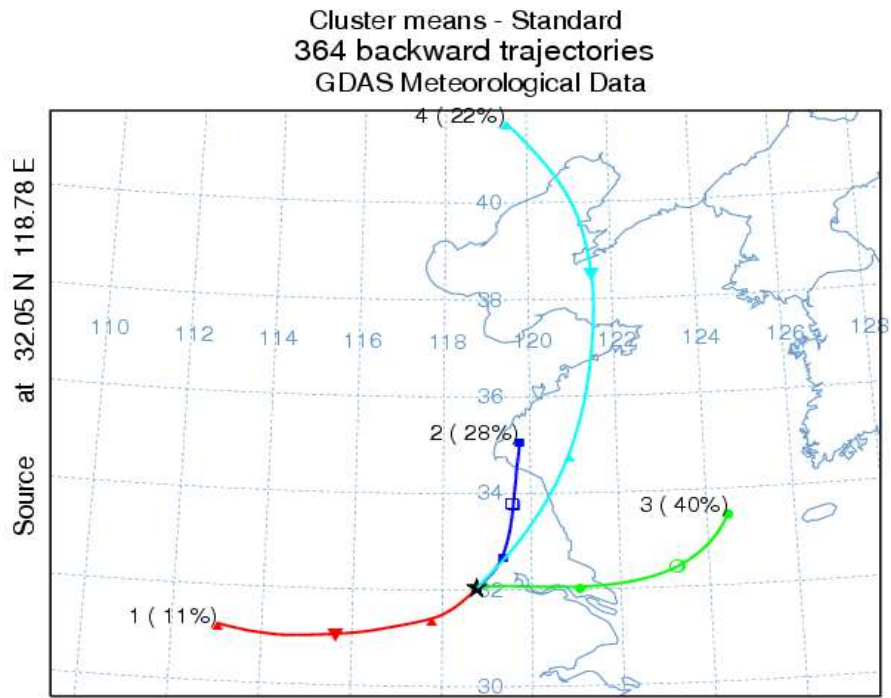


2326

2327

Fig 10. Scatter plots of (a) CO-NO_x, (b) PM_{2.5}-NO_x, and (c) BC-NO_x color-coded with O₃.

2328



2329

2330

Fig 11. Clusters of 96 h back trajectories arriving at the study site at 100 m in 2016 fall.

2331

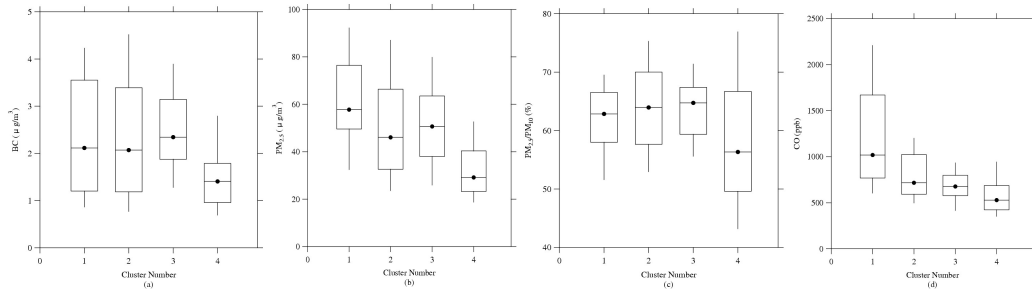
2332

2333

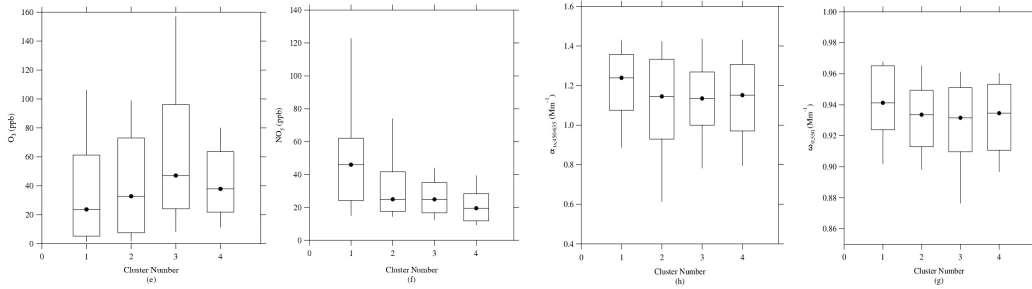
2334

2335

2336



2337



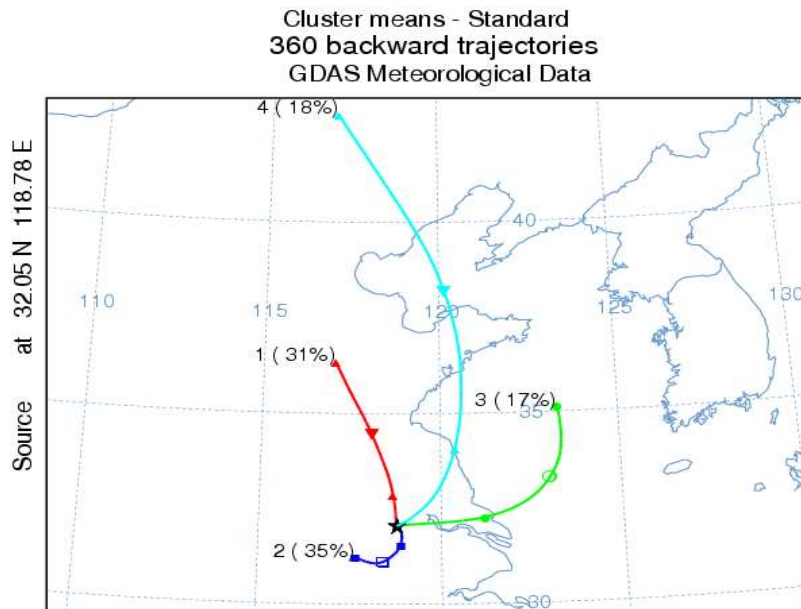
2338 Fig 12. The 10, 25, 50, 75, and 90% percentile values in each cluster of back trajectories in 2016

2339 fall of (a) BC, (b) $\text{PM}_{2.5}$, (c) $\text{PM}_{2.5}/\text{PM}_{10}$, (d) CO, (e) O_3 , (f) NO_y , (g) α_{ts} , and (h) ω_0 . Black

2340

markers represent the averages.

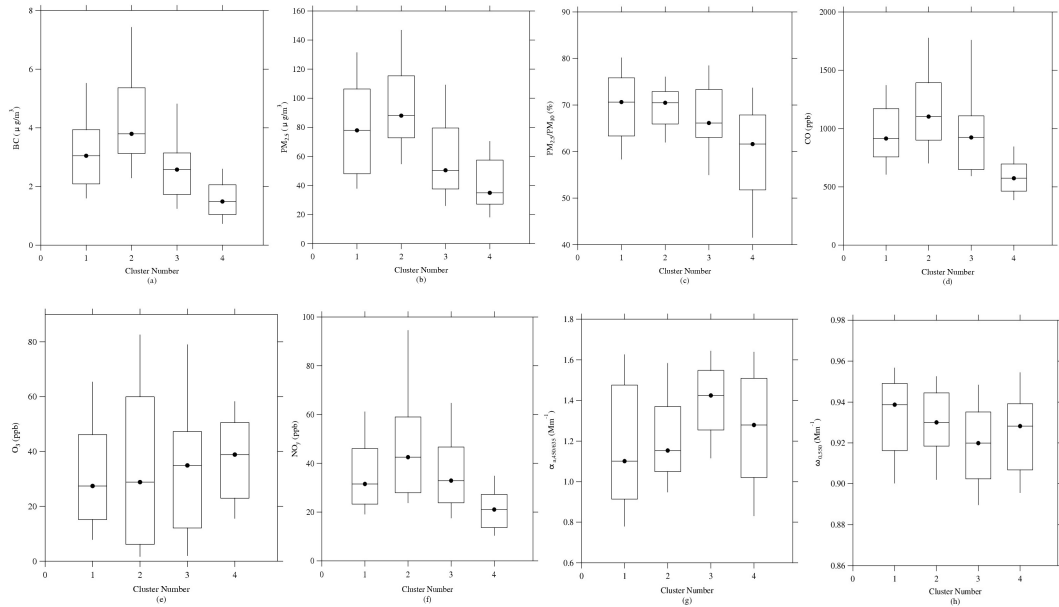
2341



2342

2343 Fig 13. Clusters of 96 h back trajectories arriving at the study site at 100m in 2016 winter.

2344



2345

2346

2347

2348 Fig 14. The 10, 25, 50, 75, and 90% percentile values in each cluster of back trajectories in 2016

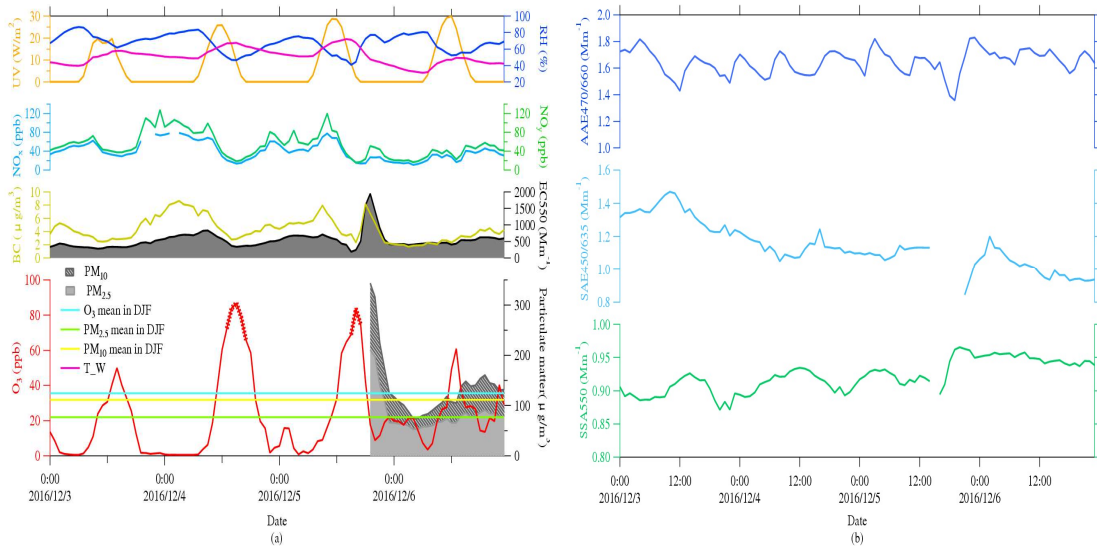
2349 winter of (a) BC, (b) PM_{2.5}, (c) PM_{2.5}/PM₁₀, (d) CO, (e) O₃, (f) NO_y, (g) α_{ts} , and (h) ω_0 . Black

2350

markers represent the averages.

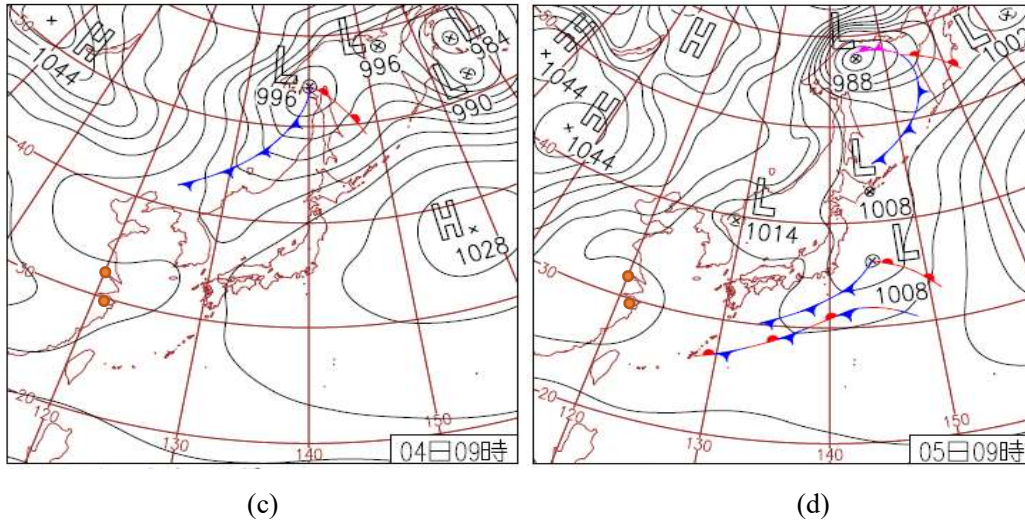
2351

2352



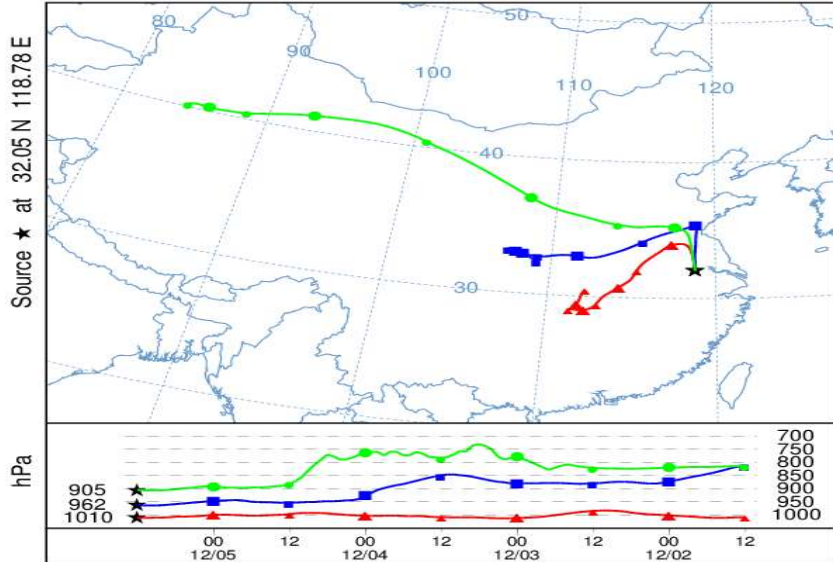
2353

2354
2355



(c) (d)

NOAA HYSPLIT MODEL
Backward trajectories ending at 1200 UTC 05 Dec 16
GDAS Meteorological Data



2356
2357

(f)

2358 Fig 15. Time series during December 3-6, 2016, for (a) PM2.5, BC and O3 with associated
2359 meteorological parameters, trace gases and (b) optical parameters. Red markers represent O3 over
2360 daily maximum average during winter. Weather charts on (c) 4th and (d) 5th December. (f) 96h
2361 backward trajectories analysis ending at 1200 UTC on 5th December.